

# Quantum optical implementation of quantum information processing \*

J. I. Cirac, Luming Duan, and P. Zoller  
*Institute for Theoretical Physics, University of Innsbruck*  
*Technikerstrasse 25-2, A-6020 Innsbruck, Austria*  
 (Dated: 2001 10 17)

We review theoretical proposals for implementation of quantum computing and quantum communication with quantum optical methods.

## I. INTRODUCTION

It is generally recognized that all the microscopic phenomena that we observed can be described and explained by the principles of Quantum Mechanics. These principles have been extensively tested, and some of them are commonly used in several technological applications. Other principles, like the ones related to the superposition principle and the measurement process, and which are in the realm of most of the paradoxes and strange phenomena related to Quantum Mechanics, have only recently become important in some applications. In particular, they form the basis of a new theory of information which may revolutionize the fields of communication and computation [1].

The basic ideas behind quantum communication and computation are very simple [1]. Quantum communication deals with sending quantum states from one place to another one in such a way that they arrive intact. The most important application so far in this field is the one in which a sender (traditionally called Alice) tries to convey a secret message to a receiver (traditionally called Bob). The message is encoded in the state  $|\Psi\rangle$  of a quantum system. Due to the fact that the quantum state of a system is distorted if somebody performs a measurement, Bob will receive a wrong state if a third (malevolent) party (Eve) tries to read the message. This way of secret communication is usually called quantum cryptography, and it is the only provably secure way in which two partners can share secret messages. In the context of quantum computation, the existence of entangled states of several particles offers the possibility of performing certain computational tasks in times much shorter than the ones taken by common (classical) computers. By acting on a system entangled to other systems, one modifies the state of the whole system at the same time, which leads to an important speed up in several computations. In particular, if one could build a quantum computer one would be able to decompose very large numbers (of  $n \gg 1$  digits) into prime factors in a time that scales polynomially with  $n$  ( $t \simeq an^b$ , with  $a$  and  $b$  constants) [2], in contrast to the exponential dependence of classi-

cal computers [3]. A quantum computer would therefore allow to break all the classical cryptographic protocols which are based on the impossibility of factorizing large numbers in relatively short times. There are also other algorithms which make use of the superposition principle in Quantum Mechanics and they are more efficient than the classical counterparts.

The experimental situation in quantum computing and quantum communication is very different. Whereas in the second case it is already a mature field, close to reaching the commercial level, the first one is still in its infancy. For the moment, it is possible to construct very small prototypes of quantum computers which, of course, do not offer any advantage over nowadays classical computers. In fact, it seems almost impossible that a *useful* quantum computer can be created in the next twenty or thirty years. Nevertheless, pursuing research in this field does not have the only goal of being useful in the near future, but there are several other goals which can be attained in the way. In particular, creating a quantum computer means that we can manipulate the quantum state of an enormous system at will which apart from being capable of bringing some surprises to our present knowledge of Quantum Mechanics, paves the way for some other applications based on this theory which may be discovered in the future and do not require a large system. On the other side, the first experiments on quantum cryptography took place between locations separated by few centimeters. At present, quantum cryptography over distances of the order of 50 km is possible. Other experiments on quantum communication achieve basically the same distances. Their extension to longer distances does not seem to be straightforward though, since the systems carrying the quantum states (i.e. photons) are eventually absorbed and therefore the quantum states are distorted before they arrive at their destination. A way to overcome this problem is to use quantum repeaters [4], in which small quantum computers amplify in a sense the quantum states so that they arrive safely to their destination.

There are very few systems in which one can implement a small quantum computer. Many of the ideas come from the field of Quantum Optics. The reason is the spectacular experimental development of this field during the last years, which has allowed, so to say, to dominate the quantum world. In particular, the internal quantum levels of atoms and ions can be manipulated very efficiently using lasers. One can basically stop them (i.e. cool them)

---

\*Proceedings of the International School of Physics Enrico Fermi **148**, *Experimental Quantum Computation and Information*, Ed. F. De Martini and C. Monroe, IOS Press, Amsterdam (2002)

with laser cooling techniques. It is also possible to manipulate their quantum state of motion by pushing them with laser light. These methods, when combined appropriately, allow, at least in principle, to perform quantum computations and to build quantum repeaters. On the other hand, very recently it has been recognized that these goals can also be achieved using atomic ensembles, instead of single atoms. The idea is to manipulate some collective degrees of freedoms of atomic ensembles using lasers, the main advantage being that the atoms do not need to be manipulated one by one, and they can be at room temperature.

The aim of this paper is to review some of the quantum optical systems that have been proposed to perform quantum computations, both using single atoms and using atomic ensembles. In the next chapter we will give a brief introduction to some of the main topics in quantum information theory, with particular emphasis on the ones that are needed in the next chapters. In the third chapter we will show how to use single atoms (ions) and photons in order to perform several tasks related to quantum information processing, whereas in the fourth chapter we will introduce several methods to deal with atomic ensembles.

## II. BASIC CONCEPTS IN QUANTUM INFORMATION THEORY

### A. Introduction

Most of the counter-intuitive predictions of Quantum Mechanics are related to the superposition principle. For example, according to Quantum Mechanics the properties of one object are generally not defined when we do not observe it. This principle, when applied to more than one system, may lead to very intriguing phenomena related to non-locality (actions in some system may affect in a special way some other systems) which have called the attention of philosophers and physicists since the advent of Quantum Mechanics. The basic ingredient of such phenomena is *entanglement*, i.e. the possibility of having two or more systems in a state which displays (quantum) correlations. Apart from its fundamental interest, entanglement plays an important role in most of the applications in the field of Quantum Information [1]. In particular, entangled states are crucial for quantum communication and computation. In this Section we will review the concept of entanglement, as well as some of the basic concepts in quantum communication and computation.

The characterization of this intriguing property of Quantum Mechanics, entanglement, is one of the central theoretical issues in Quantum Information Theory. In fact, there are still many open questions regarding the entanglement properties of two or more quantum systems. Although for pure states of two systems, entanglement is well understood, for more systems we do not yet

know how to quantify this property. The situation becomes much more complicated if the state of the system is mixed. In that case, we do not even know in general how to determine whether two systems are entangled or not. This problem has important consequences in current experiments in this field, since after preparing a quantum state of a system one would like to determine whether it is entangled or not (as we will explain, if it is not entangled this would mean that we could have created the same state in a much cheaper and straightforward way). In the first section of this chapter we will review this property, entanglement, both for pure and mixed states and will give some of the known criteria to determine whether a mixed state is entangled or not.

Mixed entangled states are not directly useful for quantum information purposes. However, there exist some methods, known under the name purification protocols, that allow us to make those states useful. We will review some of the basic purification protocols in the second subsection.

Quantum computation and communication are the most visible applications in the field of quantum information. In the last subsections of this section we will review these two topics paying special attention to the physical properties that a quantum system must possess in order to be useful for these applications. In particular, we will give a set of requirements to build a quantum computer which will serve us in the next chapters to show that several quantum optical systems serve for this purpose. We will also review one of the main tools in the field of quantum communication, teleportation, which combined with certain purification protocols allow to extend quantum communication over arbitrarily long distances.

### B. Entanglement

#### 1. Entanglement of pure states

The superposition principle is one of the basic concepts in Quantum Mechanics: If a system can be in two different states (associated to the vectors  $|0\rangle, |1\rangle \in H$ ) then it can also be in the state described by a linear superposition  $\alpha|0\rangle + \beta|1\rangle$ . This implies the existence of states in which properties are not well defined. The situation is even more intriguing when we have a composite system. For example, let us consider two subsystems A and B whose states are associated to the elements of two Hilbert spaces,  $H_A$  and  $H_B$ , respectively. We will assume that these systems are located at different places, although for most of our treatment this condition is not required. Let us consider states of the whole system in which one subsystem is in certain state  $|i\rangle_A$  and the other in  $|j\rangle_B$ . One denotes those states as  $|i\rangle_A \otimes |j\rangle_B \in H = H_A \otimes H_B$ , or simply  $|i, j\rangle \in H$ . According to the superposition principle, any superposition of these states must also be possible, i.e. the state represented by  $|\Psi\rangle \equiv \alpha|0, 0\rangle + \beta|1, 1\rangle \in H$ . A state of this

form cannot be described as a certain state for system A and some other state for system B; that is, there exist no pair of vectors  $|\phi_{1,2}\rangle_{A,B} \in H_{A,B}$  such that  $|\Psi\rangle = |\phi_1, \phi_2\rangle$ . States of this form are called entangled states and play a fundamental role in Quantum Information. Note that their existence arises from the fact that the states of the whole system must be described as elements of a Hilbert space themselves. One says that  $H$  is the tensor product of  $H_A$  and  $H_B$ , i.e.  $H = H_A \otimes H_B$ . Thus entangled states are a direct consequence of the tensor product structure of the Hilbert space describing composite systems.

In the following, we will denote by  $\{|k\rangle\}_{k=1}^{d_{A,B}}$  an orthonormal basis in  $H_{A,B}$ , respectively. Although the definitions and results apply for general dimensions, for most of the examples we will consider qubits, i.e. systems where  $d_A = d_B = 2$ . In that case we will take as a basis  $\{|0\rangle, |1\rangle\}$ . We will use the Pauli operators

$$\begin{aligned}\sigma_x &= |1\rangle\langle 0| + |0\rangle\langle 1|, \\ \sigma_y &= -i(|1\rangle\langle 0| - |0\rangle\langle 1|), \\ \sigma_z &= |1\rangle\langle 1| - |0\rangle\langle 0|.\end{aligned}$$

For qubits, there are some entangled states which play a very important role in quantum information, the so-called Bell states. They are

$$\begin{aligned}|\Psi^\pm\rangle &= \frac{1}{\sqrt{2}}(|0, 1\rangle \pm |1, 0\rangle) \\ |\Phi^\pm\rangle &= \frac{1}{\sqrt{2}}(|0, 0\rangle \pm |1, 1\rangle)\end{aligned}$$

The most important properties of entangled states is that they carry correlations. That is, if we measure an observable in A and another in B, the outcomes will be, in general, correlated. For example, if we have the state  $|\Psi^-\rangle$  and measure the observable  $\sigma_z$  in both systems we will obtain the opposite result. Actually, if we measure any observable  $\vec{\sigma} \cdot \vec{n}$  we will always obtain opposite results in A and B, the reason being that  $|\Psi^-\rangle$  is invariant under global rotations (i.e.  $U \otimes U |\Psi^-\rangle \propto |\Psi^-\rangle$  for all unitary operators  $U \in SU(2)$ ). Note that for all entangled states there always exist some correlations. For product vectors, however, the outcomes in A are independent of the outcomes in B. This can be also viewed by noting that if  $A$  and  $B$  are two observables, then  $\langle A \otimes B \rangle = \langle A \rangle \langle B \rangle$  for product vectors, but not (in general) for entangled states. The existence of correlations, by itself, is not a property of entangled states. For example, if somebody provides with two boxes A and B in which there are either two black or two white balls, when we open the box we will see correlations. However, the correlations carried by entangled states are, in some sense, different to those, since they occur for any pair of observables. In fact, classical correlations like the ones displayed by the balls in the boxes are restricted by Bell's inequalities [5], whereas the ones corresponding to entangled states may violate them. This is why with the correlations contained in entangled states we can perform things that are not possible using classical correlations.

In order to create entangled states out of product states we need interactions. This can be easily understood as follows. If we do not have interactions, the Hamiltonian describing the evolution of systems A and B will be written as  $H = H_A \otimes 1_B + 1_B \otimes H_B$ , where  $1$  is the identity operator. Since  $H_A \otimes 1_B$  and  $1_B \otimes H_B$  commute with each other, we have that the evolution operator can be always written as  $U(t) = U_A(t) \otimes U_B(t)$ , and the product state  $|\Psi(0)\rangle = |\phi_1(0)\rangle_A \otimes |\phi_2(0)\rangle_B$  will evolve into  $|\Psi(t)\rangle = |\phi_1(t)\rangle_A \otimes |\phi_2(t)\rangle_B$  which is a product state. Operators of the form  $U = U_A \otimes U_B$  are called local operators. Similarly, we cannot get entangled states by measuring observables in A and B, independently since the state after the measurement will be changed by local operators. One says that entanglement cannot be created by local operations (operations meaning any action on the systems). Note, however, that product states can be obtained by local operations (in particular, by measurements).

Let us show now how we can tell whether a state is entangled or not, and how much. We consider a state of the form

$$|\Psi\rangle = \sum_{i=1}^{d_A} \sum_{j=1}^{d_B} c_{i,j} |i, j\rangle. \quad (1)$$

All the information about the state is in the coefficients  $c_{i,j}$  which form a  $d_A \times d_B$  matrix that we will call  $C$ . Note that we could have chosen another orthonormal bases in  $H_{A,B}$  to express this state. In fact, there is a particular basis in which the matrix of the coefficients is diagonal and positive. If we choose such a basis to write the state, it will have the simple form

$$|\Psi\rangle = \sum_{k=1}^d d_k |u_k, v_k\rangle, \quad (2)$$

where  $d = \min(d_A, d_B)$ , and  $\sum_{k=1}^d d_k^2 = 1$ , with  $d_k \geq 0$ . This form is called Schmidt decomposition. Its existence directly follows from the singular value decomposition of the matrix  $C$ , i.e., the existence of two unitaries  $U$  and  $V$  and a diagonal one  $D$  whose diagonal elements are  $d_k$  such that  $C = UDV$ . The  $d_k$  are called Schmidt coefficients and the bases  $\{|u_k\rangle\} \in H_A$  and  $\{|v_k\rangle\} \in H_B$  are called Schmidt bases. Once we have expressed the state in the Schmidt decomposition, it is very simple to obtain some other information. For example, if we are interested in predicting expectation values or probabilities of outcomes if we only measure system A (or B), all the information about them is in the reduced density operator  $\rho_A = \text{tr}_B(|\Psi\rangle\langle\Psi|)$  (analogously for  $\rho_B$ ). We obtain

$$\rho_A = \sum_{k=1}^d d_k^2 |u_k\rangle\langle u_k|, \quad \rho_B = \sum_{k=1}^d d_k^2 |v_k\rangle\langle v_k| \quad (3)$$

Conversely, the Schmidt coefficients and the corresponding bases can be easily found by simply diagonalizing both reduced density operators.

For a product state  $|\phi_1, \phi_2\rangle$ , the reduced density operators are rank one projectors, i.e.  $\rho_{A,B} = |\phi_{1,2}\rangle\langle\phi_{1,2}|$ . This means that there is only one Schmidt coefficient which is different than zero. Conversely, if we have a state with only one Schmidt coefficient then it must be a product state. Equivalently,  $|\Psi\rangle$  is a product state if and only if the corresponding reduced density operators correspond to pure states. This means that if we have an entangled state, the corresponding reduced density operators must correspond to mixed states, or, equivalently, that there must be more than one nonzero Schmidt coefficients.

Thus, we see that the entanglement of a state is directly related to the mixedness of the reduced density operators. This is intuitively clear since, as we mentioned above, entangled states give rise to correlations and if we only observe one of the systems we loose information about these correlations which results in the fact that we will effectively have a mixed state. This suggests that we can measure the degree of entanglement by the degree of mixedness of the reduced density operators. There are several measures of mixedness of density operators; perhaps the most popular one is the von Neumann entropy  $S(\rho) = -\text{tr}(\rho \ln(\rho))$ . For a pure state this entropy is zero, whereas for a maximally mixed state (described by the identity operator, properly normalized) it gives  $\log_2 d$ , where  $d$  is the dimension of the Hilbert space. The entropy is convex, i.e. for  $p \in [0, 1]$ ,  $S[p\rho_1 + (1-p)\rho_2] \geq pS(\rho_1) + (1-p)S(\rho_2)$ , which means that it always increases by mixing (i.e. by loosing information). This motivates the following definition: Given a state  $|\Psi\rangle$ , we define the *entropy of entanglement*,  $E(\Psi)$  as the von Neumann entropy of the reduced density operator [6]. Thus, we have

$$E(\Psi) = S(\rho_A) = S(\rho_B) = -\sum_{k=1}^d d_k^2 \log_2(d_k^2). \quad (4)$$

The entropy of entanglement only depends on the Schmidt coefficients, but not on the corresponding basis. This means that it is invariant under local unitary operations. That is, if  $|\Psi'\rangle = (U_A \otimes U_B)|\Psi\rangle$ , then  $E(\Psi') = E(\Psi)$ . On the other hand, one can show that it cannot increase in average by local operations [7]. That is, if we perform (independent) measurements in A and B and obtain the state  $|\Psi_k\rangle$  after the measurement with probability  $p_k$ , we have that

$$E(\Psi) \geq \sum_k p_k E(\Psi_k). \quad (5)$$

Note, however, that the previous inequality does not imply that none of the  $E(\Psi_k)$  can be larger than  $E(\Psi)$ , or even the maximum allowed  $\log_2 d$ . States  $|\Psi\rangle \in H_{AB} = C^d \otimes C^d$  for which  $E(\Psi) = \log_2(d)$  are called *maximally entangled states* in  $d$  dimensions.

Let us now consider more systems  $A_1, A_2, \dots, A_N$ . Now, we can have entangled states and product states of the different systems [8]. For example, we can have a state of the form  $|\Psi\rangle = |\phi_1\rangle_{A_1 A_3} \otimes |\phi_2\rangle_{A_2 A_5 A_6} \otimes |\phi_3\rangle_{A_4}$ ,

where  $|\phi_{1,2,3}\rangle$  cannot be written as product states. It is clear that in a state like that, the parties  $A_1$  and  $A_3$  are entangled with each other, but not to the rest; similarly, the parties  $A_2, A_5$ , and  $A_6$  are entangled among them, and the party  $A_4$  is completely disentangled.

In general we can consider all possible partitions of those systems in which we group certain of them. For example, we can consider the partition  $(A_1 A_3), (A_2 A_5 A_6), (A_4)$ . We can classify the entangled states according to the different partitions. That is, a state is entangled according to some partition if it can be written as a product state of the corresponding disjoint elements of the groups, but not within each of the groups. In order to determine the partition corresponding to a particular state we can calculate all possible reduced density operators and look whether they correspond to mixed states or not.

The quantification of the multipartite entanglement is a more complicated question which can be illustrated by the following example. Let us consider three parties and the states [9],

$$|\text{GHZ}\rangle = \frac{1}{\sqrt{2}}(|0, 0, 0\rangle - |1, 1, 1\rangle) \quad (6)$$

$$|W\rangle = \frac{1}{\sqrt{3}}(|0, 0, 1\rangle + |0, 1, 0\rangle + |1, 0, 0\rangle). \quad (7)$$

Those are entangled states according to the partition  $(A_1 A_2 A_3)$ . However it is hard to say which one is more entangled. Certainly, the first one possesses a sticking non-local behavior, in the sense that it can be used to prove Bell's theorem without using inequalities [9]. However, it is very weak in the sense that if one party does not participate in the measurement (or is lost), then all the entanglement disappears. However, the second one retains some entanglement even if one particle is lost (in fact it is the most robust against particle losses) [10].

## 2. Entanglement of mixed states

The states that we have considered in the previous Section are idealized. In reality, all systems interact with some sort of environment. Thus, we should include the state of the environment in our description in order to be consistent. In fact, due to the interaction between system and environment they will become entangled even if initially they were in a product state:  $|\Psi_S(0)\rangle_A \otimes |\Psi_E(0)\rangle_E \rightarrow |\Psi(t)\rangle_{SE}$ . Since we are only interested in our system, all the information that we can acquire (without performing measurements in the environment) are contained in the reduced density operator  $\rho_S(t) = \text{tr}_E[|\Psi(t)\rangle_{SE}\langle\Psi(t)|]$ , which will correspond to a mixed state. Actually, this process in which a pure state is converted into a mixed state via its interaction with the environment is some times called decoherence. The term decoherence comes from a process which makes the coherence (non-diagonal elements of the density operator in a given basis) to vanish. However, since this definition

depends on the basis some authors prefer to call decoherence any process which is not describable by a unitary operator, i.e. which comes from the interaction of the system with some other system.

Note that density operators can be always be written in the form

$$\rho = \sum_k p_k |\phi_k\rangle\langle\phi_k| \quad (8)$$

where the  $p_k$  are positive and add up to one. One particular decomposition of this form is the spectral decomposition, in which, additionally, the vectors  $|\phi_k\rangle$  form an orthonormal basis. In general, except for pure states (rank one density operators) there are infinitely many decompositions. Note that a decomposition like (8) tells us one way of creating a state described by  $\rho$ . We simply have to prepare the system in state  $|\phi_k\rangle$  with probability  $p_k$ . The fact that there exist infinitely many decompositions of a state means that it can be prepared in infinitely many different forms. For example, the state  $\rho = I/2$  of one qubit can be prepared by choosing randomly one among the states  $\{|0\rangle, |1\rangle\}$  or one among the states  $\{|+\rangle, |-\rangle\}$ , where  $|\pm\rangle = (|0\rangle \pm |1\rangle)/\sqrt{2}$ . It is also worth stressing that even though the systems are prepared in different forms, they are completely indistinguishable. The reason is that the probability of any outcome after a measurement is completely determined by the density operator, so that if two systems have the same density operator they cannot be distinguished by performing any measurement (and therefore by any means). Density operators are linear and self-adjoint ( $\rho = \rho^\dagger$ ), have trace one ( $\text{tr}(\rho) = 1$ ), and are positive ( $\rho \geq 0$ ).

We thus have to define entanglement for mixed states [11]. Following what happens with pure states, it makes sense to define entangled states as those that require interactions between the systems in order to be prepared, and non-entangled (or separable) as the ones that can be created without interactions. More specifically, in Quantum Information a state is called entangled if it cannot be prepared by local operations (and classical communication) out of a product state. As we will see, this definition is equivalent to imposing that mixtures of product states are not entangled. Let us give some examples with two qubits: The state described by  $\rho = |0,0\rangle\langle 0,0|$  is not entangled since it is already a product state. Any density operator of the form  $\rho = \rho_A \otimes \rho_B$  is not entangled since the states  $\rho_{A,B}$  can be prepared locally out of the state  $|0\rangle$ . To see this, if we write  $\rho$  as in (8) we can simply transform the state  $|0\rangle$  into  $|\phi_k\rangle$  with probability  $p_k$ . The state

$$\rho = \frac{1}{2}(|0,0\rangle\langle 0,0| + |1,1\rangle\langle 1,1|)$$

is not entangled since it can be locally prepared as follows. We choose randomly 0 or 1. If we have 0, we prepare both A and B in state  $|0\rangle$  and otherwise in  $|1\rangle$ . Obviously, in this way we do not need any interaction between the systems. We just need classical communication

between the location of A and B so that the corresponding preparers can agree on the state they prepare. With these examples we see that the definition of entanglement is equivalent to the following mathematical characterization:  $\rho$  is separable if and only if there exist  $p_k \geq 0$  and  $\{|a_k\rangle\} \in H_A$  and  $\{|b_k\rangle\} \in H_B$  such that

$$\rho = \sum_k p_k |a_k, b_k\rangle\langle a_k, b_k|.$$

Otherwise it is entangled. It turns out that it is very hard in practice to determine whether a given state is entangled or not. There exists, however, an important sufficient criterion that may be useful in some occasions. It states [12] that if  $\rho^{TA}$  has a negative eigenvalue (i.e. it is not positive) then  $\rho$  is entangled. Here  $\rho^{TA}$  stands for the partial transpose of  $\rho$  with respect to the first system in the basis  $\{|k\rangle\}_{k=1}^{d_A} \in H_A$ , i.e.  ${}_A\langle k|\rho^{TA}|k'\rangle_A = {}_A\langle k'|\rho|k\rangle$ . In general, the converse of this criterion is not true [13]. That is, there exist entangled states fulfilling  $\rho^{TA} \geq 0$ . However, in low dimensions (if  $d_A \times d_B \leq 6$ ) this criterion (called Peres-Horodecki criterion [12, 14]) gives a necessary and sufficient condition:  $\rho$  is separable if and only if  $\rho^{TA} \geq 0$ . For other separability criteria see [15].

Given some state, sometimes we would like to know 'how close' it is to some pure state, like for example a Bell state. In order to measure this quantity we define the fidelity of  $\rho$  with respect to some state  $|\Phi\rangle$  as

$$F = \langle\Phi|\rho|\Phi\rangle.$$

A fidelity  $F \simeq 1$  means that our state is very close to the desired one. Note that a completely random state has a fidelity  $F = 1/d$ , where  $d$  is the dimension of the total Hilbert space.

A particular useful family of mixed states are the so-called Werner-like states. Let us consider two systems A and B with corresponding Hilbert spaces of dimension  $d$  both. Given a state  $\rho$  we depolarize it locally by applying the same random unitary operator to system A and system B. One can show that the state after this process has the form

$$\rho_F = F \frac{P_a}{d_a} + (1 - F) \frac{P_s}{d_s} \quad (9)$$

where  $P_s = (1 + \pi_{AB})/2$  and  $P_a = (1 - \pi_{AB})/2$  are the projector onto the symmetric and antisymmetric subspaces ( $\pi_{AB}$  is the permutation operator), and  $d_s = d(d+1)/2$  and  $d_a = d(d-1)/2$  the corresponding dimensions. Here,  $F = \text{tr}(P_a \rho)$ .  $\rho_F$  is called Werner-like state, since Werner [11] was the first one who introduced them for the case of qubits. One can easily show that  $\rho_F$  is entangled if and only if  $\rho_F^{TA}$  is not positive.

### C. Purification

Most of the applications in the field of Quantum Information are based on the use of superpositions of pure

states. However, in practice, the state that one has at disposal are mixed. For example, if one would like to perform quantum cryptography over long distances using entangled photons, when they arrive at the final location their state will also be entangled to the environment and therefore mixed. The longer the distance the photons have to travel, the more mixed they will become. Unfortunately, if they are significantly mixed, the security of the corresponding cryptographic protocol will no longer be ensured. This fact considerably limits the distances over which one can perform secure quantum cryptography. Fortunately, there is a method that allows to make the states more pure, and even more entangled. The idea is to use several copies of a state which is not useful for the applications of Quantum Information, but that it is still entangled [16, 17]. Using local operations and classical communication it is sometimes possible to obtain fewer copies of particles in a state which is closer to a maximally entangled states, for example the state  $|\Phi^+\rangle$ . This process is called entanglement purification (or distillation), and will be the subject of the present section.

Let us consider the two-qubit Werner state,

$$\rho_F = F|\Psi^-\rangle\langle\Psi^-| + \frac{(1-F)}{3}(|\Psi^+\rangle\langle\Psi^+| + |\Phi^+\rangle\langle\Phi^+| + |\Phi^-\rangle\langle\Phi^-|)$$

where all the vectors appearing here are Bell states. In the present scenario, Alice and Bob share two pairs of qubits in that state. Let us denote by  $A_1$  and  $A_2$  Alice's particles and by  $B_1$  and  $B_2$  Bob's, so that their state is  $\rho_F \otimes \rho_F$ . The distillation procedure presented in Ref. [16] is as follows. First, Alice applies the unitary transformation  $\sigma_y$  to her two qubits. This transforms in each pair  $|\Psi^\pm\rangle \rightarrow |\Phi^\mp\rangle$ . Thus, the resulting state will have now the maximum contribution coming from  $|\Phi^+\rangle$ . Then, both apply locally a controlled-NOT operation to their two particles, where  $A_1$  and  $B_1$  act like sources, and the other two ( $A_2$  and  $B_2$ ) as targets. The control-NOT operation acts as follows:

$$|0\rangle_{A_1}|0\rangle_{A_2} \rightarrow |0\rangle_{A_1}|0\rangle_{A_2} \quad (10)$$

$$|0\rangle_{A_1}|1\rangle_{A_2} \rightarrow |0\rangle_{A_1}|1\rangle_{A_2} \quad (11)$$

$$|1\rangle_{A_1}|0\rangle_{A_2} \rightarrow |1\rangle_{A_1}|1\rangle_{A_2} \quad (12)$$

$$|1\rangle_{A_1}|1\rangle_{A_2} \rightarrow |1\rangle_{A_1}|0\rangle_{A_2} \quad (13)$$

and similarly with  $B$ . Alice and Bob then measure the state of their target particle in the basis  $\{|0\rangle, |1\rangle\}$  (i.e., they measure  $\sigma_z^{A_2}$  and  $\sigma_z^{B_2}$ ) and broadcast their results. If the results are the same, they keep the source particles, and otherwise they discard them. One can easily see that this is equivalent to projecting the initial states onto the subspace in which either both the sources and the targets are  $\Phi$  states or both are  $\Psi$  states. The probability of having at the end of the process the state  $|\Phi^+\rangle$  is

$$F' = \frac{F^2 + (1-F)^2/9}{F^2 + 2F(1-F)/3 + 5(1-F)^2/9} \quad (14)$$

For  $1 > F > 1/2$ , we have that  $F' > F$ . Therefore, the fidelity after this operation increases. To finish the

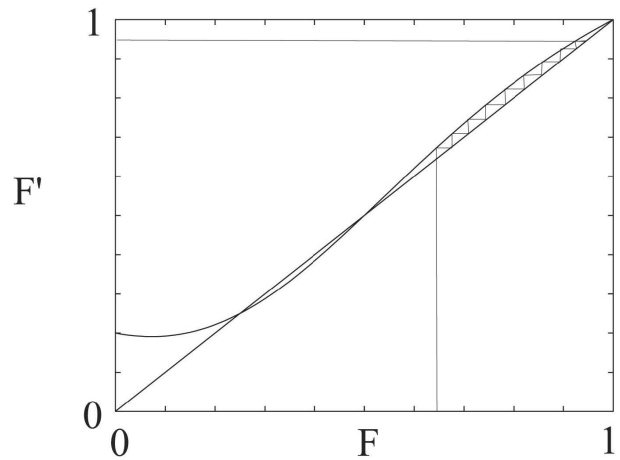


FIG. 1: New fidelity in terms of the old fidelity for the purification protocol. Successive applications lead to a fidelity as close to one as one wishes.

process, the output states should be left in a Werner state, so that this process can be continued. Alice applies the operation  $\sigma_y$  to his source particle, which transforms  $|\Phi^+\rangle \rightarrow |\Psi^-\rangle$  and then they depolarize. In summary, if the process is successful, Alice and Bob are left with a single pair in a Werner state but with fidelity  $F'$ . Then, they can take two successful pairs and repeat the same procedure to obtain a higher fidelity. By proceeding in this way they can reach a fidelity as close to one as they wish, but at the expenses of wasting many pairs. In Fig. II C we have plotted  $F'$  as a function of  $F$  and show how the fidelity increases as one repeats it with the successful pairs.

So far we have assumed that the operations that take place during the purification protocol (Controlled-NOT, measurements, etc.) are perfect. In reality there will be imperfections in all these operations. One can take them into account by using some explicit models [4] or by studying the worst case scenario [18]. The result is schematized in Fig. II C. Now, there is a minimum value of the original fidelity of the state  $F_{\min}$  for which purification is possible. Apart from that, there is a maximum achievable fidelity  $F_{\max}$  due to the imperfections.

## D. Quantum computing

### 1. What is a quantum computer?

A computation can be considered as a physical process that transforms an input into an output. A classical computation is that in which the physical process is based on classical laws (without coherent quantum phenomena). A quantum computation is that based on quantum laws (and in particular on the superposition principle). In quantum computation, inputs and outputs

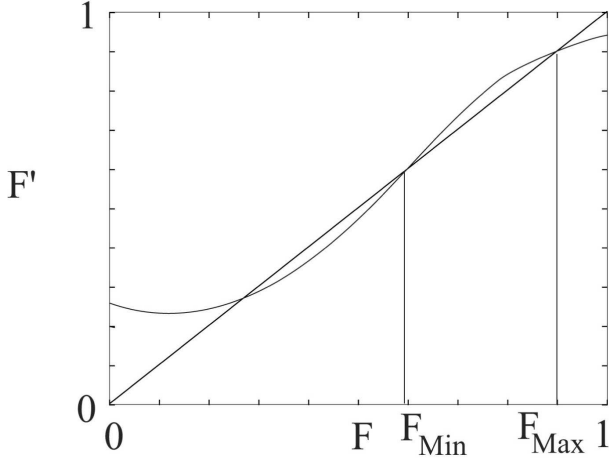


FIG. 2: Same as in the previous figure, but with imperfections.

are represented by states of the system. For example, enumerating the state of a given basis as  $\{|1\rangle, |2\rangle, \dots\}$ , the number  $N$  would be represented by the  $N$ th state of this basis. A quantum computation consists of evolving the system with a designed Hamiltonian interaction, such that the states are transformed as we want. Note that the operation that transforms input into outputs has to be unitary. For example, the operation that gives 1 if a number is odd and 2 if it is even could not be implemented:  $|2n+1\rangle \rightarrow |1\rangle$  and  $|2n\rangle \rightarrow |2\rangle$  (where  $n$  is an integer). This operation cannot be unitary since it does not conserve the scalar product (i.e.  $\langle 1|3\rangle = 0$  but the corresponded mapped states are not orthogonal). One can, however, use an auxiliary system so that the output is written in that system while keeping the unitarity of the operation:  $|2n+1\rangle \otimes |0\rangle \rightarrow |2n+1\rangle \otimes |1\rangle$  and  $|2n\rangle \otimes |0\rangle \rightarrow |2n\rangle \otimes |2\rangle$  (where  $n$  is an integer). In general, if our algorithm consists of evaluating a given function  $f$ , we can design an interaction Hamiltonian such that the evolution operator transforms the input states according to the following table:

$$\begin{aligned} |1\rangle \otimes |0\rangle &\rightarrow |1\rangle \otimes |f(1)\rangle \\ |2\rangle \otimes |0\rangle &\rightarrow |2\rangle \otimes |f(2)\rangle \\ &\dots \\ |N\rangle \otimes |0\rangle &\rightarrow |N\rangle \otimes |f(N)\rangle \end{aligned}$$

Note that using this transformation we can, at least, do the same computations with quantum computers as with classical computers. However, with quantum computers we can do even more. We can prepare the input state that in a superposition

$$|\Psi\rangle = \frac{1}{\sqrt{N}} \sum_{k=1}^N |k\rangle \otimes |0\rangle \rightarrow \frac{1}{\sqrt{N}} \sum_{k=1}^N |k\rangle \otimes |f(k)\rangle$$

after a single run. In principle, all the values of  $f$  are present in this superposition. Note, however, that we do

not have access to this information since if we perform a measurement we will only obtain a result (with certain probability). Nevertheless, we see that with a quantum computer we can do at least the same as with a classical computer, ... and even more. This property of using quantum superpositions to run only once the computer was termed by Feynman quantum parallelism.

## 2. Requirements

A quantum computer consists of a quantum register (a quantum system) that can be manipulated and measured in a controlled way. In order to build a quantum computer, one needs the following elements (see also Ref. [19]):

1. **A set of qubits:** These are two-level systems perfectly identified and which form the quantum register. We denote by  $\{|0\rangle_k, |1\rangle_k\}$  two orthogonal states of the  $k$ -th qubit, so that the state of all the qubits (the quantum register) can be written as

$$|\Psi\rangle = \sum_{k_1, k_2, \dots, k_N=0}^1 c_{k_1 k_2 \dots k_N} |k_1\rangle_1 \otimes |k_2\rangle_2 \otimes \dots \otimes |k_N\rangle_N.$$

In the following, we will simplify the notation and write  $|k_1, k_2, \dots, k_N\rangle$  instead of the cumbersome notation that uses tensor products. Note that these qubits can be in superposition and entangled states, which gives the extraordinary power to the quantum computer. Note that the state of the qubits must be kept almost pure since otherwise the power of the superpositions would not be effective. This means that the qubits must be well isolated from the environment in such a way that process of decoherence is sufficiently slow.

2. **Universal set of quantum gates:** The controlled manipulation of the qubits means that we can perform any unitary operation  $U$  on the qubits so that  $|\Psi\rangle \rightarrow U|\Psi\rangle$ . In principle, if we want to perform general operations we should be able to engineer arbitrary interactions between the qubits. Fortunately, this task is enormously simplified given the fact that any  $U$  can be decomposed as a product of gates belonging to a small set, the so-called universal set of gates. This means that if we are able to perform the gates of this set we will be able to perform any computation (unitary operations on the register) by simply applying a sequence of them. There are many sets of universal

gates, and of course, they are all equivalent. The most convenient set is the one that contains one two-qubit gate (an operation acting on two qubits only) plus a set of single-qubit gates. Let us recall here some of the gates of this sort ( $\sigma_{x,y,z}$  are the Pauli operators acting on a qubit):

(a) Single-qubit gates: act on a single qubit.

i. Phase gate:  $U_z^{(1)}(\varphi) = e^{-i\varphi\sigma_z}$ ,

$$|0\rangle \rightarrow e^{i\varphi/2}|0\rangle$$

$$|1\rangle \rightarrow e^{-i\varphi/2}|1\rangle$$

ii. Excitations:  $U_z^{(1)}(\theta) = e^{-i\theta\sigma_x}$ ,

$$|0\rangle \rightarrow \cos\theta|0\rangle - i\sin\theta|1\rangle$$

$$|1\rangle \rightarrow -i\sin\theta|0\rangle + \cos\theta|1\rangle$$

(b) Two-qubit gates: act on two qubits.

i. Controlled-not:  $U_{\text{CNOT}}^{(2)} = |0\rangle\langle 0| \otimes 1 + |1\rangle\langle 1| \otimes \sigma_x$

$$|0,0\rangle \rightarrow |0,0\rangle$$

$$|0,1\rangle \rightarrow |0,1\rangle$$

$$|1,0\rangle \rightarrow |1,1\rangle$$

$$|1,1\rangle \rightarrow |1,0\rangle$$

This gate changes the state of the second qubit conditioned to the state of the first one. The first qubit is therefore called control qubit, whereas the second one is called target.

ii. Controlled-phase:  $U_\pi^{(2)} = |0\rangle\langle 0| \otimes 1 - |1\rangle\langle 1| \otimes \sigma_z$

$$|0,0\rangle \rightarrow |0,0\rangle$$

$$|0,1\rangle \rightarrow |0,1\rangle$$

$$|1,0\rangle \rightarrow |1,0\rangle$$

$$|1,1\rangle \rightarrow -|1,1\rangle$$

Two different universal sets of gates are [1]:

$$S_1 = \{U_{\text{CNOT}}^{(2)}, U_x^{(1)}(\pi/4), U_z^{(1)}(\varphi), \varphi \in [0, 2\pi)\},$$

$$S_2 = \{U_\pi^{(2)}, U_z^{(1)}(\pi/4), U_x^{(1)}(\varphi), \varphi \in [0, 2\pi)\}.$$

Note that the two-qubit gates require interactions between the qubits, and therefore are the more difficult ones in practice. The fact that the operations are unitary (and therefore reversible) means that the uncontrolled interaction with any other part of the quantum computer must be avoided.

3. **Detection:** One should be able to measure  $\sigma_z$  on each of the qubits (or, equivalently, to detect whether they are in state  $|0\rangle$  or  $|1\rangle$ ). Note that this process requires the interaction with a measurement apparatus in an irreversible way.
4. **Erase:** We must be able to prepare the initial state of the system, for example the state  $|0, 0, \dots, 0\rangle$ . Actually, this is not an extra requirement since if one is able to detect and to apply the single-qubit gate  $U_x^{(1)}(\pi)$  this is enough.

5. **Scalability:** The difficulty of performing gates, measurements, etc., should not grow (exponentially) with the number of qubits. Otherwise, the gain in the quantum algorithms would be lost.

For the moment, we know very few systems which fulfill the requirements to implement a quantum computer with them. Perhaps, the most important problem is related to the necessity of finding a quantum system which is sufficiently isolated, and for which the required controlled interactions can be produced. For the moment, there exist three kind of physical systems that fulfill, at least, most of the requirements (see Ref. [20]):

1. **Quantum optical systems :** Qubits are atoms (ions), and the manipulation takes place with the help of a laser. This systems are very clean in the sense that with them it is possible to observe quantum phenomena very clearly. In fact, with them several groups have managed to prepare certain states which lead to phenomena that present certain analogies with the Schrödinger cat paradox, Zeno effect, etc. Moreover, those systems are currently used to create atomic clocks, and with them one can perform the most precise measurements that exist nowadays. For the moment, experimentalist have been able to perform certain quantum gates, and to entangle 3 or 4 atoms. The most important difficulty with those systems is to scale up the models so that one can perform computations with many atoms.
2. **Solid state systems :** There have been several important proposals to construct quantum computers using Cooper pairs or quantum dots as qubits. The highest difficulty in these proposals is to find the proper isolation of the system, since in a solid it seems hard to avoid interactions with other atoms, impurities, phonons, etc. For the moment, only single quantum gates have been experimentally reported. However, these systems posses the advantage that they are easily scalable.
3. **Nuclear magnetic resonance systems:** In this case the qubits are represented by atoms within the same molecule, and the manipulation takes place using the NMR technique. Initially, these systems seemed to be very promising for quantum computation, since it was thought that the cooling of the molecules was not required, which otherwise would make the experimental realization very difficult. However, it seems that without cooling, these systems loose all the advantages of quantum computation.

### 3. Error correction

In any computation (classical and quantum) or during storing of information there will be errors. One way to



fight against these errors is to improve the hardware and make it better. However, this is expensive, and not always possible. Shannon realized that instead of trying to avoid the errors it is much better to correct them. This is done by giving redundant information, and using this extra information to find out if an error occur. One can distinguish two kind of errors:

*Memory errors:* Those that occur to the information that is stored, regardless of whether an operation takes place or not.

*Operation errors:* Those that occur during an operation.

Here we will concentrate on memory errors, since the corresponding correction procedures are easier to understand. On the other hand, they play an important role not only in quantum computing, but also in quantum communication and information. Once one knows how memory errors can be corrected, (with some modifications) one can understand how to correct operation errors. We will first revise the most straightforward way of correcting errors in a classical computer, and then we will show how to do it in a quantum computer.

#### Classical error correction:

Imagine that one wants to store a single bit for a time  $t$  (we will call this bit a *logical bit*). Let us denote by  $P_\tau$  the probability that one error occurs in a time interval  $\tau$ ; that is, the probability that the bit flips (if it was 0 then it changes to 1 and vice versa). If  $P_\tau \simeq 1$  there will be problems in achieving the goal. One way to correct the errors is based on what is called *redundant coding*. This consists of using three bits to store the logical bit. That is, we encode the information such that if the logical bit is 0 the three bits are 0, and if it is 1, the three bits are 1:  $0_L \equiv 000$ , and  $1_L \equiv 111$ . These logical qubits are called *code words*. After at time  $\tau$ , we will have

- Probability of no errors:  $(1 - P_\tau)^3$  (for example, if we had initially 000, after the time  $\tau$  it is 000).
- Probability of error in one bit:  $3P_\tau(1 - P_\tau)^2$  (for example, if we had initially 000, after the time  $\tau$  it is 100, 010 or 001).
- Probability of two or more errors:  $3P_\tau^2(1 - P_\tau) + P_\tau^3$ .

The error correction consists of measuring if the three bits are in the same state or not. If they are in the same state, then we do nothing. If they are in a different state, we use majority vote to change the bit that is different. For example, if we have that the first and the third bit are equal and the second is different (010 or 101), we flip the second bit (000 and 111, respectively). After the correction we will have the correct state with a probability  $P_\tau^c = 1 - 3P_\tau^2 + 2P_\tau^3$ . Thus, one gains if  $P_\tau^c < 1 - P_\tau$ , that is, if (roughly)  $P_\tau < 1/3$ . If one wants to keep the state for very long times  $t$ , one has to perform many measurements. More precisely, assume that  $P_\tau = 1 - e^{-\gamma\tau} \simeq \gamma\tau$  for times  $\tau$  sufficiently short. Let us divide  $t$  in  $N$  intervals of duration  $\tau = t/N$ . For  $N$  sufficiently large, the

probability of having the correct state after performing the correction after the time  $t$  will be

$$P_t^c \geq \left[ 1 - 3 \left( \frac{\gamma t}{N} \right)^2 \right]^N \quad (15)$$

For  $N$  large, this probability can be made as close to one as desired. One can generalize this method to the case in which one wants to store  $k$  logical bits and allow for errors in  $l$  bits. For example, encoding  $0_L \equiv 00000$ ,  $1_L \equiv 11111$ , one can allow for two errors.

#### Quantum error correction:

Imagine that one wants to store a single quantum bit in an unknown state  $|\Psi\rangle = c_0|0\rangle + c_1|1\rangle$  for a time  $t$  (we will call this qubit a *logical qubit*). Let us assume that after a time  $\tau$  with a probability  $1 - P_\tau$  the qubit remains intact and that with a probability  $P_\tau$  it changes to  $|\Psi'\rangle = c_0|1\rangle + c_1|0\rangle$ . This error is called spin flip, and it can be represented by the action of  $\sigma_x$  onto the state of the qubit. One can correct the above error by using *redundant coding* [21, 22]. For example, one can encode the state of the logical qubit in 3 qubits as  $|0\rangle_L \equiv |000\rangle$  and  $|1\rangle_L \equiv |111\rangle$  (code words). The subspace spanned by these states is called subspace of code words. After time  $\tau$ , we will have:

- Probability of no errors:  $(1 - P_\tau)^3$  (the state will be  $|\Psi\rangle_L$ ).
- Probability of error in one bit:  $3P_\tau(1 - P_\tau)^2$  (the state will be  $\sigma_x^1|\Psi\rangle_L$ , or  $\sigma_x^2|\Psi\rangle_L$ , or  $\sigma_x^3|\Psi\rangle_L$ ).
- Probability of two or more errors:  $3P_\tau^2(1 - P_\tau) + P_\tau^3$ .

Note that in order to correct the errors, we cannot do the same as in the classical case, since measuring the state of the qubit will collapse it in a different state (for example  $|000\rangle$ ), and therefore the superposition will be destroyed. What we can do is to detect whether the three bits are in the same state or not, without disturbing the state. If the qubits are in the same state, then we do nothing. If they are a different state, we use majority vote to change the bit that is different. All these measurements have to be performed without destroying the superposition. This can be done as follows: first we measure the projector  $P = |000\rangle\langle 000| + |111\rangle\langle 111|$  (which corresponds to an incomplete measurement). If we obtain 1, then we leave the qubits as they are. If we obtain 0 then we measure the projector  $P_1 = |100\rangle\langle 100| + |011\rangle\langle 011|$ : if we obtain 1 we apply the local unitary operator  $\sigma_x^1$  and if not we proceed. We measure  $P_2 = |010\rangle\langle 010| + |101\rangle\langle 101|$ ; if we obtain 1 we apply the local unitary operator  $\sigma_x^2$  and if not we apply the operator  $\sigma_x^3$  (note that if we measure the operator  $P_3$  we would obtain 1 with probability 1). As a result, if there was either no error or one error, it will be corrected. If there were two or more errors, they will not be corrected. Using this method, we achieve the same results as in the classical correction method, namely, by

correcting very often we can keep the unknown state of a qubit for as long as we want. The idea of the method for quantum error correction is based on designing the code words in such a way that every possible error (in the first, second, or third qubit) transforms the subspace of code words onto another subspace which is orthogonal to it, but without modifying its internal structure. Then, by performing an incomplete measurement, we can detect in which subspace our state is, and therefore we know how to correct the error. This method can be generalized to the case in which other kinds of errors can occur. For example, imagine that with a small probability we can have errors consisting of applying the operator  $\sigma_\alpha$  ( $\alpha = x, y, z$ ) to a qubit. We want to preserve the state of  $k$  qubits against arbitrary errors in  $t$  different qubits. We will denote by  $E$  the possible operators corresponding to the errors that we want to correct. For example,  $\sigma_x^1 \otimes \sigma_y^4$ . We encode the  $k$  logical qubits in  $n$  qubits. The subspace of code words  $H_L$  has dimension  $2^k$ , whereas the Hilbert space  $H$  of all the qubits has dimensions  $2^n$ . Each of the possible error operators (consisting of up to  $t$  tensor products of Pauli operators) transform  $H_L$  into a subspace of dimension  $2^k$  (Note that the  $E$ 's are unitary and therefore they conserve the dimension of the subspace on which they are applied). The subspace of code words has to be such that all these subspaces are mutually orthogonal. This condition imposes a minimum bound (the quantum Hamming bound) to the number of qubits needed, since all these orthogonal subspaces have to fit in  $H$ . One can easily show that this bound implies that

$$2^k \sum_{l=0}^t 3^l \binom{n}{l} < 2^n. \quad (16)$$

For  $k = 1$  the minimum  $n$  is 5. Methods have been devised to construct codewords for each of these cases [23, 24]. On the other hand, one can take into account the errors that are produced while errors are being corrected, as well as the ones produced during operations. There is a whole theory dealing with the so-called fault tolerant error correction [25], which basically shows that this is always possible provided the error per gate is smaller than some error threshold, which lies between  $10^{-4}$ – $10^{-6}$  depending on the error model. This result implies that if the error per gate is smaller than this threshold, then quantum computation is possible by using fault tolerant error correction.

The above error correction schemes work in the presence of (undesired) coupling to the environment which leads to decoherence. In order to show that, one can expand the operator that describes the evolution of the  $i$ th qubit with its local environment as

$$U^i = \alpha^i 1^i \otimes E_0^i + \epsilon_1^i \sigma_x^i \otimes E_1^i + \epsilon_2^i \sigma_y^i \otimes E_2^i + \epsilon_3^i \sigma_z^i \otimes E_3^i \quad (17)$$

where the  $E$ 's are operators acting on the environment, and  $\alpha^i$  and  $\epsilon_{1,2,3}^i$  are constant numbers. Note that we can

always use this expansion given the fact that the Pauli operators (plus the identity) form a basis in the space of operators acting on a qubit. We will consider that the time is sufficiently short so that all  $\alpha^i \simeq 1$  and  $\epsilon_{1,2,3}^i \ll 1$ . The state of all the qubits after some interaction time  $U|\psi\rangle|E\rangle = \otimes_{i=1}^n U^i|\psi\rangle|E\rangle$  can be expanded in terms of the epsilon keeping only the lowest orders. The error correction explained above will project the state onto only one of the terms of the resulting expression. The state of the environment will therefore factorize, and all the analysis made before remains valid.

## E. Quantum communication

The situation one has in mind in quantum communication is the following: Alice wants to send Bob an unknown state  $|\Psi\rangle$ . One way of doing this is to send the particle carrying the state directly. However, the particle will very likely interact with the environment which may result in a different state, generally mixed. There are some ways of avoiding this. In the following we will describe a basic tool in quantum communication which allows to send one quantum state from one place to another provided one has a maximally entangled state shared between the two places, and is able to communicate classically without errors.

### 1. Teleportation

By teleportation we define to transfer an intact quantum state from one place to another, by a sender who knows neither the state to be teleported nor the location of the intended receiver [26]. The term teleportation comes from Science Fiction meaning to make a person or object disappear while an exact replica appears somewhere else. The first teleportation experiments have recently taken place. Consider two partners, Alice and Bob, located at different places. Alice has a qubit in an unknown state  $|\phi\rangle$ , and she wants to teleport it to Bob, whose location is not known. Prior to the teleportation process, Alice and Bob share two qubits in a Bell state  $|\Psi^-\rangle = \frac{1}{\sqrt{2}}(|0,1\rangle - |1,0\rangle)$ . The idea is that Alice performs a joint measurement of the two-level system to be teleported and her particle. Due to the nonlocal correlations contained in the Bell state, the effect of the measurement is that the unknown state appears instantaneously in Bob's hands, except for a unitary operation which depends on the outcome of the measurement. If Alice communicates to Bob the result of her measurement, then Bob can perform that operation and therefore recover the unknown state (for experiments, see [27–29]).

Let us call particle 1 that which has the unknown state  $|\phi\rangle_1$ , particle 2 the member of the EPR that Alice possesses and particle 3 that of Bob. We write the state of particle 1 as  $|\phi\rangle_1 = a|0\rangle_1 + b|1\rangle_1$  where  $a$  and  $b$  are (un-

known) complex coefficients. The state of particles 2 and 3 is the Bell state  $|\Psi^-\rangle$ . The complete state of particles 1, 2 and 3 is therefore

$$|\Psi\rangle_{123} = \frac{a}{\sqrt{2}}(|0, 0, 1\rangle - |0, 1, 0\rangle) + \frac{b}{\sqrt{2}}(|1, 0, 1\rangle - |1, 1, 0\rangle).$$

In order to teleport the state, Alice and Bob follow this procedure:

(1) *Alice measurement*: Alice makes a joint measurement of her particles (1 and 2) in the Bell basis

$$\begin{aligned} |\Psi^\pm\rangle &= \frac{1}{\sqrt{2}}(|0, 1\rangle \pm |1, 0\rangle) \\ |\Phi^\pm\rangle &= \frac{1}{\sqrt{2}}(|0, 0\rangle \pm |1, 1\rangle) \end{aligned}$$

(2) *Alice broadcasting*: Then she broadcasts (classically) the outcome of her measurement. That is, she has to send Bob two bits of classical information which indicate the outcome of the measurement.

(3) *Bob restoration*: Bob then applies a unitary operation to his particle to obtain  $|\phi\rangle_3$ . According to the state of the particles the possible outcomes are:

With probability  $1/4$ , Alice finds  $|\Psi^-\rangle_{12}$ . The state of the third particle is automatically projected onto  $a|0\rangle_3 + b|1\rangle_3$ . Thus, in this case Bob does not have to perform any operation.

With probability  $1/4$ , Alice finds  $|\Psi^+\rangle_{12}$ . The state of the third particle is automatically projected onto  $-a|0\rangle_3 + b|1\rangle_3$ . Teleportation occurs if Bob applies  $\sigma_z$  to his particle.

With probability  $1/4$ , Alice finds  $|\Phi^-\rangle_{12}$ . The state of the third particle is automatically projected onto  $a|1\rangle_3 + b|0\rangle_3$ . Teleportation occurs if Bob applies  $\sigma_x$  to his particle.

With probability  $1/4$ , Alice finds  $|\Phi^+\rangle_{12}$ . The state of the third particle is automatically projected onto  $a|1\rangle_3 - b|0\rangle_3$ . Teleportation occurs if Bob applies  $\sigma_z$  to his particle.

Note that Alice ends up with no information about her original state so that no violation of the no-cloning theorem occurs. In this sense, the state of particle 1 has been transferred to particle 3. On the other hand, there is no instantaneous propagation of information. Bob has to wait until he receives the (classical) message from Alice with her outcome. Before he receives the message, his lack of knowledge prevents him from having the state. Note that no measurement can tell him whether Alice has performed her measurement or not. Since teleportation is a linear operation applied to a state, it will also work for statistical mixtures, or in the case in which particle 1 is entangled with other particles.

## F. Quantum repeaters

We have now all necessary tools available to introduce the concept of the quantum repeater. Our goal is to create an EPR pair of high fidelity between two distant locations. Since nonlocal entanglement between distant particles cannot be created using only local operations, this involves the usage of a quantum channel, which is noisy in general. The bottleneck for communication over large distances is the scaling of the error probability with the length of the channel. When using, for example, optical fibers and single photons as a quantum channel, both the absorption losses and the depolarization errors scale exponentially with the length of the channel. The state of the photon or the photon itself will therefore be destroyed with almost certainty if the channel is longer than a few half-lengths of the fiber.

To overcome this problem, one can use quantum repeaters. The idea of such a repeater is to divide a long quantum channel into shorter segments, which are purified separately, before they are connected. Connecting two segments of a channel means here to build up quantum correlations across the compound channel from correlations that exist across the individual segments. This can be done by teleportation of entanglement. A quantum repeater must therefore combine the methods of entanglement purification and teleportation. Although the combination of these methods should, in principle, allow to create entanglement over arbitrary distances, it is another question how much this "costs" in terms of resources needed for purification. Resources means here the number of low fidelity entangled pairs that have to be provided for purification of each channel segment. This quantity is related to the number of particles that have to be manipulated locally (at the connection points between the segments) in a coherent fashion. If the resources grow too fast with the length of the channel, not much will be gained by the whole procedure. A further important quantity is the error tolerance for the local operations. In every real situation, the local operations applied to one or more particles will bear some imperfections. Since such operations are the building blocks for any entanglement purification protocol, their imperfections will limit the maximum attainable fidelity for an EPR pair and the efficiency of the protocol. In the context of the quantum repeater, a maximum fidelity  $F < 1$  corresponds to a residual amount of noise for each segment. When the segments are connected, this noise accumulates.

To overcome this limitation [4], we can divide the long channel into  $N$  smaller segments and create less distant entangled pairs across each segment. The number of segments  $N$  is thereby chosen in such a way that it is possible to create entangled pairs with sufficiently high initial fidelity  $F > F_{\min}$  over the distance of such a segment, such that they can be purified, according to our previous discussion. In a next step, we connect these "elementary" pairs by using teleportation. For example if we have an entangled purified pair between the nodes  $A_1$  and  $A_2$ , and

another one between  $A_2$  and  $A_3$ , we teleport the state of the first particle in  $A_2$  to  $A_3$  by using this second pair. The result of this teleportation will be that the nodes  $A_1$  and  $A_3$  will now share an entangled state. Of course, due to imperfections during the teleportation procedure, as well as the fact that the pairs used were not perfectly pure, the new entangled state will not be pure. But as long as its fidelity is larger than  $F_{\min}$ , it will be possible to purify it to a value close to  $F_{\max}$ . Thus, the crucial point is that, on the one hand, the operations that are performed cannot be too noisy since otherwise they could decrease the fidelity below  $F_{\min}$ , which would make the process impossible; on the other hand, the distance between nodes has to be such that purification be possible. This limits the number of pairs one can connect before purification becomes impossible. We therefore connect a smaller number  $L \ll N$  of pairs so that the resulting fidelity  $F_L$  stays above the threshold value for purification ( $F_L \geq F_{\min}$ ) and purification is possible.

The general strategy will be to design an alternating sequence connection and (re-)purification procedures in such a way that the number of resources needed remains as small as possible, and in particular does not grow exponentially with  $N$  and thus with  $l$ . This is possible, in principle, using a nested purification protocol [4].

### III. QUANTUM INFORMATION PROCESSING WITH SINGLE ATOMS AND PHOTONS

#### A. Introduction

This chapter discusses various schemes of quantum information processing with single trapped atoms and photons, i.e., manipulation of atoms and photons on the level of the single quantum level. Experimental realization includes laser cooled trapped ions, either in a linear trap or in arrays of micro traps, and neutral atoms stored in far-off-resonance traps or optical lattices. Single atoms can be stored in high-Q cavities, providing an interface between atoms and photons. The models discussed below share the feature that long lived internal atomic states, such as atomic hyperfine ground states or metastable states, serve as quantum memory to store the qubits. Furthermore, we assume that single qubit rotations can be performed by coupling the qubit states to laser light for an appropriate time period. In general, this requires that single atoms can be addressed by laser light. The discussion during the last few years has focused on developing various schemes for two-qubit gates. The models discussed in the literature can be classified in two categories. The first version relies on the concept of a quantum data bus: in this case the qubits are coupled to a collective auxiliary quantum mode, and entanglement of qubits is achieved by swapping qubits to excitations of the collective mode. Examples for such systems are the collective phonon modes in ion traps [30], and photons in cavity QED [31, 32]. Requirements often include the

initialization of the quantum data bus in a pure initial state, e.g. laser cooling to the motional ground state in ion traps. However, recently specific protocols for “hot gates” have been developed which loosen these requirements [33, 34]. The second concept for performing the two-qubit gate is controllable internal-state dependent two-body interactions between atoms. Examples for this latter scheme are coherent cold collisions of atoms in optical traps and optical dipole-dipole interactions [35, 36]. A third example is the “fast” two-qubit gate based on large permanent dipole interactions between laser excited Rydberg atoms in static electric fields [37]. We note that the unitary operations, which can be decomposed in a series of single and two-qubit operations on the qubits, can either be performed *dynamically*, i.e. based on the time evolution generated by a specific Hamiltonian, or *geometrically* as in holonomic quantum computing [38, 39]. Finally, a common feature of the quantum optical models is that read out of the atomic qubit is performed using the method of quantum jumps.

This chapter is arranged as follows: we start with a detailed description of trapped ions as a physical system to implement quantum computing in Sec. 2. This is followed by a Section on cavity QED which discusses optical interconnects between atoms as quantum memory and photons for transmission of quantum information. Finally, Sec. 3 discusses examples of two-qubit gates with neutral atoms based on cold coherent collisions and interaction between laser excited Rydberg atoms in electric fields.

#### B. Trapped Ions

In this section we give a theoretical description of quantum state engineering [40] and entanglement engineering [30, 41] in a system of trapped and laser cooled ions. The development of the theory starts with the description of Hamiltonians, state preparation, laser cooling and state measurements first for single ions, which is then generalized to the case of many ions. This serves as the basis of our discussion of quantum computer models [30, 33, 34, 38, 43, 44].

##### 1. The Model

##### 2. Single Trapped Ion

*Motional degrees of freedom:* We consider a single ion confined in a harmonic trap and interacting with laser light [40]. We assume that the lasers are directed along one of the principal axes of the harmonic potential, which allows us to consider ion motion in only one dimension. Hence, the Hamiltonian describing the free motion of the ion in the trap is

$$H_{0T} = \frac{\hat{p}^2}{2M} + \frac{1}{2}M\nu^2\hat{x}^2. \quad (18)$$

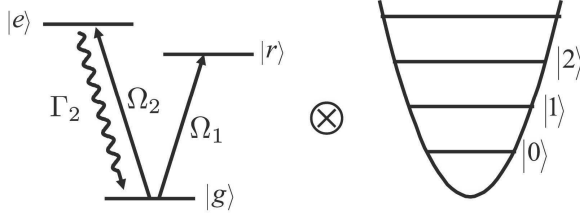


FIG. 3: Energy levels of an ion trap. Left: internal level structure with  $|g\rangle \rightarrow |r\rangle$  a metastable transition, and  $|g\rangle \rightarrow |e\rangle$  a strong dissipative transition coupled by Rabi frequencies  $\Omega_1$  and  $\Omega_2$ , respectively. Right: quantized energy levels in the harmonic trapping potential

Here  $\hat{x}$  and  $\hat{p}$  are the position and momentum operators respectively,  $M$  is the ion mass,  $\nu$  is the oscillation frequency (Fig. III B 2). We can rewrite this Hamiltonian in the familiar form  $H_{0T} = \nu(a^\dagger a + 1/2)$  with raising and lowering operators  $a$  and  $a^\dagger$ , defined according to  $\hat{x} = \sqrt{1/2M\nu}(a + a^\dagger)$  and  $\hat{p} = i\sqrt{M\nu/2}(a^\dagger - a)$  (we set  $\hbar = 1$ ).

*Internal degrees of freedom:* We assume that the internal electronic structure of the ion is modelled by a three-level system, with levels  $|g\rangle$ ,  $|e\rangle$  and  $|r\rangle$ , where the first transition  $|g\rangle \rightarrow |r\rangle$  is a dipole-forbidden, and  $|g\rangle \rightarrow |e\rangle$  is dipole-allowed (Fig. III B 2). In our model system we will employ the transition to the metastable state  $|r\rangle$  for *quantum state engineering*, while the strongly dissipative transition coupling  $|e\rangle$  to the ground state will be used for *laser cooling* and *state measurement*. These transitions can be excited by laser beams of frequencies close to the corresponding resonance frequencies. Obviously, emission or absorption of laser photons will modify the atomic motion. We confine our discussion to the Lamb-Dicke limit (LDL), i.e., to the limit where the ion motion is restricted to a region much smaller than the wavelength of the laser light exciting a given transition [48]. This allows us to expand the Hamiltonian describing the interaction of the ion with the laser light in terms of the Lamb-Dicke parameter  $\eta_i = 2\pi a_0/\lambda_i$ , where  $a_0 = 1/(2M\nu)^{1/2}$  is the size of the ground state of the harmonic potential, and  $\lambda_i$  is the wavelength of the laser light exciting transition  $i$ . We will now write out in details the Hamiltonians describing the coupling of the ion to laser light in the LDL.

*Dipole forbidden transition  $|g\rangle \rightarrow |r\rangle$  transition:* We first consider the situation in which only the laser driving the dipole-forbidden transition  $|g\rangle \rightarrow |r\rangle$  is on. We assume for the moment that the interaction time with the laser beam is much shorter than the lifetime of level  $|r\rangle$ , so that we can neglect dissipation. The corresponding Hamiltonian is

$$H_1 = H_{0T} + H_{0A_1} + H_{A_1L}, \quad (19)$$

where the first two terms are the bare trap and atomic Hamiltonian, and  $H_{A_1L}$  describes the interaction with

the laser. In a frame rotating with the laser frequency, we have  $H_{0A_1} = \delta_1|g\rangle\langle g|$  and

$$H_{A_1L} = \frac{1}{2}\Omega_1 \sin[\eta_1(a + a^\dagger) + \phi_1] (|r\rangle\langle g| + |g\rangle\langle r|) \quad (20)$$

$$H_{A_1L}^\pm = \frac{1}{2}\Omega_1 \{|r\rangle\langle g| \exp[\pm i\eta_1(a + a^\dagger)] + \text{h.c.}\}, \quad (21)$$

for standing-wave and travelling-wave configurations, respectively. Here,  $\delta_1 = \omega_{L_1} - \omega_{rg}$  is the laser detuning from the internal transition,  $\Omega_1$  is the Rabi frequency, and  $\eta_1$  is the Lamb-Dicke parameter for this particular transition. The index  $+$  ( $-$ ) denotes that the laser plane wave propagates in the positive (negative)  $x$  direction, while  $\phi_1$  defines the position of the center of the trap in the laser standing wave.

In lowest order in the Lamb-Dicke expansion we have

$$H_{A_1L} = \frac{1}{2}\Omega_1 \{|r\rangle\langle g| [\alpha_0 + \alpha_\pm(a + a^\dagger) + \mathcal{O}(\eta_1^2)] + \text{h.c.}\}. \quad (22)$$

where  $\alpha_0 = 1$ ,  $\alpha_\pm = \pm i\eta_1$  and  $\alpha_0 = \sin(\phi_1)$ ,  $\alpha_\pm = \eta_1 \cos(\phi_1)$  for a travelling and standing-wave configuration, respectively. The Hamiltonian (22) can be further simplified if the laser field is sufficiently weak so that only pairs of bare atom + trap levels are coupled resonantly. We denote by  $|n, g\rangle$  and  $|n, r\rangle$  the eigenstates of the bare Hamiltonian  $H_{0T} + H_{0A_1}$ , where the internal two-level system is in the ground (excited) state and  $n$  is the excitation number of the harmonic oscillator. These states are degenerate for  $\omega_{L_1} - \omega_{rg} = k\nu$  ( $k = 0, \pm 1, \dots$ ), i.e., whenever the laser is tuned to one of the “motional sidebands”, corresponding to a degeneracy between  $|n, g\rangle$  and  $|n+k, r\rangle$ . In the presence of the laser these degeneracies become avoided crossings, and for sufficiently weak laser excitation these avoided crossings will be isolated (non-overlapping). For example, for  $|\omega_{L_1} - \omega_{rg}| \ll \nu$ , i.e.  $k = 0$ , transitions changing the harmonic oscillator quantum number  $n$  are off-resonance and can be neglected. In this case the Hamiltonian (19) can be approximated by

$$H_0 = \nu a^\dagger a - \frac{1}{2}\delta_1 \sigma_z + \frac{1}{2}\Omega_1(\alpha_0 \sigma_+ + \text{h.c.}), \quad (23)$$

where we have used the spin- $\frac{1}{2}$  notation  $\sigma_+ = (\sigma_-)^\dagger = |r\rangle\langle g|$ ,  $\sigma_z = |r\rangle\langle r| - |g\rangle\langle g|$ . For laser frequencies close to the lower motional sideband resonance  $|\omega_{L_1} - (\omega_{rg} - \nu)| \ll \nu$  ( $k = -1$ ), only transitions decreasing the quantum number  $n$  by one are important, and  $H_1$  can be approximated by a Hamiltonian of the Jaynes-Cummings type:

$$H_{JC\pm} = \nu a^\dagger a - \frac{1}{2}\delta_1 \sigma_z + \frac{1}{2}\Omega_1(\alpha_\pm \sigma_+ a + \text{h.c.}). \quad (24)$$

Similarly, for  $|\omega_{L_1} - (\omega_{rg} + \nu)| \ll \nu$ , only transitions increasing the quantum number  $n$  by one ( $k = +1$ ) contribute, so that  $H_1$  can be approximated by the *anti*-Jaynes-Cummings Hamiltonian

$$H_{AJC\pm} = \nu a^\dagger a - \frac{1}{2}\delta_1 \sigma_z + \frac{1}{2}\Omega_1(\alpha_\pm \sigma_+ a^\dagger + \text{h.c.}). \quad (25)$$

(see Fig. III B 2) For the above approximations to be valid we require that the effective Rabi frequencies to the non-resonant states have to be much smaller than the trap frequency  $(\alpha_i \Omega_1 / \nu)^2 \ll 1$  ( $i = 0, \pm$ ). Note in particular that for an ion at the node of a standing light wave corrections to the JC Hamiltonian (24) are of the order  $(\eta_1 \Omega_1 / \nu)^2 \ll 1$ , i.e. the conditions of validity are greatly relaxed.

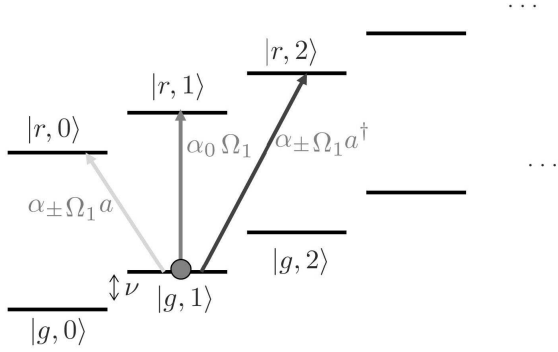


FIG. 4: Coupling to the atom + trap levels according to the Hamiltonians (23), (24 and (25, respectively, in lowest order Lamb-Dicke expansion.

Eigenstates of the Hamiltonians  $H_0$ ,  $H_{JC\pm}$  and  $H_{AJC\pm}$  are the dressed states familiar from cavity QED, which are obtained by diagonalizing the  $2 \times 2$  matrices of nearly degenerate states. Applying a laser pulse on resonance,  $\omega_{L_1} = \omega_{rg}$ , will according to (23) induce Rabi flopping between the states  $|n, g\rangle$  and  $|n, r\rangle$ , while a laser tuned for example to the lower motional sideband  $\omega_{L_1} = \omega_{rg} - \nu$  will lead to Rabi oscillations coupling  $|n, g\rangle$  and  $|n-1, r\rangle$ . The above Hamiltonians are the basic building blocks to engineer quantum states. As an example, Refs. [45, 46] give a protocol to build the general motional superposition states  $\sum_{n=0}^M c_n |g, n\rangle$  starting from the (pure) ground state  $|g, 0\rangle$ . The unitary operation effecting this transformation can be decomposed into unitary operations generated by the Hamiltonians (24) and (23), i.e. by applying a sequence of laser pulses with proper detunings and duration.

*The dipole-allowed transition  $|g\rangle \rightarrow |e\rangle$  transition:* For a laser beam exciting the dipole-allowed transition  $|g\rangle \rightarrow |e\rangle$  spontaneous emission is expected to play a significant role, and thus the dynamics must be described in terms of a master equation [47–49],

$$\dot{\rho} = -i[H_2, \rho] + \mathcal{L}_2 \rho. \quad (26)$$

In a rotating frame the Hamiltonian is  $H_2 = \nu a^\dagger a + \delta_2 |g\rangle\langle g| + H_{A_2L}$  with  $\delta_2 = \omega_{L_2} - \omega_{eg}$  laser detuning from the internal transition. The laser atom coupling  $H_{A_2L}$  has a structure analogous to (19) with the replacements  $|r\rangle \rightarrow |e\rangle$ , a Rabi coupling  $\Omega_2$ , position of the center of the trap in the laser standing wave  $\phi_2$ , and Lamb-Dicke parameter  $\eta_2$ . The dissipative part of the master

equation (26) can be written as [49]

$$\mathcal{L}_2 \rho = \Gamma_2 |g\rangle\langle g| \langle e| \tilde{\rho} |e\rangle - \frac{1}{2} \Gamma_2 (|e\rangle\langle e| \rho + \rho |e\rangle\langle e|), \quad (27)$$

where  $\Gamma_2$  is the spontaneous emission rate from level  $|e\rangle$ , and

$$\tilde{\rho} = \int_{-1}^1 du N(u) e^{-i\eta_2 u(a+a^\dagger)} \rho e^{i\eta_2 u(a+a^\dagger)}, \quad (28)$$

with  $N(u)$  the dipole emission pattern for spontaneous emission from  $|e\rangle$  to  $|g\rangle$ . For example, for a  $\Delta m_J = \pm 1$  transition,  $N(u) = 3/8(1+u^2)$ . Master equations of this type have been derived and studied in the context of laser cooling [47–49]. Physically speaking, Eqs. (26,27) describe the excitation of the atomic electron by the laser, which can either return to the ground state by either a laser induced process or by spontaneous emission. The emission of the spontaneous photon according to the angular distribution  $N(u)$  is accompanied by a momentum transfer to the atom, as described by the recycling term (28).

*Spontaneous emission and laser cooling to the motional ground state:* A prerequisite for many of the schemes for quantum engineering of nonclassical states of motion, or entangled atomic states is that the initial motional state of the ion is prepared in a well defined pure state, e.g., the ground state  $|0\rangle$  [30, 40]. The standard approach to preparing such a pure state of the atomic motion is sideband cooling [42].

The theoretical description is particularly simple in the Lamb-Dicke limit, where the separation of the time scale for the internal and external dynamics allows the adiabatic elimination of the internal degree of freedom [48]. For details of the calculations we refer to [49] and references cited therein. The physical picture of laser cooling in the Lamb-Dicke limit is as follows: in the rest frame of the ion, the ion “sees” a laser field consisting of a carrier at frequency  $\omega_{L_2}$  and small (motional) sidebands at frequencies  $\omega_{L_2} \pm \nu$ . Cooling occurs when absorption of laser photons from the upper laser sideband (at  $\omega_{L_2} + \nu$ ) is stronger than from the lower sideband, since the former absorption reduces the external energy, whereas the latter increases the external energy. Hence, laser cooling is particularly efficient in the strong confinement limit when one is able to tune the laser frequency in such a way that the upper laser sideband is on resonance with the two-level transition, since in this case only the photons of the upper sideband are absorbed, and consequently the ion ends up in the ground state of the harmonic trapping potential. This is the basic mechanism of *sideband cooling*. For many of the ions currently in use in Paul traps, the strong confinement condition  $\nu \gg \Gamma_2$  is not fulfilled for dipole-allowed transitions, and hence sideband cooling is not possible. However, employing auxiliary internal atomic levels and additional laser excitation allows one to effectively “design” two-level atoms for sideband cooling [42, 50].

*State measurement by the quantum jump technique:* Implementation of quantum computing and communication protocols require measurement of the internal state of the atom [30]. In an ion trap this can be achieved with essentially 100% efficiency using the method of quantum jumps [42, 47]. The theoretical understanding of quantum jumps is based on the continuous measurement theory, and we refer to [47] for a detailed mathematical description of the underlying theory. For our purpose it suffices to summarize the results as follows. Consider a *single* ion prepared initially in a superposition state on the metastable transition,  $\alpha|g\rangle + \beta|r\rangle$ . Switching on the laser on the strongly dissipative transition will give with probability  $|\alpha|^2$  a burst of photon emissions  $|e\rangle \rightarrow |g\rangle$  on the time scale  $1/\Gamma_2$ , or with probability  $|\beta|^2$  the appearance on an emission window on the strong line. Measuring an emission window, or no window thus corresponds to a projective measurement of  $|r\rangle$  or  $|g\rangle$ .

### 3. Ions in a linear trap

The above model is readily extended to describe a string of  $N$  ions in a linear trap [42] which is the basis of the ion trap '95 quantum computer proposal [30, 41] described below. A linear trap corresponds to a confinement of the motion along  $x, y$  and  $z$  directions in an (anisotropic) harmonic potential of frequencies  $\nu \equiv \nu_x \ll \nu_y, \nu_z$ . The equilibrium position of the ions will be given by the confining forces of the trapping potential balancing the Coulomb repulsion between the ions. If the ions have been previously laser cooled in all three dimensions they undergo small oscillations around these equilibrium position. In this case, the motion of the ions is described in terms of normal modes.

As an example, a 1D model for two ions in a linear trap with internal levels  $|g\rangle$  and  $|r\rangle$  and coupled to laser light is given by the following Hamiltonian

$$H = \nu a_{\text{cm}}^\dagger a_{\text{cm}} + \sqrt{3}\nu a_r^\dagger a_r - \delta_1 |r\rangle_{11} \langle r| - \delta_2 |r\rangle_{22} \langle r| \quad (29)$$

$$+ \frac{1}{2} \Omega_1(t) [|r\rangle_{11} \langle g| e^{-i\eta_{\text{cm}}(a_{\text{cm}} + a_{\text{cm}}^\dagger)} e^{-i\eta_r(a_r + a_r^\dagger)} + \text{h.c.}] \quad (30)$$

$$+ \frac{1}{2} \Omega_2(t) [|r\rangle_{22} \langle g| e^{-i\eta_{\text{cm}}(a_{\text{cm}} + a_{\text{cm}}^\dagger)} e^{+i\eta_r(a_r + a_r^\dagger)} + \text{h.c.}] \quad (31)$$

Here, the first line are the Hamiltonians for the harmonic collective oscillations of center-of-mass and stretch mode with oscillation frequency  $\nu$  and  $\sqrt{3}\nu$ , respectively, and the bare atomic Hamiltonian for the first and second ion in the rotating frame with  $\delta_{1,2}$  the laser detunings. The second and third line are the laser couplings to the ions with  $\Omega_{1,2}$  Rabi frequencies of the laser acting on each ion, respectively, and  $\eta_{\text{cm},r}$  are the corresponding Lamb-Dicke parameters. In the general case of  $N$  ions there will be a set of  $N$  collective modes of ion motion, where again the minimum frequency of collective mode oscillations is that of the center-of-mass (CM) mode in the  $x$ -direction  $\nu_x \equiv \nu$ , and the next frequency is the stretch mode  $\sqrt{3}\nu_x$ ,

and all the others are larger. It is an important feature for the quantum computer proposal below that the frequency spacing of the low lying modes is essentially *independent* of the number of ions  $N$  in the trap.

Our previous discussion of the Lamb-Dicke expansion of the Hamiltonian is readily extended to the string of  $N$  ions. In a similar way, we can model spontaneous emission of the ions by a master equation. In a typical experimental situation, the distance between the ions will be much larger than the optical wave length, so that the spontaneous emission of the ions is independent, and the master equation will contain a sum of the independent spontaneous emission terms of the ions of the form (27).

### 4. Ion trap quantum computer '95

As first proposed in Ref. [30],  $N$  cold ions interacting with laser light and moving in a linear trap provide a realistic physical system to implement a quantum computer. The distinctive features of this system are: (i) it allows the implementation of a complete set of quantum gates between any set of (not necessarily neighboring) ions; (ii) decoherence is comparatively small, and (iii) the final readout can be performed with essentially unit efficiency [41, 51–58].

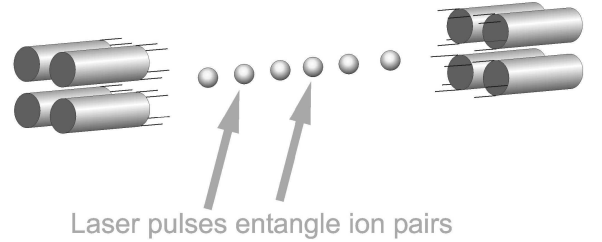


FIG. 5: Ion trap quantum computer (schematic).

Fig. III B 4 illustrates the basic setup. The qubits are represented by the long-lived internal states of the ions, with  $|g\rangle_j \equiv |0\rangle_j$  representing the ground state, and  $|r_0\rangle_j \equiv |1\rangle_j$  a metastable excited state ( $j = 1, \dots, N$ ). (In addition, we assume that there is a second metastable excited state  $|r_1\rangle$  which serves below the role of an auxiliary state.) In this system independent manipulation of each individual qubit is accomplished by addressing the ions with individual laser beams and inducing a Rabi rotation. The heart of the proposal is the implementation of a two-qubit gate between two (or more) arbitrary ions in the trap by exciting the collective quantized motion of the ions with lasers, i.e. the collective phonon mode plays the role of a quantum data bus. For this we assume that the collective phonon modes have been cooled to the ground state [52, 53].

Single qubit rotations can be performed tuning a laser on resonance with the internal transition ( $\delta_j = 0$ ) with

polarization  $q = 0$ . In an interaction picture the corresponding Hamiltonian is

$$\hat{H}_j = (\Omega/2) [ |r_0\rangle_j \langle g| e^{-i\phi} + |g\rangle_j \langle r_0| e^{i\phi} ]. \quad (32)$$

For an interaction time  $t = k\pi/\Omega$  (i.e., using a  $k\pi$  pulse), this process is described by the following unitary evolution operator

$$\hat{V}_j^k(\phi) = \exp \left[ -ik\frac{\pi}{2} (|e_0\rangle_j \langle g| e^{-i\phi} + h.c.) \right], \quad (33)$$

so that we achieve a Rabi rotation

$$\begin{aligned} |g\rangle_j &\rightarrow \cos(k\pi/2) |g\rangle_j - ie^{i\phi} \sin(k\pi/2) |r_0\rangle_j, \\ |r_0\rangle_j &\rightarrow \cos(k\pi/2) |r_0\rangle_j - ie^{-i\phi} \sin(k\pi/2) |g\rangle_j. \end{aligned}$$

If the laser addressing the  $j$ -th ion is tuned to the lower motional sideband of, for example, the center-of-mass mode, we have in the interaction picture the Hamiltonian

$$H_{j,q} = \frac{\eta}{\sqrt{N}} \frac{\Omega}{2} [ |r_q\rangle_j \langle g| a e^{-i\phi} + |g\rangle_j \langle r_q| a^\dagger e^{i\phi} ]. \quad (34)$$

Here  $a^\dagger$  and  $a$  are the creation and annihilation operator of CM phonons, respectively,  $\Omega$  is the Rabi frequency,  $\phi$  the laser phase, and  $\eta$  is the Lamb-Dicke parameter. The subscript  $q = 0, 1$  refers to the transition excited by the laser, which depends on the laser polarization. Equation (34) follows from the Hamiltonian for the case of a linear trap, similar to the derivation of (24). The factor  $\sqrt{N}$  appears since the effective mass of the CM motion is  $NM$ , and the amplitude of the mode scales like  $1/\sqrt{NM}$  (Mössbauer effect).

If this laser beam is on for a certain time  $t = k\pi/(\Omega\eta/\sqrt{N})$  (i.e., using a  $k\pi$  pulse), the evolution of the system will be described by the unitary operator:

$$\hat{U}_j^{k,q}(\phi) = \exp \left[ -ik\frac{\pi}{2} (|r_q\rangle_j \langle g| a e^{-i\phi} + h.c.) \right]. \quad (35)$$

It is easy to prove that this transformation keeps the state  $|g\rangle_j |0\rangle$  unaltered, whereas

$$\begin{aligned} |g\rangle_j |1\rangle &\rightarrow \cos(k\pi/2) |g\rangle_j |1\rangle - ie^{i\phi} \sin(k\pi/2) |r_q\rangle_j |0\rangle, \\ |r_q\rangle_j |0\rangle &\rightarrow \cos(k\pi/2) |r_q\rangle_j |0\rangle - ie^{-i\phi} \sin(k\pi/2) |g\rangle_j |1\rangle, \end{aligned}$$

where  $|0\rangle$  ( $|1\rangle$ ) denotes a state of the CM mode with no (one) phonon.

Let us now show how a two-bit gate can be performed using this interaction. We consider the following three-step process (see Fig. IIIB 4): (i) A  $\pi$  laser pulse with polarization  $q = 0$  and  $\phi = 0$  excites the  $m$ th ion. The evolution corresponding to this step is given by  $\hat{U}_m^{1,0} \equiv \hat{U}_m^{1,0}(0)$  (Fig. IIIB 4a). (ii) The laser directed on the  $n$ -th ion is then turned on for a time of a  $2\pi$ -pulse with polarization  $q = 1$  and  $\phi = 0$ . The corresponding evolution operator  $\hat{U}_n^{2,1}$  changes the sign of the state  $|g\rangle_n |1\rangle$  (without affecting the others) via a rotation through the auxiliary state  $|e_1\rangle_n |0\rangle$  (Fig. IIIB 4b). (iii)

Same as (i). Thus, the unitary operation for the whole process is  $\hat{U}_{m,n} \equiv \hat{U}_m^{1,0} \hat{U}_n^{2,1} \hat{U}_m^{1,0}$  which is represented diagrammatically as follows:

$$\begin{array}{ccccccc} & \hat{U}_m^{1,0} & & \hat{U}_n^{2,1} & & \hat{U}_m^{1,0} & \\ |g\rangle_m |g\rangle_n |0\rangle & \rightarrow & |g\rangle_m |g\rangle_n |0\rangle & \rightarrow & |g\rangle_m |g\rangle_n |0\rangle & \rightarrow & |g\rangle_m |g\rangle_n |0\rangle \\ |g\rangle_m |r_0\rangle_n |0\rangle & \rightarrow & |g\rangle_m |r_0\rangle_n |0\rangle & \rightarrow & |g\rangle_m |r_0\rangle_n |0\rangle & \rightarrow & |g\rangle_m |r_0\rangle_n |0\rangle \\ |r_0\rangle_m |g\rangle_n |0\rangle & \rightarrow & -i |g\rangle_m |g\rangle_n |1\rangle & \rightarrow & i |g\rangle_m |g\rangle_n |1\rangle & \rightarrow & |r_0\rangle_m |g\rangle_n |0\rangle \\ |r_0\rangle_m |r_0\rangle_n |0\rangle & \rightarrow & -i |g\rangle_m |r_0\rangle_n |1\rangle & \rightarrow & -i |g\rangle_m |r_0\rangle_n |1\rangle & \rightarrow & -|r_0\rangle_m |r_0\rangle_n |0\rangle \end{array} \quad (36)$$

The effect of this interaction is to change the sign of the state only when both ions are initially excited. Note that the state of the CM mode is restored to the vacuum state  $|0\rangle$  after the process. Equation (36) is phase gate  $|\epsilon_1\rangle |\epsilon_2\rangle \rightarrow (-1)^{\epsilon_1 \epsilon_2} |\epsilon_1\rangle |\epsilon_2\rangle$  ( $\epsilon_{1,2} = 0, 1$ ) which together with single qubit rotations becomes equivalent to a controlled-NOT.

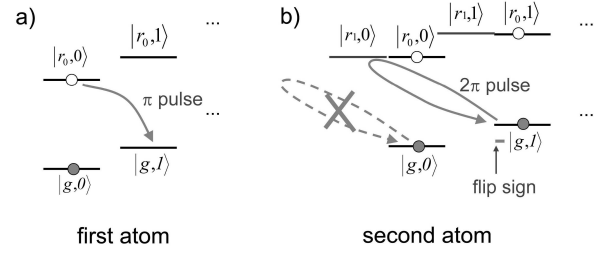


FIG. 6: The two-qubit quantum gate. a) First step according to (36): the qubit of the first atom is swapped to the photonic data bus with a  $\pi$ -pulse on the lower motional sideband, b) Second step: the state  $|g,1\rangle$  acquires a minus sign due to a  $2\pi$ -rotation via the auxiliary atomic level  $|r_1\rangle$  on the lower motional sideband.

Final readout of the quantum register (state measurement of the individual qubits) at the end of the computation can be accomplished using the quantum jumps technique with unit efficiency [42, 47].

The above proposal for the implementation of quantum computing with trapped ions has been the basis and has provided the stimulus for a significant body of experimental and theoretical work over the last few years [41, 51–58]. Highlights of the series of experimental work in particular by Chris Monroe and Dave Wineland at NIST Boulder [51, 52, 55–58], and Rainer Blatt at the University of Innsbruck [53, 54], are the implementation of a 2 qubit quantum gate with a single ion [51], ground state cooling of a string of ions [52, 53], addressing of single ions to perform single qubit operations [54], the generation of Bell states [58], and - as the most remarkable achievement - preparation of a maximally entangled state of four ions by the NIST Boulder group [56]. For a detailed discussion of the experimental situation we refer to the lecture notes by D. Wineland and R. Blatt in this volume. On theory side various extensions to finite temperature gates have been given, as well as schemes



which might allow faster gate operation times [33, 34, 59]. One of the most interesting contributions is a scheme by Mølmer and Sørensen [33] which allows preparation of a maximally entangled state of  $N$  ions with a single pulse without addressing the individual ions, as employed in the four-ion NIST experiment [56]. A quantum computer model based on geometric variants of the gate [39, 60, 61] was recently proposed by Duan *et al.* [38]. Error correction of the phonon data bus was studied in [62].

### 5. Ion trap quantum computer 2000

While in the ion trap '95 scheme a two-qubit gate was realized using the collective phonon mode as an auxiliary quantum degree of freedom, we describe now briefly a version on an ion trap computer where entanglement is achieved by designing an *internal-state dependent two-body interaction* between the ions [43, 44]. This proposal has the advantage being conceptually simpler (e.g. there is no zero temperature requirement), and obviously scalable. The model assumes that ions are stored in an *array of microtraps* (Fig. III B 5). Similar to the ion trap '95 proposal, it is assumed that long lived internal states of the ions serve as carriers of the qubits, and that single qubit operations can be performed by addressing ions with a laser.

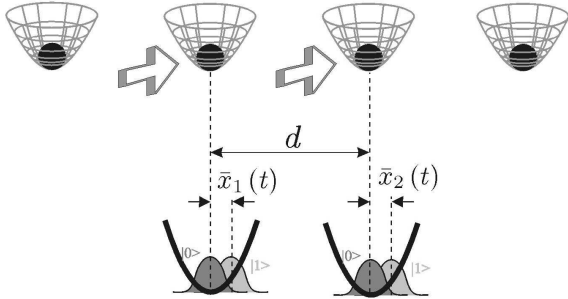


FIG. 7: Ions stored in an array of microtraps. By addressing two adjacent ions with an external field the ion wave packet is displaced conditional to its internal state.

The model assumes a set of  $N$  ions confined in independent harmonic potential wells separated by some constant distance  $d$ , where  $d$  is large enough so that: (i) the Coulomb repulsion is not able to excite the vibrational state of the ions; (ii) the ions can be individually addressed. Two-qubit gates between two neighboring ions can be performed by slightly displacing them for a short time  $T$  if they are in a particular internal state, say  $|1\rangle$ . In that case, and provided the ions come back to their original motional state after being pushed, the Coulomb interaction will provide the internal wave function (quantum register) with different phases depending on the internal states of the ions. Choosing the time

appropriately, the complete process will give rise to the two-qubit gate  $|\epsilon_1\rangle|\epsilon_2\rangle \rightarrow e^{i\epsilon_1\epsilon_2\phi}|\epsilon_1\rangle|\epsilon_2\rangle$ . In order to analyze this in a more quantitative way, we consider two ions 1 and 2 of mass  $m$  confined by two harmonic traps of frequency  $\omega$  in one dimension (Fig. III B 5). We denote by  $\hat{x}_{1,2}$  the position operators of the two ions. The potential seen by the ions is

$$V = \sum_{i=1,2} \frac{1}{2} m \omega^2 (\hat{x}_i - \bar{x}_i(t) |1\rangle_i \langle 1|)^2 + \frac{e^2}{4\pi\epsilon_0} \frac{1}{|d + \hat{x}_2 - \hat{x}_1|} \quad (37)$$

where  $\bar{x}_i(t)$  is the state dependent displacement induced by the force. We are interested in the limit, where the displacements are much smaller than the distance between the traps,  $|\hat{x}_{1,2}| \ll d$ , and where the Coulomb energy is small compared with the trapping potentials,  $\epsilon|\hat{x}_1\hat{x}_2|/a_0^2 \ll 1$ . Furthermore, we assume that the motional state of the pushed ions will change adiabatically with the potential. Expansion of the Coulomb term in powers of  $\hat{x}_{1,2}/d$  gives rise to a term  $-m\omega^2\epsilon\hat{x}_1\hat{x}_2$  in the potential (37). It is this term which is responsible for entangling the atoms, giving rise to a conditional phase shift, which can be simply interpreted as arising from the energy shifts due to the Coulomb interactions of atoms accumulated on different trajectories according to their internal states (Fig. III B 5),

$$\phi = -\frac{e^2}{4\pi\epsilon_0} \int_0^T dt \left[ \frac{1}{d + \bar{x}_2 - \bar{x}_1} - \frac{1}{d + \bar{x}_2} - \frac{1}{d - \bar{x}_1} + \frac{1}{d} \right],$$

where the four terms are due to atoms in  $|1\rangle_1|1\rangle_2$ ,  $|1\rangle_1|0\rangle_2$ ,  $|0\rangle_1|1\rangle_2$  and  $|0\rangle_1|0\rangle_2$ , respectively. The expression (III B 5) depends only on mean displacement of the atomic wavepacket and thus is insensitive to the temperature (the width of the wave packet) which will appear only in the problem in higher orders in  $x_{1,2}/d$  of our expansion of the potential (37), or in cases of non-adiabaticity. A detailed theory of this proposal including an analysis of imperfections has been given by Calarco *et al.* [44].

### C. Cavity QED

Cavity QED (CQED) realizes a situation where one or a few atoms interact strongly with a single quantized high-Q cavity mode, where the light field can be either in the optical or in the microwave domain (see the lecture notes by G. Rempe, S. Haroche and H. Walther). The coupling of atoms via the cavity mode can be used to engineer entanglement between the atoms [31, 32, 63–69]. The underlying physics is described by the Jaynes-Cummings Hamiltonian [47] which for a single two-level atom has the form

$$H = \frac{1}{2} \hbar \omega_0 \sigma_z + \hbar \omega_c a^\dagger a + \hbar \frac{1}{2} [\Omega_{eg}(\mathbf{r}) a^\dagger \sigma_- + \Omega_{eg}(\mathbf{r})^* \sigma_+ a], \quad (38)$$

where the  $\sigma$ 's are the Pauli spin operators describing the two-level atom, and  $a^\dagger$  and  $a$  are the boson creation and annihilation operators of the field mode, respectively. The term proportional to  $\Omega_0(\mathbf{r})$  in (38) describes the coherent oscillatory exchange of energy between the atom and the field mode. In optical cavity QED dissipation in this system due to spontaneous emission of the atom in the excited state, and cavity decay, which can be modeled by a master equation.

From a formal point of view there is a close analogy between the ion trap models discussed in the previous section and the Jaynes-Cummings type models of CQED, where the role of the collective phonon modes of trapped ions is now taken by photons in the high-Q cavity mode. Thus, in many cases schemes for quantum state and entanglement engineering proposed in the ion traps are readily translated to their CQED counterparts. A first example of a CQED model of a quantum computer is the scheme by Pellizzari *et al.* [31]. In this scheme atoms representing the qubits are stored in a high-Q cavity, and the photon mode in the cavity plays the role of an auxiliary quantum degree of freedom. This allows entanglement of pairs of atoms, where the specific feature of Ref. [31] is that photon exchange between atoms is performed using adiabatic passage along (the decoherence free subspace of) dark states, so that spontaneous emission as a decoherence channel is completely eliminated. On the other hand, CQED provides a natural interface between atoms as carriers of qubits and photons, which - once they leave the cavity - can be guided by optical fibers to transport qubits to distant locations. CQED thus serves as the paradigm for an *optical interconnect* between atoms as quantum memory and photons as carriers of qubits for quantum communication [32, 63].

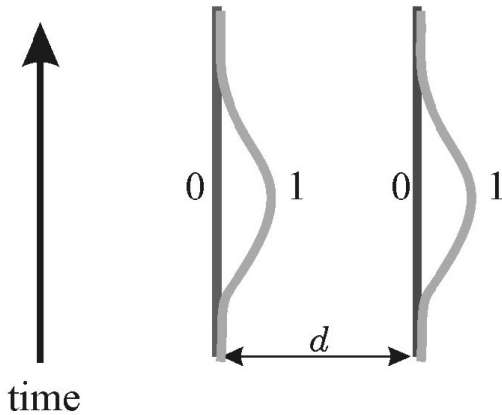


FIG. 8: Trajectories of the qubits as a function of time. Depending on the internal state different phases are accumulated.

### 1. Optical interconnects

The goal of quantum communications is to transmit an unknown quantum state from a first to a second node in a quantum network. We consider a situation where the state of a qubit is stored in internal state of atoms. The task is to transmit the qubit according to

$$(\alpha|0\rangle_1 + \beta|1\rangle_1) \otimes |0\rangle_2 \rightarrow |0\rangle_1 \otimes (\alpha|0\rangle_2 + \beta|1\rangle_2) \quad (39)$$

from the first to the second atom. Below we study a model of an optical interconnect based on storing atoms in high-Q optical cavities (see Fig. III C 1). By applying laser beams, one first transfers the internal state of an atom (qubit) at the first node to the optical state of the cavity mode. The generated photons leak out of the cavity, propagate as a wavepacket along the transmission line, and enter an optical cavity at the second node. Finally, the optical state of the second cavity is transferred to the internal state of an atom. Multiple-qubit transmissions can be achieved by sequentially addressing pairs of atoms (one at each node), as entanglements between arbitrarily located atoms are preserved by the state-mapping process.

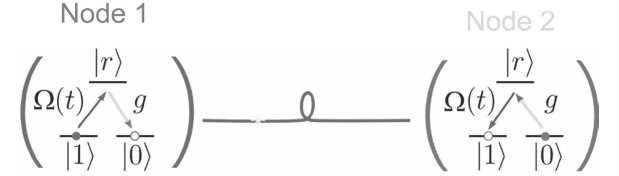


FIG. 9: Transmission of a qubit from an atom at the first node to an atom at the second node according to (39) and (41).

The distinguishing feature of the protocol described below [32] is that by controlling the atom-cavity interaction, one can absolutely avoid the reflection of the wavepackets from the second cavity, effectively switching off the dominant loss channel that would be responsible for decoherence in the communication process. For a physical picture of how this can be accomplished, let us consider that a photon leaks out of an optical cavity and propagates away as a wavepacket. Imagine that we were able to “time reverse” this wavepacket and send it back into the cavity; then this would restore the original (unknown) superposition state of the atom, provided we would also reverse the timing of the laser pulses. If, on the other hand, we are able to drive the atom in a transmitting cavity in such a way that the outgoing pulse were already symmetric in time, the wavepacket entering a receiving cavity would “mimic” this time reversed process, thus “restoring” the state of the first atom in the second one.

The simplest possible configuration of quantum transmission between two nodes consists of two three-level

atoms 1 and 2 which are strongly coupled to their respective cavity modes (see Fig. III C 1). The qubit is stored in a superposition of the two degenerate ground states  $|g\rangle \equiv |0\rangle$  and  $|e\rangle \equiv |1\rangle$ . The states  $|e\rangle$  and  $|g\rangle$  are coupled by a Raman transition, where a laser excites the atom from  $|e\rangle$  to  $|r\rangle$  with to a time-dependent Rabi frequency, followed by a transition  $|r\rangle \rightarrow |e\rangle$  which is accompanied by emission of a photon into the corresponding cavity mode. In order to suppress spontaneous emission from the excited state during the Raman process, we assume that the laser is strongly detuned from the atomic transition. In such a case, one can eliminate adiabatically the excited states  $|r\rangle$ . The Hamiltonian for the dynamics of the two ground states becomes, in a rotating frame for the cavity modes at the laser frequency, is of the Jaynes-Cummings form with time-dependent coupling  $g_i(t)$

$$\hat{H}_i = -\delta \hat{a}_i^\dagger \hat{a}_i - i g_i(t) [|e\rangle_i \langle g| a_i - \text{h.c.}], \quad (i = 1, 2) \quad (40)$$

where  $\hat{a}_i$  are the destruction operators for the cavity modes  $i = 1, 2$ , and  $\delta$  denotes the Raman detuning between the ground state levels. For simplicity we ignore here AC-Stark shifts of the ground states due to the cavity mode and laser field, which can be easily include in a complete model [32]. The last term is a Jaynes-Cummings interaction, with an effective time-dependent coupling constant  $g_i(t)$ .

The goal is now to select a laser pulse shape  $g_i(t)$  to accomplish *ideal quantum transmission*

$$(c_g |g\rangle_1 + c_e |e\rangle_1) |g\rangle_2 \otimes |0\rangle_1 |0\rangle_2 |\text{vac}\rangle \rightarrow |g\rangle_1 (c_g |g\rangle_2 + c_e |e\rangle_2) \otimes |0\rangle_1 |0\rangle_2 |\text{vac}\rangle, \quad (41)$$

where  $c_{g,e}$  are complex numbers. In (41),  $|0\rangle_i$  and  $|\text{vac}\rangle$  represent the vacuum state of the cavity modes and the free electromagnetic modes connecting the cavities. Transmission will occur by photon exchange via these modes.

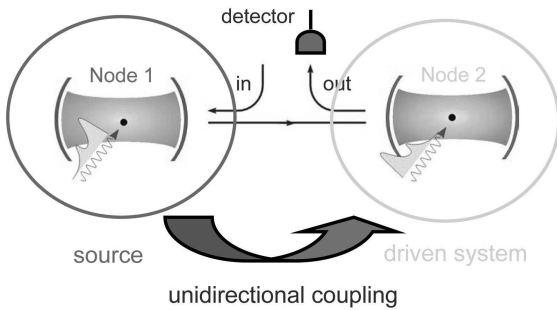


FIG. 10: Transmission of a qubit between two atoms as a cascaded quantum system

It is useful to formulate this problem in the language of cascaded quantum systems. A cascaded quantum system consists of a quantum *source* driving in a unidirectional coupling a quantum *system*. In our case the

source is the first node emitting a photon while the system is the second node (Fig. III C 1). In case of perfect transmission of the qubit we require that the photon is not reflected from the second cavity, and thus there is no back reaction on the first node, i.e. the coupling becomes unidirectional. A theory of cascaded quantum systems has been developed independently by Gardiner and Carmichael [47, 71, 72]. In the present context it is convenient to use a quantum trajectory formulation [47] of cascaded quantum system [72]. To this end, we consider a fictitious experiment where the output field of the second cavity is continuously monitored by a photodetector (Fig. III C 1). The evolution of the quantum system under continuous observation, conditional to observing a particular trajectory of counts, can be described by a pure state wavefunction  $|\Psi_c(t)\rangle$  in the system Hilbert space of the two nodes (where the radiation modes outside the cavity have been eliminated). During the time intervals when no count is detected, this wavefunction evolves according to a Schrödinger equation with *non-hermitian* effective Hamiltonian

$$\hat{H}_{\text{eff}}(t) = \hat{H}_1(t) + \hat{H}_2(t) - i\kappa \left( \hat{a}_1^\dagger \hat{a}_1 + \hat{a}_2^\dagger \hat{a}_2 + 2\hat{a}_2^\dagger \hat{a}_1 \right). \quad (42)$$

The detection of a count at time  $t_r$  is associated with a quantum jump according to  $|\Psi_c(t_r + dt)\rangle \propto \hat{c} |\Psi_c(t_r)\rangle$ , where  $\hat{c} = \hat{a}_1 + \hat{a}_2$ , while the probability density for a jump (detector click) to occur during the time interval from  $t$  to  $t + dt$  is  $\langle \Psi_c(t) | \hat{c}^\dagger \hat{c} | \Psi_c(t) \rangle dt$  [47].

We wish to design the laser pulses in both cavities in such a way that ideal quantum transmission condition (41) is satisfied. A necessary condition for the time evolution is that a quantum jump (detector click, see Fig. III C 1) never occurs, i.e.  $\hat{c} |\Psi_c(t)\rangle = 0 \forall t$ , and thus the effective Hamiltonian will become a hermitian operator. In other words, the system will remain in a *dark* state of the cascaded quantum system. Physically, this means that the wavepacket is not reflected from the second cavity. We expand the state of the system as

$$\begin{aligned} |\Psi_c(t)\rangle = & |c_g |gg\rangle |00\rangle_c \\ & + |c_e [\alpha_1(t) |eg\rangle |00\rangle_c + \alpha_2(t) |ge\rangle |00\rangle_c \\ & + \beta_1(t) |gg\rangle |10\rangle_c + \beta_2(t) |gg\rangle_c |01\rangle_c] \end{aligned} \quad (43)$$

Ideal quantum transmission (41) will occur for  $\alpha_1(-\infty) = \alpha_2(+\infty) = 1$ . We can now easily derive evolution equations for the amplitudes  $\alpha_i(t)$ ,  $\beta_i(t)$  ( $i = 1, 2$ ). Starting from these equations Cirac *et al.* derives a class of solutions for pulses shapes in analytical form, guided by the physical expectation that the time evolution in the second cavity should reverse the time evolution in the first one, i.e. one looks for solutions satisfying the *symmetric pulse condition*  $g_2(t) = g_1(-t)$ . Numerical examples and a discussion of imperfection due to photon loss and spontaneous emission can be found in the quoted references.

Motivated by this CQED scheme various transmission protocols have been discussed based on this *photonic*

channel [74, 75], including a protocol for a *quantum repeater* [4].

#### D. Collisional interactions for neutral atoms

In atomic physics with *neutral atoms* recent advances in cooling and trapping have led to an exciting new generation of experiments with Bose condensates, experiments with optical lattices, and atom optics and interferometry (see the lecture notes by E. Cornell and S. Rolston). The question therefore arises, to what extent these new experimental possibilities and the underlying physics can be adapted to the field of experimental quantum computing. In the previous section we have outlined possibilities of entangling neutral atoms in Cavity QED schemes. Here we will discuss two examples of entangling atoms directly using controlled two-body interactions. The specific examples to be discussed are cold coherent collisions between ground state atoms [35], and interaction of atoms via large dipole-dipole coupling of Rydberg atoms [37]. A scheme for entangling atoms with laser induced dipole-dipole interactions was proposed by G. K. Brennen *et al.* [36, 77, 78].

##### 1. Entanglement via coherent ground state collisions

Below we study coherent cold collisions [79] as the basic mechanism to entangle neutral atoms [35]. The picture of *atomic collisions as coherent interactions* has emerged in the field of Bose Einstein condensation (BEC) of (ultracold) gases. In a field theoretic language these interactions correspond to Hamiltonians which are quartic in the atomic field operators, analogous to Kerr nonlinearities between photons in quantum optics. By storing ultracold atoms in arrays of microscopic potentials provided, for example, by optical lattices these collisional interactions can be controlled via laser parameters [35]. Furthermore, these nonlinear atom-atom interactions can be large [35], even for interactions between individual pairs of atoms, thus providing the necessary ingredients to implement quantum logic.

Consider a situation where two atoms with electrons populating the internal states  $|a\rangle$  and  $|b\rangle$ , respectively, are trapped in the ground states  $\psi_0^{a,b}$  of two potential wells  $V^{a,b}$  (Fig. III D 1). Initially, these wells are centered at positions  $\bar{x}^a$  and  $\bar{x}^b$ , sufficiently far apart (distance  $d = \bar{x}_b - \bar{x}_a$ ) so that the particles do not interact. The positions of the potentials are moved along trajectories  $\bar{x}^a(t)$  and  $\bar{x}^b(t)$  so that the wavepackets of the atoms overlap for certain time, until finally they are restored to the initial position at the final time. This situation is described by the Hamiltonian

$$H = \sum_{\beta=a,b} \left[ \frac{(\hat{p}^\beta)^2}{2m} + V^\beta(\hat{x}^\beta - \bar{x}^\beta(t)) \right] + u^{ab}(\hat{x}^a - \hat{x}^b). \quad (44)$$

Here,  $\hat{x}^{a,b}$  and  $\hat{p}^{a,b}$  are position and momentum operators,  $V^{a,b}(\hat{x}^{a,b} - \bar{x}^{a,b}(t))$  describe the displaced trap potentials and  $u^{ab}$  is the atom-atom interaction term. Ideally, we would like to implement the transformation from before to after the collision,

$$\psi_0^a(x^a - \bar{x}^a) \psi_0^b(x^b - \bar{x}^b) \rightarrow e^{i\phi} \psi_0^a(x^a - \bar{x}^a) \psi_0^b(x^b - \bar{x}^b), \quad (45)$$

where each atom remains in the ground state of its trapping potential and preserves its internal state. The phase  $\phi$  will contain a contribution from the interaction (collision). The transformation (45) can be realized in the *adiabatic limit*, whereby we move the potentials slowly on the scale given by the trap frequency, so that the atoms remain in the ground state. Moving non-interacting atoms will induce kinetic single particle kinetic phases. In the presence of interactions ( $u^{ab} \neq 0$ ), we define the time-dependent energy shift due to the interaction as

$$\Delta E(t) = \frac{4\pi a_s \hbar^2}{m} \int dx |\psi_0^a(x - \bar{x}^a(t))|^2 |\psi_0^b(x - \bar{x}^b(t))|^2, \quad (46)$$

where  $a_s$  is the  $s$ -wave scattering length. We assume that  $|\Delta E(t)| \ll \hbar\nu$  with  $\nu$  the trap frequency so that no sloshing motion is excited. In this case, (45) still holds with  $\phi = \phi^a + \phi^b + \phi^{ab}$ , where in addition to (trivial) single particle kinetic phases  $\phi^a$  and  $\phi^b$  arising from moving the potentials, we have a *collisional phase shift*

$$\phi^{ab} = \int_{-\infty}^{\infty} dt \Delta E(t) / \hbar. \quad (47)$$

The assumption behind the *colliding atoms by hand*, as described above, is that different internal states of the atom see a different trapping non-dissipative potential. In practice, this can be achieved by trapping atoms in a far-off-resonant trap or optical lattice, where the lasers are tuned in such a way that the atomic states  $|a\rangle$  and  $|b\rangle$  couple differently to the excited atomic states, so that their AC Stark shifts differ. A specific laser configuration achieving this state dependent trapping has been analyzed in Ref. [35] for Alkali atoms, based on tuning

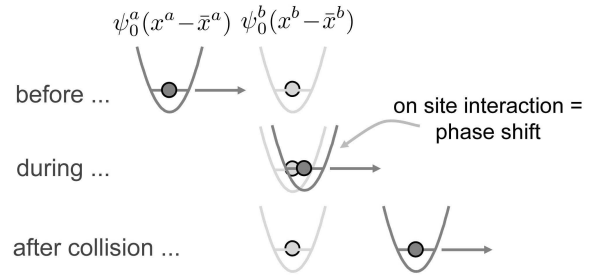


FIG. 11: We collide a first atom in the internal state  $|a\rangle$  with a second atom in state  $|b\rangle$ . In the collision the wave function accumulates a phase according to (45)

the laser between the fine structure excited states. The trapping potentials can be moved by changing the laser parameters. Such trapping potentials could also be realized with magnetic and electric microtraps [76].

So far, we have argued that one can use cold collisions as a coherent mechanism to induce phase shifts in two-atom interactions in a controlled way. We can use these interactions to implement conditional dynamics. By the above arguments, the atomic wave packet in a superposition of the two internal levels can be "split" by moving the state dependent potentials, very much like a beam splitter in atom interferometry. Thus we can move the potentials of neighboring atoms such that only the  $|a\rangle$  component of the first atom "collides" with the state  $|b\rangle$  of the second atom

$$\begin{aligned} |a\rangle_1|a\rangle_2 &\rightarrow e^{i2\phi^a}|a\rangle_1|a\rangle_2, \\ |a\rangle_1|b\rangle_2 &\rightarrow e^{i(\phi^a+\phi^b+\phi^{ab})}|a\rangle_1|b\rangle_2, \\ |b\rangle_1|a\rangle_2 &\rightarrow e^{i(\phi^a+\phi^b)}|b\rangle_1|a\rangle_2, \\ |b\rangle_1|b\rangle_2 &\rightarrow e^{i2\phi^b}|b\rangle_1|b\rangle_2, \end{aligned} \quad (48)$$

where the motional states remain unchanged in the adiabatic limit, and  $\phi^a$  and  $\phi^b$  are single particle kinetic phases. The transformation (48) corresponds to a fundamental two-qubit gate. The fidelity of this gate is limited by nonadiabatic effects, decoherence due to spontaneous emission in the optical potentials and collisional loss to other unwanted states, or collisional to unwanted states. According to Ref. [35] the fidelity of this gate operation is remarkably close to one in a large parameter range. We note that loading of single atoms in laser traps has been achieved recently [81], and movable arrays of trapping potential have been created with arrays of microlenses [82]. Finally, by filling the lattice from a Bose condensate, and using the ideas related to Mott transitions in optical lattices [80] it is possible to achieve uniform lattice occupation ("optical crystals") or even specific atomic patterns, as well as the low temperatures necessary for performing the experiments proposed above.

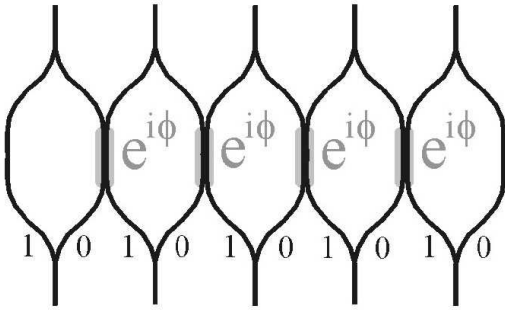


FIG. 12: By moving an optical lattice in a state-dependent way neighboring atoms collide and acquire a phase shift.

It is interesting to generalize these ideas to the dynamics of a two-component Bose gas in an optical lattice. For example, in the adiabatic regime we denote by  $a_i$  and  $b_i$  the annihilation operators for a particle in the ground state of the potential centered at the position  $i$ , and corresponding to the internal levels  $|a\rangle$  and  $|b\rangle$ , respectively. The effective Hamiltonian in this regime is a time dependent Bose-Hubbard model [80],

$$H = \sum_i \left[ \omega^a(t) a_i^\dagger a_i + \omega^b(t) b_i^\dagger b_i + u^{aa}(t) a_i^\dagger a_i^\dagger a_i a_i + u^{bb}(t) b_i^\dagger b_i^\dagger b_i b_i \right] + \sum_{i,j} u_{ij}^{ab}(t) a_i^\dagger a_i b_j^\dagger b_j, \quad (49)$$

where the  $\omega$ 's and  $u$ 's depend on the specific way the potentials are moved. In quantum optics this Hamiltonian corresponds to a quantum non-demolition situation [47], whereby the particle number can be measured non-destructively.

## 2. Rydberg atoms

Entanglement via cold coherent collisions, as described above, requires moving atoms and accumulating a phase due to (comparatively small) onsite interactions, which makes this a slow process. For neutral atoms there is a difficulty in identifying *strong and controllable long-range two-body interactions*, which is required to design a gate. Furthermore, the strength of two-body interactions does not necessarily translate into a useful fast quantum gate: large interactions are usually associated with strong mechanical forces on the trapped atoms. Thus, internal states of the trapped atoms (the qubits) may become entangled with the motional degrees of freedom during the gate, resulting effectively in an additional source of decoherence. This leads to the typical requirement that the process is *adiabatic* on the time scale of the oscillation period of the trapped atoms in order to avoid entanglement with motional states. As a result, extremely tight traps and low temperatures are required. A fast two-qubit phase gate for neutral trapped atoms, which addresses these problems, was proposed in Ref. [35]. The scheme is based on (i) the very large interactions of permanent dipole moments of laser excited Rydberg states in a constant electric field to entangle atoms, and (ii) allows gate operation times set by the time scale of the laser excitation or the two particle interaction energy, which can be significantly shorter than the trap period. Among the attractive features of the gate are the insensitivity to the temperature of the atoms and to the variations in atom-atom separation.

Rydberg states [84] of a hydrogen atom within a given manifold of a fixed principal quantum number  $n$  are degenerate. This degeneracy is removed by applying a constant electric field  $\mathcal{E}$  along the  $z$ -axis (linear Stark effect). For electric fields below the Inglis-Teller limit the mixing of adjacent  $n$ -manifolds can be neglected,

and the energy levels are split according to  $\Delta E_{nqm} = 3nqea_0\mathcal{E}/2$  with parabolic and magnetic quantum numbers  $q = n - 1 - |m|, n - 3 - |m|, \dots, -(n - 1 - |m|)$  and  $m$ , respectively,  $e$  the electron charge, and  $a_0$  the Bohr radius. These Stark states have permanent dipole moments  $\mu \equiv \mu_z \mathbf{e}_z = 3/2 nqea_0 \mathbf{e}_z$ . In alkali atoms the  $s$  and  $p$ -states are shifted relative to the higher angular momentum states due to their quantum defects, and the Stark maps of the  $m = 0$  and  $m = 1$  manifolds are correspondingly modified [84].

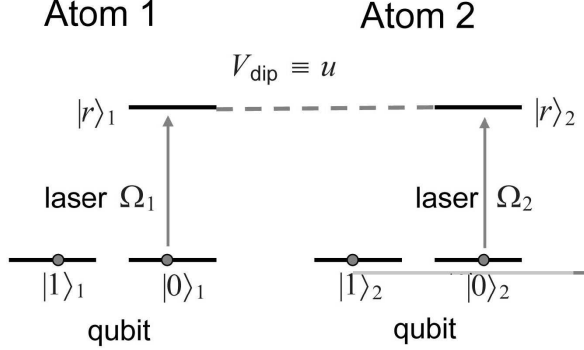


FIG. 13: Atomic level scheme of the two-qubit gate. The laser excites the atoms in state  $|1\rangle$  to Rydberg states in an electric field. The Rydberg states interact via a dipole-dipole interaction.

Let us consider two atoms 1 and 2 initially prepared in Rydberg Stark eigenstates, with a dipole moment along  $z$  and a given  $m$ , as selected by the polarization of the exciting laser. They interact and evolve according to the dipole-dipole potential

$$V_{\text{dip}}(\mathbf{r}) = \frac{1}{4\pi\epsilon_0} \left[ \frac{\mu_1 \cdot \mu_2}{|\mathbf{r}|^3} - 3 \frac{(\mu_1 \cdot \mathbf{r})(\mu_2 \cdot \mathbf{r})}{|\mathbf{r}|^5} \right], \quad (50)$$

with  $\mathbf{r}$  the distance between the atoms. We are interested in the limit where the electric field is sufficiently large so that the energy splitting between two adjacent Stark states is much larger than the dipole-dipole interaction. For two atoms in the given initial Stark eigenstate, the diagonal terms of  $V_{\text{dip}}$  provide an energy shift whereas the non-diagonal terms couple  $(m, m) \rightarrow (m \pm 1, m \mp 1)$  adjacent  $m$  manifolds with each other. We will assume that these transitions are suppressed by an appropriate choice of the initial Stark eigenstate. For a hydrogen state  $|r\rangle = |n, q = n - 1, m = 0\rangle$ , for example, and we find for a fixed distance  $\mathbf{r} = R\mathbf{e}_z$  of the two atoms a dipole-dipole interaction  $u(R) = \langle r | V_{\text{dip}}(R\mathbf{e}_z) | r \rangle \otimes | r \rangle$  with  $u(R) = -9[n(n-1)]^2(a_0/R)^3(e^2/8\pi\epsilon_0 a_0) \propto n^4$ . In alkali atoms we have to replace  $n$  by the effective quantum number  $\nu$  [84]. We will use this large energy shift to entangle atoms.

We study a configuration where two atoms are for the moment assumed to be at fixed positions  $\mathbf{x}_j$  (with  $j = 1, 2$  labelling the atoms), at a distance at a distance

$R = |\mathbf{x}_1 - \mathbf{x}_2|$ . We store qubits in two internal atomic ground states denoted by  $|g\rangle_j \equiv |0\rangle_j$  and  $|e\rangle_j \equiv |1\rangle_j$ . The ground states  $|g\rangle_j$  are coupled by a laser to a given Stark eigenstate  $|r\rangle_j$ . The internal dynamics is described by a model Hamiltonian

$$H^i(t, \mathbf{x}_1, \mathbf{x}_2) = u |r\rangle_1 \langle r| \otimes |r\rangle_2 \langle r| + \sum_{j=1,2} \left[ (\delta_j(t) - i\gamma) |r\rangle_j \langle r| - \frac{1}{2} \Omega_j(t, \mathbf{x}_j) (|r\rangle_j \langle g| + |g\rangle_j \langle r|) \right]$$

Here  $\Omega_j(t, \mathbf{x}_j)$  are Rabi frequencies,  $\delta_j(t)$  are the detunings of the exciting lasers, and  $\gamma$  accounts for loss from the excited states  $|r\rangle_j$ .

When we include the atomic motion, the complete Hamiltonian has the structure

$$H(t, \hat{\mathbf{x}}_1, \hat{\mathbf{x}}_2) = H^T(\hat{\mathbf{x}}_1, \hat{\mathbf{x}}_2) + H^i(t, \hat{\mathbf{x}}_1, \hat{\mathbf{x}}_2) \quad (51)$$

$$\equiv H^e(t, \hat{\mathbf{x}}_1, \hat{\mathbf{x}}_2) + H^i(t, \mathbf{x}_1, \mathbf{x}_2), \quad (52)$$

where  $H^T$  describes the motion of the trapped atoms, and  $\hat{\mathbf{x}}_j$  are the atomic position operators, and we define  $\hat{\mathbf{r}} = \hat{\mathbf{x}}_1 - \hat{\mathbf{x}}_2$ . Our goal is to design a phase gate for the internal states with a gate operation time  $\Delta t$  with the internal Hamiltonian  $H^i(t, \mathbf{x}_1, \mathbf{x}_2)$  in Eq. (51), where (the c-numbers)  $\mathbf{x}_j$  now denote the centers of the initial atomic wave functions as determined by the trap, while avoiding motional effects arising from  $H^e(t, \hat{\mathbf{x}}_1, \hat{\mathbf{x}}_2)$ . This requires that the gate operation time  $\Delta t$  is short compared to the typical time of evolution of the external degrees of freedom,  $H^e \Delta t \ll 1$ . Under this condition, the initial density operator of the two atoms evolves as  $\rho_e \otimes \rho_i \rightarrow \rho_e \otimes \rho'_i$  during the gate operation. Thus the motion described by  $\rho_e$  does not become entangled with the internal degrees of freedom given by  $\rho_i$ . Typically, the Hamiltonian  $H^T$  will be the sum of the kinetic energies of the atoms and the trapping potentials for the various internal states. We will assume that the potentials are harmonic with a frequency  $\omega$  for the ground states, and  $\omega'$  for the excited state.

Physically, for the splitting of the Hamiltonian according to Eq. (51) to be meaningful we require the initial width of the atomic wave function  $a$ , as determined by

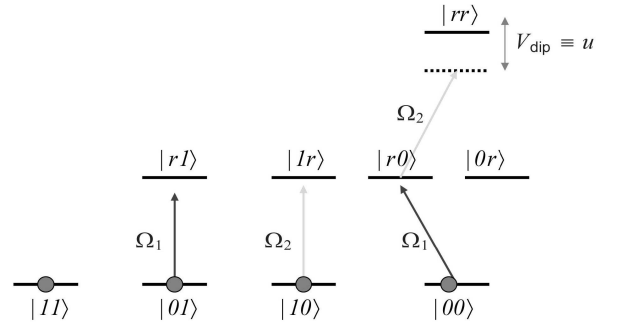


FIG. 14: Laser excitation sequence of the dipole-dipole gate with Rydberg atoms. Qubits are stored in two internal atomic ground states denoted by  $|0\rangle_j$  and  $|1\rangle_j$ .

the trap, to be much smaller than the mean separation between the atoms  $R$ . We expand the dipole-dipole interaction around  $R$ ,  $V_{\text{dip}}(\hat{\mathbf{r}}) = u(R) - F(\hat{\mathbf{r}}_z - R) + \dots$ , with  $F = 3u(R)/R$ . Here the first term gives the energy shift if both atoms are excited to state  $|r\rangle$ , while the second term contributes to  $H^e$  and describes the mechanical force on the atoms due to  $V_{\text{dip}}$ . Other contributions to  $H^e$  arise from the photon kick in the absorption  $|g\rangle \rightarrow |r\rangle$ , but these terms can be suppressed in a Doppler-free two photon absorption, for example. We obtain  $H^e(\hat{\mathbf{x}}_1, \hat{\mathbf{x}}_2) = H^T - F(\hat{\mathbf{r}}_z - R)|r\rangle_1\langle r| \otimes |r\rangle_2\langle r|$ .

We can study our model for a phase gate according to dynamics induced by  $H^i$  in various parameter regimes. First, in the limit  $\Omega_j \gg u$ , it is possible to perform a gate by exciting the Rydberg atoms with  $\pi$ -pulses, so that the state  $|r\rangle_1|r\rangle_2$  picks up the extra phase  $\varphi = u\Delta t$  from the dipole-dipole interaction. Thus, this scheme realizes a fast phase gate operating on the time scale  $\Delta t \propto 1/u$ . We note, however, that the accumulated phase depends on the precise value of  $u$ , i.e. is sensitive to the atomic distance. In addition, during the gate operation there are large mechanical effects due to the force  $F$ .

These problems can be avoided by operating the gate in the parameter regime  $u \gg \Omega_j$ . In the simplest case we assume that the two atoms can be addressed individually, i.e.  $\Omega_1(t) \neq \Omega_2(t)$ . We set  $\delta_j = 0$  and perform the gate operation in three steps: (i) We apply a  $\pi$ -pulse to the first atom, (ii) a  $2\pi$ -pulse (in terms of the unperturbed states, i.e. it has twice the pulse area of pulse applied in (i)) to the second atom, and, finally, (iii) a  $\pi$ -pulse to the first atom. As can be seen from Fig. III D 2, the state  $|ee\rangle$  is not affected by the laser pulses. If the system is initially in one of the states  $|ge\rangle$  or  $|eg\rangle$  the pulse sequence (i)-(iii) will cause a sign change in the wave function. If the system is initially in the state  $|gg\rangle$  the first pulse will bring the system to the state  $i|rg\rangle$ , the second pulse will be *detuned* from the state  $|rr\rangle$  by the interaction strength  $u$ , and thus accumulate a *small* phase  $\tilde{\varphi} \approx \pi\Omega_2/2u \ll \pi$ . The third pulse returns the system to the state  $e^{i(\pi-\tilde{\varphi})}|gg\rangle$ , which realizes a phase gate with  $\varphi = \pi - \tilde{\varphi} \approx \pi$  (up to trivial single qubit phases). The time needed to perform the gate operation is of the order  $\Delta t \approx 2\pi/\Omega_1 + 2\pi/\Omega_2$ . It is possible to formulate an *adiabatic* version of this gate with the advantage that individual addressing of the two atoms is not required,  $\Omega_{1,2}(t) \equiv \Omega(t)$  and  $\delta_{1,2}(t) \equiv \delta(t)$ .

A remarkable feature of the second model is that, in the ideal limit, the doubly excited state  $|rr\rangle$  is never populated, because the double excited state is shifted by the large dipole-dipole interaction, i.e. we have a dipole-blockade mechanism (reminiscent of the Coulomb blockade in quantum dots). Hence, the mechanical effects due to atom-atom interaction are greatly suppressed. Furthermore, this version of the gate is only weakly sensitive to the exact distance between the atoms, since the distance-dependent part of the entanglement phase  $\tilde{\varphi} \ll \pi$ .

We now turn to a discussion of decoherence mecha-

nisms, which include spontaneous emission, transitions induced by black body radiation, ionization of the Rydberg states due to the trapping or exciting laser fields, and motional excitation of the trapped atoms. While dipole-dipole interaction increases with  $\nu^4$ , the spontaneous emission and ionization of the Rydberg states by optical laser fields decreases proportional to  $\nu^{-3}$ . The Rabi frequency coupling the ground to the Rydberg states scales as  $n^{-3/2}$ . For  $\nu < 20$  the black body radiation is negligible in comparison with spontaneous emission, and similar conclusions hold for typical ionization rates from the Rydberg states. For typical numbers one expects errors on the percent level [35].

## IV. QUANTUM INFORMATION PROCESSING WITH ATOMIC ENSEMBLES

### A. Introduction

In the previous chapter, all the schemes for quantum information processing are based on laser manipulation of single trapped particles. In this chapter, we will show that many quantum information protocols can also be implemented simply by laser manipulation of atomic ensembles containing a large number of identical neutral atoms (see also the lecture notes by M. Fleischhauer). The experimental candidate systems for the atomic ensembles can be either laser-cooled atoms confined in a magnetic optical trap [85–88], or room-temperature atoms contained in a glass cell with coated walls to avoid bad collisions [89–91]. Quantum information is stored in the ground-state manifold of the atoms, such as in Zeeman sublevels with different atomic spins, or in some hyperfine atomic levels which are stable or metastable under optical transitions. Long coherence time of the relevant states has been observed in both kinds of the experimental systems mentioned above [85–91]. The motivation of using atomic ensembles instead of single-particles for quantum information processing is three-folds: first, laser manipulation of atomic ensembles without separate addressing of individual atoms is much easier than the laser manipulation of single particles; Secondly, the quantum information encoded in atomic ensembles is robust against some practical noise. For instance, the loss of few atoms in a large atomic ensemble has negligible influence on its carried quantum information; Finally and perhaps most importantly, the use of the atomic ensembles provides a novel way for enhancing the signal-to-noise ratio with some collective effects existing in this system. We know that in physical implementations of quantum information protocols, the central problem is to enhance the signal-to-noise ratio, that is, to enhance the ratio of the magnitudes between the coherent information processing and the decoherence process caused by the noisy coupling to the environment. For instance, in cavity-QED schemes, one needs to build a high-finesse cavity around the atoms to achieve strong light-atom coupling, and

needs to enter the challenging strong coupling regime for a high signal-to-noise ratio. However, we will see that due to the collective enhancement induced by the many-atom coherence, the signal-to-noise ratio in atomic ensembles can be greatly increased by encoding quantum information into some collective excitations of the ensembles. As a result of this effect, quantum information processing is made possible with much simplified experimental systems, such as atomic ensemble in weak-coupling cavities or even in free space.

This chapter is arranged as follows: In Sec. 4.2, we describe the interaction of light with atomic ensembles with various level configurations. Our attention is focused on collective enhancement of the signal-to-noise ratio in these systems. For simple demonstration of the collective enhancement, in the first two level configurations we assume that there is a weak-coupling cavity around the atomic ensemble, following the approaches in Refs. [92–95]; and in the last level configuration, we directly describe the interaction of light with a free-space atomic ensemble using a one-dimensional light propagation model, following the approaches in Refs. [96–98]. Some discussions on the three-dimensional light propagation effects can be found in Ref. [99]. In these two different approaches, one can find basically the same kind of collective enhancement of the signal-to-noise ratio. The systems discussed in Sec. 4.2 provide the basic elements for physical implementation of many quantum information protocols. In Sec. 4.3, we show how to use atomic ensembles combined with linear optical elements to realize scalable long-distance quantum communication, such as quantum key distribution, quantum teleportation, and Bell-inequality detections. Long-distance quantum communication is necessarily based on the use of photonic channels. However, due to losses and decoherence in the channel, the communication fidelity decreases exponentially with the channel length. To overcome the problem associated with the exponential fidelity decay, one needs to use quantum repeaters [4], which provide the only known way for robust long-distance quantum communication. In Sec. 4.3, we review the recent scheme proposed in Ref. [95] for physical implementation of quantum repeaters and robust quantum communication over long lossy channels. The scheme involves laser manipulation of atomic ensembles, beam splitters, and single-photon detectors with moderate efficiencies, and therefore well fits the status of the current experimental technology. The communication efficiency in this scheme scales polynomially with the channel length thereby facilitating scalability to very long distances. In Sec. 4.4, we investigate other applications of atomic ensembles in quantum information processing. In particular, we show that atomic ensembles can be used to realize quantum light memory [93, 94, 97, 100] and single-photon sources with controllable emission time, direction, and pulse shape. Quantum light memory and a controllable single-photon source provide the basic elements for realization of a recent quantum computation scheme [101]. Another quan-

tum computation scheme using atomic ensembles was proposed in Ref. [102], which combines laser manipulation of atomic ensembles with the idea of dipole blockades from Rydberg atoms. In that scheme, one needs to exploit direct dipole-dipole interactions between atoms which are induced by exciting atoms to high Rydberg levels. This scheme will not be investigated in this review since the concept of direct atom-atom interaction is outside the scope of the current chapter. In Sec. 4.5, we review the applications of atomic ensembles in continuous variable quantum information processing. Laser manipulation of atomic ensembles provides a simple way for realizing continuous variable quantum teleportation between distant atomic ensembles [98]. Probabilities of using atomic ensembles for realizing continuous variable quantum computation are also briefly remarked.

## B. Interaction of light with atomic ensembles and collective enhancement of the signal-to-noise ratio

We consider in the following the interaction of propagating light with atomic ensembles. In particular, we demonstrate that when a sample of identical atoms with suitable level configurations are shined by a propagating optical signal, the signal will only interact with the (symmetric) collective atomic mode, whereas atomic spontaneous emissions caused by the coupling to vacuum noise fields are distributed over all the modes. As a result of this property, the signal-to-noise ratio for the collective atomic mode can be greatly enhanced. We consider three types of level configurations for the atoms: two  $\Lambda$ -level configurations with different kinds of coupling to the signal light and one four-level configuration. All these level schemes are useful in subsequent sections for different purposes of quantum information processing. In all these schemes, besides the propagating quantum signal, there is some driving field provided by a classical laser. We always assume that the classical driving field and the quantum signal are co-propagating to assure a collective coupling condition. For a simple demonstration of the collective enhancement of the signal-to-noise ratio, first in the two  $\Lambda$ -level configurations we assume that there is a low-Q ring cavity around the ensemble, and a ring cavity mode, driven by the input and output quantum light signal, is then coupled to a desired atomic transition. Due to the collective enhancement, we can get a large signal-to-noise ratio even without a cavity to enhance the light-atom coupling. As an example to explicitly show this, in the four-level configuration we assume interaction of quantum light with free-space atomic ensembles under a one-dimensional light propagation model. The result confirms that we have the same kind of collective enhancement in the signal-to-noise ratio.



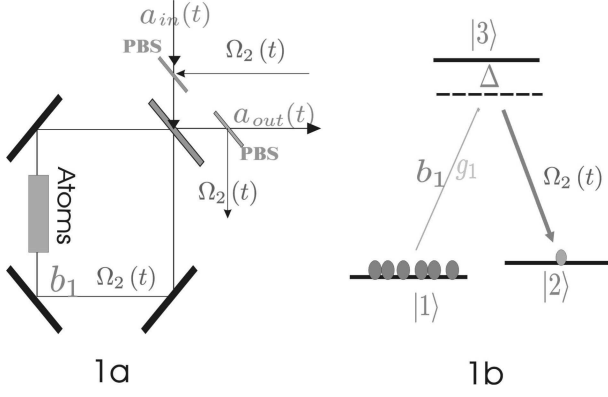


FIG. 15: (1a) An atomic ensemble in a weak coupling cavity. (1b) The  $\Lambda$ -level configuration.

### 1. $\Lambda$ -level configuration

In the first level configuration, we assume that the atoms have two ground states  $|1\rangle$ ,  $|2\rangle$  and one excited state  $|3\rangle$  (see Fig. IV B 1). All the atoms initially occupy the ground level  $|1\rangle$ . The transition  $|1\rangle \rightarrow |3\rangle$  is coupled with a coupling coefficient  $g_1$  to a ring cavity mode  $b_1$ , which is then driven by the input and output quantum signals  $a_{in}(t)$  and  $a_{out}(t)$ . The transition  $|3\rangle \rightarrow |2\rangle$  is driven by a classical laser field with a Rabi frequency  $\Omega_2$  ( $\Omega_2$  can be time-dependent). The driving laser and the ring cavity mode (quantum signal) are copropagating to satisfy the collective coupling condition  $(k_l - k_s)L_a \ll \pi$ , where  $k_l$  and  $k_s$  are respectively the wave vectors of the laser and the quantum signal, and  $L_a$  is the length of the atomic ensemble. We assume off resonant coupling with a large detuning  $\Delta$  as shown in Fig. IV B 1. This level scheme has been considered in Refs. [93, 94, 97, 100] for quantum light memory (Refs. [93, 97] considered this level scheme with resonant coupling). Here we follow Ref. [94] for a simple theoretical description. A description of the resonant coupling based on dark states can be found in Refs. [93, 103], and a free-space description of this level scheme with the one-dimensional light propagation model can be found in Refs. [97].

In the case of a large detuning  $\Delta$ , we can adiabatically eliminate the excited level  $|3\rangle$ , and under the collective coupling condition, the interaction shown in Fig. IV B 1 is described by the following Hamiltonian in the rotating frame

$$H = \hbar (\Omega_2 g_1 / \Delta) b_1^\dagger \sum_{i=1}^{N_a} \sigma_{12}^i + \text{h.c.}, \quad (53)$$

where  $N_a$  is the total atom number, and  $\sigma_{12}^i = |1\rangle_i \langle 2|$  is the atomic lowering operator for the  $i$ th atom. We have neglected the light shift terms such as  $(\Omega_2 / \Delta)^2 \sum_{i=1}^{N_a} \sigma_{22}^i$  in Eq. (53), which can be trivially cancelled by refining the laser frequency. We assume that the quantum signal is weak so that nearly all the atoms still remain in

the level  $|1\rangle$  with  $\langle |1\rangle_i \langle 1| \rangle \simeq 1$ . Under this weak excitation condition, we introduce an effective bosonic operator  $s = \sum_{i=1}^{N_a} \sigma_{12}^i / \sqrt{N_a}$  with  $[s, s^\dagger] \simeq 1$  for the (symmetric) collective atomic mode. With the collective atomic operator, the Heisenberg-Langevin equations corresponding to the Hamiltonian (1) has the form [47]

$$\dot{s} = -i \left( \sqrt{N_a} \Omega_2 g_1^* / \Delta \right) b_1, \quad (54)$$

$$\dot{b}_1 = -i \left( \sqrt{N_a} \Omega_2 g_1 / \Delta \right) s - (\kappa/2) b_1 - \sqrt{\kappa} a_{in}(t) \quad (55)$$

where  $\kappa$  is the cavity decay rate, and  $a_{in}(t)$  is the input quantum signal with the properties  $[a_{in}(t), a_{in}^\dagger(t')] = \delta(t - t')$ . The output quantum signal  $a_{out}(t)$  from the cavity is connected with the input by the input-output relation  $a_{out}(t) = a_{in}(t) + \sqrt{\kappa} b_1$ . In the bad-cavity limit with the cavity decay rate  $\kappa$  much larger than the coupling rate  $\sqrt{N_a} \Omega_2 g_1 / \Delta$ , we can adiabatically eliminate the cavity mode  $b_1$ , and obtain a direct Langevin equation for the collective atomic mode  $s$

$$\dot{s} = -\frac{\kappa'}{2} s - \sqrt{\kappa'} a_{in}(t), \quad (56)$$

where the effective coupling rate  $\kappa' = 4N_a |\Omega_2 g_1|^2 / (\Delta^2 \kappa)$ , and without loss of generality we have assumed that the phase of the laser is chosen in the way to make  $i\Omega_2 g_1 = |\Omega_2 g_1|$ . The output quantum signal, expressed by the atomic operator  $s$ , has the form  $a_{out}(t) = -a_{in}(t) - \sqrt{\kappa'} s$ . Eq. (56) serves as the basic equation in dealing with quantum light memory in Sec. IV.

To show that we have a collective enhancement of the signal-to-noise ratio, let us consider the atomic spontaneous emissions. There are two spontaneous emission processes: first, the (about  $N_a$ ) atoms in the level  $|1\rangle$  can absorb photons from the quantum signal to go up to the level  $|3\rangle$ , and then go down through spontaneous emissions; and second, the very few atoms in the level  $|2\rangle$  can absorb photons from the classical driving laser to go up and then go down through spontaneous emissions. We assume that the atomic ensemble is dilute with  $k_s / \sqrt[3]{\rho_n} \geq 1$  (where  $\rho_n$  is the atomic number density) so that there are no superradiant effects for spontaneous emissions which go to all the possible directions. In this case, the total spontaneous emission rate is given by  $\gamma_{t1} = N_a |g_1|^2 \gamma_s / \Delta^2$  for the first process, and by  $\gamma_{t2} = |\Omega_2|^2 \gamma_s / \Delta^2$  for the second process, where  $\gamma_s$  is the resonant spontaneous emission rate (the natural bandwidth of the level  $|3\rangle$ ). When the classical driving laser is strong with  $|\Omega_2|^2 \geq N_a |g_1|^2$ , the signal-to-noise ratio  $R_{sn}$  in this configuration is estimated by  $R_{sn} \sim \kappa' / \gamma_{t2} \sim 4N_a |g_1|^2 / (\kappa \gamma_s)$ . This result should be compared with the corresponding one in the case with single atoms trapped in a high-Q cavity, where the signal-to-noise ratio is given by  $|g_1|^2 / (\kappa \gamma_s)$  [104]. Therefore, for atomic ensembles with the  $\Lambda$ -level configuration, the signal-to-noise ratio is greatly enhanced by the large fac-

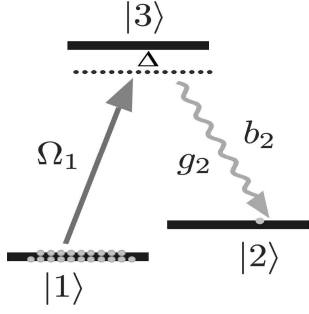


FIG. 16: The AII-level configuration.

tor of the atom number  $N_a$  due to the many-atom collective effects in coupling to the co-propagating quantum signal.

## 2. AII-level configuration

In the second level configuration, each atom still has three levels  $|1\rangle$ ,  $|2\rangle$  and  $|3\rangle$ . The difference is now that the classical driving laser is coupling to the transition  $|1\rangle \rightarrow |3\rangle$ , and the quantum signal to the transition  $|3\rangle \rightarrow |2\rangle$  (see Fig. IV B 2). This level configuration was considered before for a quantum description of the Raman stimulating process [96], and recently it has been shown in [95] to be useful for physical implementation of long-distance quantum communication. Here, we follow Ref. [95] for a simple description and demonstration of the collective enhancement of the signal-to-noise ratio. In this level configuration, the effective Hamiltonian after adiabatic elimination of the upper level  $|3\rangle$  has the following form

$$H = \hbar \left( \sqrt{N_a} \Omega_1 g_2 / \Delta \right) s^\dagger b_2^\dagger + \text{h.c.}, \quad (57)$$

where  $s$  is the collective atomic annihilation operator defined as before, and we have neglected the trivial light shift terms. Similar to the configuration I, we can write the Heisenberg-Langevin equations corresponding to the Hamiltonian (57), and then adiabatically eliminate the mode  $b_2$  in the bad-cavity limit to obtain a direct Langevin equation for the collective atomic mode  $s$

$$\dot{s}^\dagger = \frac{\kappa'}{2} s^\dagger - \sqrt{\kappa'} a_{in}(t), \quad (58)$$

where the effective coupling rate  $\kappa' = 4N_a |\Omega_1 g_2|^2 / (\Delta^2 \kappa)$ , and without loss of generality we have assumed  $i\Omega_1^* g_2^* = |\Omega_1 g_2|$ . The output quantum signal  $a_{out}(t)$  is connected with the input  $a_{in}(t)$  by the input-output relation  $a_{out}(t) = -a_{in}(t) + \sqrt{\kappa'} s^\dagger$ .

The atomic ensembles with the AII-level configuration described before provide us the basic elements for implementing quantum repeaters and long-distance quantum

communication which will be detailed in the next section. For the applications there, we explicitly solve the basic equation (58) with a vacuum input quantum signal  $a_{in}(t)$  which satisfies the properties  $\langle a_{in}^\dagger(t) a_{in}(t') \rangle = 0$  and  $\langle a_{in}(t) a_{in}^\dagger(t') \rangle = \delta(t - t')$ . Equation (58) is linear and has the simple solution

$$s^\dagger(t) = s^\dagger(0) e^{\kappa' t/2} - \sqrt{\kappa'} \int_0^t e^{\kappa'(t-\tau)/2} a_{in}(\tau) d\tau. \quad (59)$$

What we are interested in the quantum repeater scheme is some measurable quantity constructed from the output signal  $a_{out}(t)$ . If we use photon detectors for measurement, what we detect is the integration of the output photon current during the detection time interval  $t_\Delta$ , which is proportional to the intensity integration of the output field  $a_{out}(t)$ . So in fact we measure the operator  $Q_m = \int_0^{t_\Delta} a_{out}^\dagger(\tau) a_{out}(\tau) d\tau$ . One can find an explicit expression for  $Q_m$  by substituting the solution of  $a_{out}(t)$  from the input-output relation. To simplify the expression of  $Q_m$ , we define an effective single-mode bosonic operator  $a$  from the continuous field  $a_{in}(t)$  by the form

$$a \equiv -\frac{\sqrt{\kappa'}}{\sqrt{e^{\kappa' t_\Delta} - 1}} \int_0^{t_\Delta} e^{\kappa'(t_\Delta - \tau)/2} a_{in}(\tau) d\tau. \quad (60)$$

With this operator, the measured quantity is expressed as

$$Q_m = a_{t_\Delta}^\dagger a_{t_\Delta} + \int_0^{t_\Delta} a_{in}^\dagger(\tau) a_{in}(\tau) d\tau, \quad (61)$$

where  $a_{t_\Delta} = a \cosh r_c + s^\dagger(0) \sinh r_c$ , a Bogoliubov transformation of  $a$  and  $s^\dagger(0)$  with  $\cosh r_c \equiv e^{\kappa' t_\Delta/2}$ . The last term of Eq. (61) is a trivial integration of the intensity of the vacuum field, which has no contribution to the measurement result. So what we measure is in fact the photon number in the effective single mode  $a_{t_\Delta}$ . Note that Eq. (59) can also be written in the Bogoliubov form  $s^\dagger(t_\Delta) = s^\dagger(0) \cosh r_c + a \sinh r_c$ . Both of  $s^\dagger(0)$  and  $a$  are initially in vacuum states, which will be denoted by  $|0_a\rangle$  and  $|0_p\rangle$  respectively in the following (the subscripts “ $a$ ” for atoms, and “ $p$ ” for photons). Transferring the solution to the Schrödinger picture, we conclude that after time  $t_\Delta$  the collective atomic mode  $s$  and the effective single mode for the output quantum signal are in a two-mode squeezed state

$$|\phi\rangle = \sec r_c \sum_n (S^\dagger a \tanh r_c)^n / n! |0_a\rangle |0_p\rangle. \quad (62)$$

This is the basic result which will be used in the next section.

Now let us take into account the atomic spontaneous emissions and calculate the signal-to-noise ratio for this level configuration. The current situation is quite different from the AI-level configuration in the sense that if one directly calculates the total spontaneous emission rate in

this system, one would find that the total rate is given by  $N_a (\Omega_1^2/\Delta^2) \gamma_s$  since almost all the atoms remain in the level  $|1\rangle$ . If one takes this rate as the noise rate, there will be no enhancement of the signal-to-noise ratio compared with the single-atom case. However, in our scheme we only concern about the collective atomic mode  $s$  since the output quantum signal is only entangled with this mode as shown by Eq. (62). So instead of the calculation of the total spontaneous emission rate, we need to calculate the noise rate for the mode  $s$ . The spontaneous emissions are independent for different atoms without superradiance, and they introduce a coherence decay term to the Langevin equation of each individual atomic operator  $s_i = \sigma_{12}^i$

$$\dot{s}_i^\dagger = -(\gamma'_s/2) s_i^\dagger + \text{noise}, \quad (63)$$

where the decay rate  $\gamma'_s = (\Omega_1^2/\Delta^2) \gamma_s$ . The last term in Eq. (63) represents the corresponding fluctuation from the noise field which results in heating, and we have left out the coherent interaction term from the Hamiltonian (57). By taking summation of Eq. (63) over all the atoms, we immediately see that there is a coherence decay term to the Langevin equation (58) of the collective atomic operator  $s^\dagger$  with the decay rate still given by  $\gamma'_s$ . The signal-to-noise ratio  $R_{sn}$  for the collective atomic mode is thus given by  $R_{sn} = \kappa'/\gamma'_s = 4N_a |g_2|^2 / (\kappa\gamma_s)$ . So compared with the single-atom case, the signal-to-noise ratio is still greatly enhanced by the large factor of the atom number  $N_a$ . This collective enhancement comes from the fact that the coherent interaction producing the output quantum signal involves only the collective atomic mode  $s$ , whereas the independent spontaneous emissions distribute over all the atomic modes, and thus only have small influence on the interesting mode  $s$ .

To best understand this point, it is helpful to also have a look at the master equation for the atomic density operator. The whole density operator  $\rho_w$  for the atomic states and the cavity mode obeys the following master equation [47]

$$\dot{\rho}_w = i[\rho_w, H] + \kappa \hat{L}[b] \rho_w + \gamma'_s \sum_i \hat{L}[s_i^\dagger] \rho_w, \quad (64)$$

where the Liouville superoperators  $\hat{L}[X]$  ( $X = b, s_i^\dagger$ ) are defined as  $\hat{L}[X] \rho_w \equiv X \rho_w X^\dagger - (X^\dagger X \rho_w + \rho_w X^\dagger X) / 2$ . In Eq. (64), the first term of the right hand side (r.h.s.) comes from the coherent Hamiltonian interaction, the second term represents the cavity output coupling, and the last term describes independent spontaneous emissions for individual atomic operators. In the bad cavity limit, after adiabatically eliminating the cavity mode, we get from Eqs. (64) and (57) the following master equation for the traced atomic density operator  $\rho_a$

$$\dot{\rho}_a = \kappa' \hat{L}[s^\dagger] \rho_a + \gamma'_s \sum_i \hat{L}[s_i^\dagger] \rho_a, \quad (65)$$

where  $\hat{L}[s^\dagger]$  is the Liouville superoperator for the collective atomic mode. The above equation can be further simplified if we introduce the Fourier transformation to the individual atomic operators  $s_j$  ( $j = 0, 1, \dots, N_a - 1$ ) with the form  $s_\mu \equiv \sum_j S_j e^{ij\mu/N_a} / \sqrt{N_a}$ , where  $s_{\mu=0}$  gives exactly the collective atomic operator  $s$ . In terms of the operators  $s_\mu$ , the master equation has the form

$$\dot{\rho}_a = (\kappa' + \gamma'_s) \hat{L}[s^\dagger] \rho_a + \gamma'_s \sum_{\mu \neq 0} \hat{L}[s_\mu^\dagger] \rho_a, \quad (66)$$

Under the weak excitation condition  $\langle s_j^\dagger s_j \rangle \ll 1$ , the operators  $s_\mu$  ( $\mu = 0, 1, \dots, N_a - 1$ ) commute with each other, so they represent independent atomic modes. We are only interested in the collective atomic mode  $s$ , and the populations in all the other modes  $s_\mu$  with  $\mu \neq 0$  have no influence on the state of the mode  $s$ . So we can trace over the modes  $s_\mu$  ( $\mu \neq 0$ ) and eliminate the last term in Eq. (66). There are two contributions to the population in the collective atomic mode  $s$ : the one with a rate  $\kappa'$  produces a coherent output signal, and the one with a rate  $\gamma'_s$  emits photons to other random directions. The signal-to-noise ratio for the mode  $s$  is thus given by  $R_{sn} = \kappa'/\gamma'_s \sim 4N_a |g_c|^2 / (\kappa\gamma_s)$ , and we get exactly the same result as before. It is interesting to note from Eq. (66) that the total spontaneous emission rate of all the modes is  $N_a \gamma'_s$ , which could be much larger than the coherent interaction rate  $\kappa'$ ; however, the spontaneous emission rate for the collective atomic mode is  $N_a$  times smaller than the total rate. This is why we still have collective enhancement and a large signal-to-noise ratio for this level configuration.

### 3. Four-level configuration

In the above two configurations of the light-atom interaction, the signal-to-noise ratio is greatly enhanced by the many-atom collective effects. Due to the collective enhancement, we by no means need a good cavity in these schemes. In fact, we can even assume to continuously decrease the cavity finesse down to 1, which corresponds to the free-space limit. In the free-space limit, the cavity decay rate  $\kappa$  is estimated by  $c/L_a$ , the inverse of the travelling time of the optical pulse in the ensemble. With the well known expressions for the coupling coefficient  $g_1$  (or  $g_2$ ) and the resonant spontaneous emission rate  $\gamma_s$  [47], one can estimate the signal-to-noise ratio in the free-space limit by  $R_{sn} \sim 4N_a |g_c|^2 / (\kappa\gamma_s) \sim 3\rho_n L_a / k_s^2 \sim d_o$ , where  $d_o$  denotes the on-resonance optical depth of the atomic ensemble which can be quite large with the current experimental technology [85–91]. So we can have a considerably large signal-to-noise ratio even without a cavity. This demonstrates that collective effects in many-atom ensembles provide us another way besides high-Q cavities to achieve strong coherent light-atom coupling. To show this more directly, we consider another light-atom interaction configuration with four levels, and in

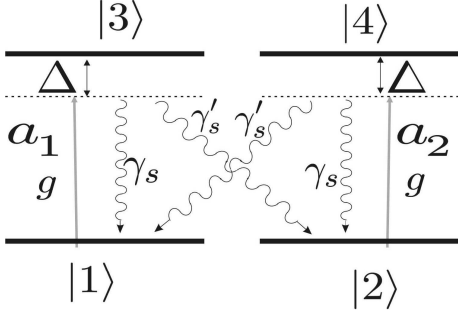


FIG. 17: The four-level configuration.

this level scheme, we solve directly the interaction of light with free-space atomic ensembles by assuming a one-dimensional light propagation model.

The relevant atomic level structure is shown by Fig. IV B 3. Each atom has two degenerate ground states and two degenerate excited states. The transitions  $|1\rangle \rightarrow |3\rangle$  and  $|2\rangle \rightarrow |4\rangle$  are coupled with a large detuning  $\Delta$  to different circularly polarized propagating light due to the angular-momentum selection rule. This kind of interaction has been analyzed semiclassically in [105, 106], and recently shown to be applicable for quantum non-demolition measurements [92, 107–109] and for continuous variable quantum teleportation [98, 110]. Here, we follow Ref. [98] for a free-space quantum description of the light-atomic-ensemble interaction. The atomic spontaneous emissions are included in the description to demonstrate the collective enhancement of the signal-to-noise ratio.

We assume a one-dimensional model for the propagating light field. As shown in Ref. [99], this is justified if the atomic ensemble is of a pencil shape with Fresnel number  $F = A/\lambda_0 L_a \approx 1$ . Here  $A$  and  $L_a$  are the cross section and the length of the ensemble, respectively, and  $\lambda_0$  is the optical wave length. The input laser pulse is linearly polarized and expressed as  $E^{(+)}(z, t) = \sqrt{\frac{\hbar\omega_0}{4\pi\epsilon_0 A}} \sum_{i=1,2} a_i(z, t) e^{i(k_0 z - \omega_0 t)}$ , where  $\omega_0 = k_0 c = 2\pi c/\lambda_0$  is the carrier frequency, and  $i$  denotes two orthogonal circular polarizations, with the standard commutation relations  $[a_i(z, t), a_j(z', t)] = \delta_{ij} \delta(z - z')$ . The light is weakly focused with cross section  $A$  to match the atomic ensemble. For the input of a strong coherent light with linear polarization, the initial condition is expressed as  $\langle a_i(0, t) \rangle = \alpha_t$ , with the total photon number over the pulse duration  $T$  satisfies  $2N_p = 2c \int_0^T |\alpha_t|^2 dt \gg 1$ . The Stokes operators are introduced for the free-space input and output light (light before entering or after leaving the atomic ensemble) by  $S_x^p = \frac{c}{2} \int_0^T (a_1^\dagger a_2 + a_2^\dagger a_1) d\tau$ ,  $S_y^p = \frac{c}{2i} \int_0^T (a_1^\dagger a_2 - a_2^\dagger a_1) d\tau$ ,  $S_z^p = \frac{c}{2} \int_0^T (a_1^\dagger a_1 - a_2^\dagger a_2) d\tau$ . In free space,  $a_i(z, t)$  only depends on  $\tau = t - z/c$ , and in this case one can check the Stokes operators satisfy the spin commutation rela-

tions  $[S_y^p, S_z^p] = iS_x^p$ . For our coherent input, we have  $\langle S_x^p \rangle = N_p$  and  $\langle S_y^p \rangle = \langle S_z^p \rangle = 0$ . With a very large  $N_p$ , the off-resonant interaction with atoms is only a small perturbation to  $S_x^p$ , and we can treat  $S_x^p$  classically by replacing it with its mean value  $\langle S_x^p \rangle$ . Then, we define two canonical observables for light by  $X^p = S_y^p / \sqrt{\langle S_x^p \rangle}$ ,  $P^p = S_z^p / \sqrt{\langle S_x^p \rangle}$  with a standard commutator  $[X^p, P^p] = i$ . These operators are the quantum variables we are interested in. Similar operators can be introduced for atoms. For an atomic ensemble with many atoms, it is convenient to define the continuous atomic operators  $\sigma_{\mu\nu}(z, t) = \lim_{\delta z \rightarrow 0} \frac{1}{\rho A \delta z} \sum_i^{z \leq z_i < z + \delta z} |\mu\rangle_i \langle \nu|$  ( $\mu, \nu = 1, 2, 3, 4$ ) with the commutation relations  $[\sigma_{\mu\nu}(z, t), \sigma_{\nu'\mu'}(z', t)] = (1/\rho_n A) \delta(z - z') (\delta_{\nu\nu'} \sigma_{\mu\mu'} - \delta_{\mu\mu'} \sigma_{\nu'\nu})$ . In the definition,  $z_i$  is the position of the  $i$  atom, and  $\rho_n$  is the number density of the atomic ensemble with the total atom number  $2N_a = \rho A L_a \gg 1$ . The collective spin operators are introduced for the ground states of the atomic ensemble by  $S_x^a = \frac{\rho A}{2} \int_0^{L_a} (\sigma_{12} + \sigma_{12}^\dagger) dz$ ,  $S_y^a = \frac{\rho A}{2i} \int_0^{L_a} (\sigma_{12} - \sigma_{12}^\dagger) dz$ ,  $S_z^a = \frac{\rho A}{2} \int_0^{L_a} (\sigma_{11} - \sigma_{22}) dz$ . All the atoms are initially prepared in the equal superposition of the two ground states  $(|1\rangle + |2\rangle)/\sqrt{2}$ , which is an eigenstate of  $S_x^a$  with a very large eigenvalue  $N_a$ . As before, we treat  $S_x^a$  classically, and define the canonical operators for atoms by  $X^a = S_y^a / \sqrt{\langle S_x^a \rangle}$ ,  $P^a = S_z^a / \sqrt{\langle S_x^a \rangle}$  with  $[X^a, P^a] = i$  and an initial vacuum state.

With introduction of the continuous atomic operators, the interaction between atoms and the propagating light  $E^{(+)}(z, t)$  is described by the following Hamiltonian in the rotating frame

$$H = \hbar \sum_{i=1,2} \int_0^L [\Delta \sigma_{i+2,i+2}(z, t) + (g e^{ik_0 z} a_i(z, t) \sigma_{i+2,i}(z, t) + h.c.)] \rho A dz \quad (67)$$

where the coupling constant  $g = \sqrt{\frac{\omega_0}{4\pi\hbar\epsilon_0 A}} d$  and  $d$  is the dipole moment of the  $|i\rangle \rightarrow |i+2\rangle$  transition. Corresponding to this Hamiltonian, the Maxwell-Bloch equations are written as [47]

$$\begin{aligned} \left( \frac{\partial}{\partial t} + c \frac{\partial}{\partial z} \right) a_i(z, t) &= -ig^* e^{-ik_0 z} \rho A \sigma_{i,i+2}(z, t), \\ \frac{\partial}{\partial t} \sigma_{\mu\nu} &= -\frac{i}{\hbar} [\sigma_{\mu\nu}, H] - \frac{\gamma_{\mu\nu}}{2} \sigma_{\mu\nu} \\ &\quad + \sqrt{\gamma_{\mu\nu}} (\sigma_{\nu\nu} - \sigma_{\mu\mu}) F_{\mu\nu} \quad (\mu < \nu), \end{aligned} \quad (68)$$

where the spontaneous emission rates (see Fig. IV B 3) are, respectively,  $\gamma_{13} = \gamma_{24} \equiv \gamma_s = \frac{\omega_0^3 |d|^2}{3\pi\epsilon_0 \hbar c^3}$ ,  $\gamma_{14} = \gamma_{23} \equiv \gamma_{s'}$ , and  $\gamma_{12} = 0$  (the ground state has a long coherence time). The Doppler broadening caused by the atomic motion is negligible, since it is eliminated for off-resonant interactions with the collinear input and output lights. Assuming that the spontaneous emission is independent for different atoms, the vacuum noise operators  $F_{\mu\nu}$  satisfy

the  $\delta$ -commutation relations  $[F_{\mu\nu}(z, t), F_{\mu'\nu'}^\dagger(z', t')] = (1/\rho A) \delta_{\mu\mu'} \delta_{\nu\nu'} \delta(z - z') \delta(t - t')$ . To simplify Eq. (68), first we change the variables by  $\tau = t - z/c$ , and then adiabatically eliminate the excited states  $|3\rangle$  and  $|4\rangle$  of atoms in the case of a large detuning, i.e.,  $\Delta \gg g \langle a_i(z, t) \rangle \sim g\sqrt{N_p/(cT)}$ . The resultant equations read

$$\begin{aligned} \frac{\partial}{\partial z} a_i(z, \tau) &= \frac{i|g|^2 \rho A \sigma_{ii}}{\Delta c} a_i(z, \tau) - \frac{|g|^2 \rho A \gamma_s \sigma_{ii}}{2\Delta^2 c} a_i(z, \tau) \\ &\quad + \frac{g^* e^{-ik_0 z} \rho A \sqrt{\gamma_s} \sigma_{ii}}{\Delta c} F_{i,i+2}(z, \tau), \\ \frac{\partial}{\partial \tau} \sigma_{12} &= \frac{i|g|^2 (a_2^\dagger a_2 - a_1^\dagger a_1)}{\Delta} \sigma_{12} - \frac{|g|^2 \gamma_{s'} (a_2^\dagger a_2 + a_1^\dagger a_1)}{2\Delta^2} \\ &\quad \times \sigma_{12} + \frac{\sqrt{\gamma_{s'}}}{\Delta} (g^* e^{-ik_0 z} a_2^\dagger \sigma_{11} F_{14} + g e^{ik_0 z} a_1 \sigma_{22} F_{23}). \end{aligned} \quad (69)$$

The physical meaning of the above equation is quite clear: The first term at the right hand side is the phase shift caused by the off-resonant interaction between light and atoms, and the second and the third terms represent the damping and the corresponding vacuum noise caused by the spontaneous emission, respectively. In Eq. (69), the  $\sigma_{ii}$  and  $a_i^\dagger a_i$  are approximately constant operators, only with a small damping caused by the spontaneous emission. To consider the spontaneous emission noise to the first order, it is reasonable to assume constant  $\sigma_{ii}$  and  $a_i^\dagger a_i$  for Eq. (69). Then, this equation can be easily solved by integrating over  $z, \tau$  on both sides. The result, expressed by the canonical atomic and optical operators  $X^{p,a}$  and  $P^{p,a}$  introduced before, has the following simple form

$$\begin{aligned} X^{p'} &= \sqrt{1 - \varepsilon_p} (X^p - \kappa_c P^a) + \sqrt{\varepsilon_p} X_s^p, \\ P^{p'} &= \sqrt{1 - \varepsilon_p} P^p + \sqrt{\varepsilon_p} P_s^p, \\ X^{a'} &= \sqrt{1 - \varepsilon_a} (X^a - \kappa_c P^p) + \sqrt{\varepsilon_a} X_s^a, \\ P^{a'} &= \sqrt{1 - \varepsilon_a} P^a + \sqrt{\varepsilon_a} P_s^a, \end{aligned} \quad (70)$$

where the operators with (without) a prime denote the quantities after (before) the light pulse goes through the atomic ensemble, and  $X_s^a, P_s^a, X_s^p, P_s^p$  represent the standard vacuum noise operators with variance  $1/2$ , defined from the integration of  $F_{\mu\nu}(z, t)$ ,  $X_s^p = \sqrt{\frac{c}{4N_p N_a |g|^2}} \int_0^T \int_0^L \rho A [ig^* e^{-ik_0 z} (a_2^\dagger \sigma_{11} F_{13} - a_1^\dagger \sigma_{22} F_{24}) + h.c.] dz dt$  for instance. The interaction and damping coefficients  $\kappa_c, \varepsilon_p, \varepsilon_a$  are given respectively by  $\kappa_c = -\frac{2\sqrt{N_p N_a} |g|^2}{\Delta c} = \frac{3\sqrt{N_p N_a} \gamma \lambda_0^2}{8\pi^2 \Delta A}$ ,  $\varepsilon_p = \frac{N_a |g|^2 \gamma_s}{\Delta^2 c}$ ,  $\varepsilon_a = \frac{N_p |g|^2 \gamma_{s'}}{\Delta^2 c}$ . The solution (70) is obtained under the conditions of weak excitation  $\kappa_c \ll \sqrt{N_{p,a}}$  and small noise  $\varepsilon_{p,a} \ll 1$ . For simplicity, we assume  $N_p \sim N_a$  and  $\gamma_s \sim \gamma_{s'}$  so that  $\varepsilon_p \sim \varepsilon_a \sim \varepsilon$ . The interaction parameter  $\kappa_c$  can be rewritten as  $\kappa_c = (3\rho_n \lambda_0^2 L_a \gamma_s) / (8\pi^2 \Delta)$  with  $N_p = N_a$ . For a atomic sample of density  $\rho_n \sim 5 \times 10^{12} \text{cm}^{-3}$  and of length  $L_a \sim 2 \text{cm}$ ,  $\kappa_c \sim 5$  is obtainable with the choice  $\Delta \sim 300\gamma$ , and at the

same time the loss  $\varepsilon_p \sim \varepsilon_a \sim \varepsilon < 1\%$ . The signal-to-noise ratio for this interaction scheme is quantified by  $R_{sn} = \kappa_c^2 / \varepsilon \sim 3\rho_n L_a / k_0^2 \sim d_o$ , which is more than  $10^3$  for the above example of parameters. We will see in Sec. V that these numbers are good enough for realizing high-fidelity continuous variable quantum teleportation. By directly solving the free-space problem, we get exactly the same signal-to-noise ratio as in the two previous two level schemes after taking the free-space limit of the cavity finesses. This clearly shows that collective enhancement of the signal-to-noise ratio is present for all these types of light-atom interactions, independent of the presence or absence of the optical cavities. The collective enhancement of the signal-to-noise ratio is an important feature of these systems, which facilitate various kinds of quantum information processing detailed below.

### C. Scalable long-distance quantum communication

Quantum communication is an essential element required for constructing quantum networks, and it also has the application for absolutely secret transfer of classical messages by means of quantum cryptography [111]. The central problem of quantum communication is to generate nearly perfect entangled states between distant sites. Such states can be used, for example, to implement secure quantum cryptography using the Ekert protocol [111], and to faithfully transfer quantum states via quantum teleportation [26]. All the known realistic schemes for quantum communication are based on the use of the photonic channels. However, the degree of entanglement generated between two distant sites normally decreases exponentially with the length of the connecting channel due to the optical absorption and other channel noise. To regain a high degree of entanglement, purification schemes can be used [16]. However, entanglement purification does not fully solve the long-distance quantum communication problem. Due to the exponential decay of the entanglement in the channel, one needs an exponentially large number of partially entangled states to obtain one highly entangled state, which means that for a sufficiently long distance the task becomes nearly impossible.

To overcome the difficulty associated with the exponential fidelity decay, the concept of quantum repeaters can be used [4]. In principle, it allows to make the overall communication fidelity very close to the unity, with the communication time growing only polynomially with the transmission distance. In analogy to a fault-tolerant quantum computing [112, 113], the quantum repeater proposal is a cascaded entanglement purification protocol for communication systems. The basic idea is to divide the transmission channel into many segments, with the length of each segment comparable to the channel attenuation length. First, one generates entanglement and purifies it for each segment; the purified entanglement is

then extended to a longer length by connecting two adjacent segments through entanglement swapping [26, 114]. After entanglement swapping, the overall entanglement is decreased, and one has to purify it again. One can continue the rounds of the entanglement swapping and purification until a nearly perfect entangled states are created between two distant sites.

To implement the quantum repeater protocol, one needs to generate entanglement between distant quantum bits (qubits), store them for sufficiently long time and perform local collective operations on several of these qubits. The requirement of quantum memory is essential since all purification protocols are probabilistic. When entanglement purification is performed for each segment of the channel, quantum memory can be used to keep the segment state if the purification succeeds and to repeat the purification for the segments only where the previous attempt fails. This is essentially important for polynomial scaling properties of the communication efficiency since with no available memory we have to require that the purifications for all the segments succeeds at the same time; the probability of such event decreases exponentially with the channel length. The requirement of quantum memory implies that we need to store the local qubits in the atomic internal states instead of the photonic states since it is difficult to store photons for a reasonably long time. With atoms as the local information carriers it seems to be very hard to implement quantum repeaters since normally one needs to achieve the strong coupling between atoms and photons with high-finesse cavities for atomic entanglement generation, purification, and swapping [32, 75], which, in spite of the recent significant experimental advances [104, 115, 116], remains a very challenging technology.

To overcome this difficulty, Ref. [95] proposes a very different scheme to realize quantum repeaters based on the use of atomic ensembles with the  $\Lambda$ -level configuration. The laser manipulation of the atomic ensembles, together with some simple linear optics devices and moderate single-photon detectors, do the whole work for long-distance quantum communication. The setup is much simpler compared with the single-atom and high-Q cavity approach discussed in the previous chapter. To achieve this, the scheme makes significant advances in each step of entanglement generation, connection, and applications, with each step having built-in entanglement purification and resilient to the realistic noise. As a result, the scheme circumvents the realistic noise and imperfections, and at the same time keeps the overhead in the communication time increasing with the distance only polynomially. In this section, we will review the realization of quantum repeaters and long-distance quantum communication following the approach in Ref. [95].

### 1. Entanglement generation

To realize long-distance quantum communication, first we need to entangle two atomic ensembles within the channel attenuation length. The entanglement generation scheme described here is based on single-photon interference at photodetectors, and is fault-tolerant to realistic noise. This scheme is an extension of a proposal first proposed in [73, 117] to entangle single-atoms. The extension was made in [95] to entangle atomic ensembles with significant improvements in the communication efficiency thanks to the collective enhancement of the signal-to-noise ratio for many-atom ensembles.

The system is a sample of atoms prepared in the ground state  $|1\rangle$  with the  $\Lambda$ -level configuration (see Fig. IV C 1). It has been shown in the previous section that one can define an effective single-mode bosonic annihilation operator  $a$  for the cavity output signal (it is called the forward-scattered Stokes signal in the free space case). After the light-atom interaction, the signal mode  $a$  and the collective atomic mode  $s \equiv (1/\sqrt{N_a}) \sum_i |1\rangle_i \langle 2|$  are in a two-mode squeezed state with the squeezing parameter  $r_c$  proportional to the interaction time  $t_\Delta$  (see Eq. (62)). If the interaction time  $t_\Delta$  is very small, the whole state of the collective atomic mode and the signal mode can be written in the perturbative form

$$|\phi\rangle = |0_a\rangle |0_p\rangle + \sqrt{p_c} S^\dagger a^\dagger |0_a\rangle |0_p\rangle + o(p_c), \quad (71)$$

where  $p_c = \tanh^2 r_c$  is the small excitation probability and  $o(p_c)$  represents the terms with more excitations whose probabilities are equal or smaller than  $p_c^2$ . The  $|0_a\rangle$  and  $|0_p\rangle$  are respectively the atomic and optical vacuum states with  $|0_a\rangle \equiv \bigotimes_i |1\rangle_i$ . There is also a fraction of light from the transition  $|3\rangle \rightarrow |2\rangle$  emitted in other directions which contributes to spontaneous emissions. We have shown in the previous section that the contribution to the population in the collective atomic mode  $s$  from the spontaneous emissions is very small for many-atom ensembles due to the collective enhancement of the signal-to-noise ratio for this mode.

Now we show how to use this setup to generate entanglement between two distant ensembles L and R using the configuration shown in Fig. IV C 1. Here, two laser pulses excited both ensembles simultaneously, and the whole system is described by the state  $|\phi\rangle_L \otimes |\phi\rangle_R$ , where  $|\phi\rangle_L$  and  $|\phi\rangle_R$  are given by Eq. (71) with all the operators and states distinguished by the subscript L or R. The forward scattered Stokes signal from both ensembles is combined at the beam splitter and a photodetector click in either D1 or D2 measures the combined radiation from two samples,  $a_+^\dagger a_+$  or  $a_-^\dagger a_-$  with  $a_\pm = (a_L \pm e^{i\varphi} a_R) / \sqrt{2}$ . Here,  $\varphi$  denotes an unknown difference of the phase shifts in the two-side channels. We can also assume that  $\varphi$  has an imaginary part to account for the possible asymmetry of the setup, which will also be corrected automatically in our scheme. But the

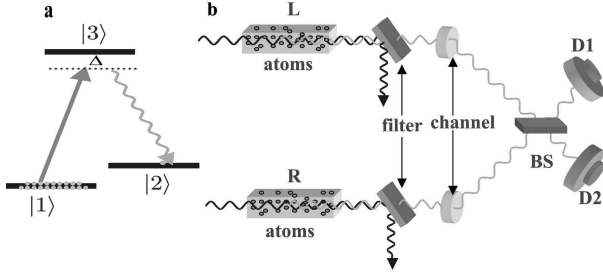


FIG. 18: (4a) The relevant level structure of the atoms in the ensemble with  $|1\rangle$ , the ground state,  $|2\rangle$ , the metastable state for storing a qubit, and  $|3\rangle$ , the excited state. The transition  $|1\rangle \rightarrow |3\rangle$  is coupled by the classical laser with the Rabi frequency  $\Omega$ , and the forward scattering Stokes light comes from the transition  $|3\rangle \rightarrow |2\rangle$ . For convenience, we assume off-resonant coupling with a large detuning  $\Delta$ . (4b) Schematic setup for generating entanglement between the two atomic ensembles L and R. The two ensembles are pencil shaped and illuminated by the synchronized classical laser pulses. The forward-scattering Stokes pulses are collected after the filters (polarization and frequency selective) and interfered at a 50%-50% beam splitter BS after the transmission channels, with the outputs detected respectively by two single-photon detectors D1 and D2. If there is a click in D1 or D2, the process is finished and we successfully generate entanglement between the ensembles L and R. Otherwise, we first apply a repumping pulse to the transition  $|2\rangle \rightarrow |3\rangle$  on the ensembles L and R to set the state of the ensembles back to the ground state  $|0\rangle_a^L \otimes |0\rangle_a^R$ , then the same classical laser pulses as the first round are applied to the transition  $|1\rangle \rightarrow |3\rangle$  and we detect again the forward-scattering Stokes pulses after the beam splitter. This process is repeated until finally we have a click in the D1 or D2 detector.

setup asymmetry can be easily made very small, and for simplicity of expressions we assume that  $\varphi$  is real in the following. Conditional on the detector click, we should apply  $a_+$  or  $a_-$  to the whole state  $|\phi\rangle_L \otimes |\phi\rangle_R$ , and the projected state of the ensembles L and R is nearly maximally entangled with the form (neglecting the high-order terms  $o(p_c)$ )

$$|\Psi_\varphi\rangle_{LR}^\pm = \left( S_L^\dagger \pm e^{i\varphi} S_R^\dagger \right) / \sqrt{2} |0_a\rangle_L |0_a\rangle_R. \quad (72)$$

The probability for getting a click is given by  $p_c$  for each round, so we need repeat the process about  $1/p_c$  times for a successful entanglement preparation, and the average preparation time is given by  $T_0 \sim t_\Delta/p_c$ . The states  $|\Psi_r\rangle_{LR}^+$  and  $|\Psi_r\rangle_{LR}^-$  can be easily transformed to each other by a simple local phase shift. Without loss of generality, we assume in the following that we generate the entangled state  $|\Psi_r\rangle_{LR}^+$ .

As will be shown below, the presence of the noise modifies the projected state of the ensembles to

$$\rho_{LR}(c_0, \varphi) = \frac{1}{c_0 + 1} \left( c_0 |0_a 0_a\rangle_{LR} \langle 0_a 0_a| + |\Psi_\varphi\rangle_{LR}^+ \langle \Psi_\varphi| \right), \quad (73)$$

where the “vacuum” coefficient  $c_0$  is determined by the dark count rates of the photon detectors. It will be seen below that any state in the form of Eq. (73) will be purified automatically to a maximally entangled state in the entanglement-based communication schemes. We therefore call this state an effective maximally entangled (EME) state with the vacuum coefficient  $c_0$  determining the purification efficiency.

## 2. Entanglement connection through swapping

After the successful generation of the entanglement within the attenuation length, we want to extend the quantum communication distance. This is done through entanglement swapping with the configuration shown in Fig. IV C 2. Suppose that we start with two pairs of the entangled ensembles described by the state  $\rho_{LI_1} \otimes \rho_{I_2R}$ , where  $\rho_{LI_1}$  and  $\rho_{I_2R}$  are given by Eq. (73). In the ideal case, the setup shown in Fig. IV C 2 measures the quantities corresponding to operators  $S_\pm^\dagger S_\pm$  with  $S_\pm = (S_{I_1} \pm S_{I_2})/\sqrt{2}$ . If the measurement is successful (i.e., one of the detectors registers one photon), we will prepare the ensembles L and R into another EME state. The new  $\varphi$ -parameter is given by  $\varphi_1 + \varphi_2$ , where  $\varphi_1$  and  $\varphi_2$  denote the old  $\varphi$ -parameters for the two segment EME states. As will be seen below, even in the presence of the realistic noise and imperfections, an EME state is still created after a detector click. The noise only influences the success probability to get a click and the new vacuum coefficient in the EME state. In general we can express the success probability  $p_1$  and the new vacuum coefficient  $c_1$  as  $p_1 = f_1(c_0)$  and  $c_1 = f_2(c_0)$ , where the functions  $f_1$  and  $f_2$  depend on the particular noise properties.

The above method for connecting entanglement can be cascaded to arbitrarily extend the communication distance. For the  $i$ th ( $i = 1, 2, \dots, n$ ) entanglement connection, we first prepare in parallel two pairs of ensembles in the EME states with the same vacuum coefficient  $c_{i-1}$  and the same communication length  $L_{i-1}$ , and then perform the entanglement swapping as shown in Fig. IV C 2, which now succeeds with a probability  $p_i = f_1(c_{i-1})$ . After a successful detector click, the communication length is extended to  $L_i = 2L_{i-1}$ , and the vacuum coefficient in the connected EME state becomes  $c_i = f_2(c_{i-1})$ . Since the  $i$ th entanglement connection need be repeated in average  $1/p_i$  times, the total time needed to establish an EME state over the distance  $L_n = 2^n L_0$  is given by  $T_n = T_0 \prod_{i=1}^n (1/p_i)$ , where  $L_0$  denotes the distance of each segment in the entanglement generation.

## 3. Entanglement-based communication schemes

After an EME state has been established between two distant sites, we would like to use it in the communication protocols, such as quantum teleportation, cryptography, and Bell inequality detection. It is not obvious that the

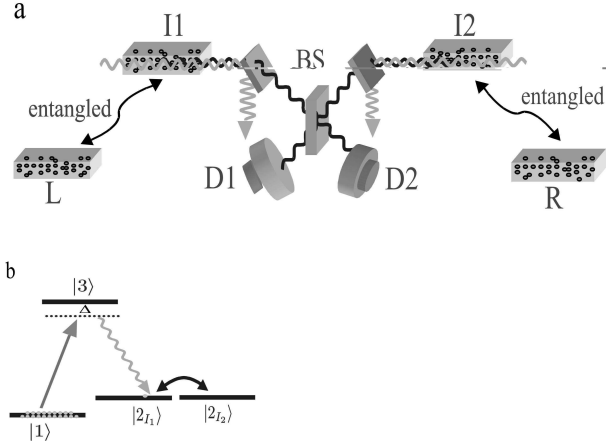


FIG. 19: (5a) Illustrative setup for the entanglement swapping. We have two pairs of ensembles L, I1 and I2, R distributed at three sites L, I and R. Each of the ensemble-pairs L, I1 and I2, R is prepared in an EME state in the form of Eq. (3). The excitations in the collective modes of the ensembles I1 and I2 are transferred simultaneously to the optical excitations by the repumping pulses applied to the atomic transition  $|2\rangle \rightarrow |3\rangle$ , and the stimulated optical excitations, after a 50%-50% beam splitter, are detected by the single-photon detectors D1 and D2. If either D1 or D2 clicks, the protocol is successful and an EME state in the form of Eq. (3) is established between the ensembles L and R with a doubled communication distance. Otherwise, the process fails, and we need to repeat the previous entanglement generation and swapping until finally we have a click in D1 or D2, that is, until the protocol finally succeeds. (5b) The two intermediated ensembles I1 and I2 can also be replaced by one ensemble but with two metastable states I1 and I2 to store the two different collective modes. The 50%-50% beam splitter operation can be simply realized by a  $\pi/2$  pulse on the two metastable states before the collective atomic excitations are transferred to the optical excitations.

EME state (73), which is entangled in the Fock basis, is useful for these tasks since in the Fock basis it is experimentally hard to do certain single-bit operations. In the following we will show how the EME states can be used to realize all these protocols with simple experimental configurations.

Quantum cryptography and the Bell inequality detection are achieved with the setup shown by Fig. IV C 3a. The state of the two pairs of ensembles is expressed as  $\rho_{L_1 R_1} \otimes \rho_{L_2 R_2}$ , where  $\rho_{L_i R_i}$  ( $i = 1, 2$ ) denote the same EME state with the vacuum coefficient  $c_n$  if we have done  $n$  times entanglement connection. The  $\varphi$ -parameters in  $\rho_{L_1 R_1}$  and  $\rho_{L_2 R_2}$  are the same provided that the two states are established over the same stationary channels. We register only the coincidences of the two-side detectors, so the protocol is successful only if there is a click on each side. Under this condition, the vacuum components in the EME states, together with the state components  $S_{L_1}^\dagger S_{L_2}^\dagger |\text{vac}\rangle$  and  $S_{R_1}^\dagger S_{R_2}^\dagger |\text{vac}\rangle$ , where  $|\text{vac}\rangle$  denotes

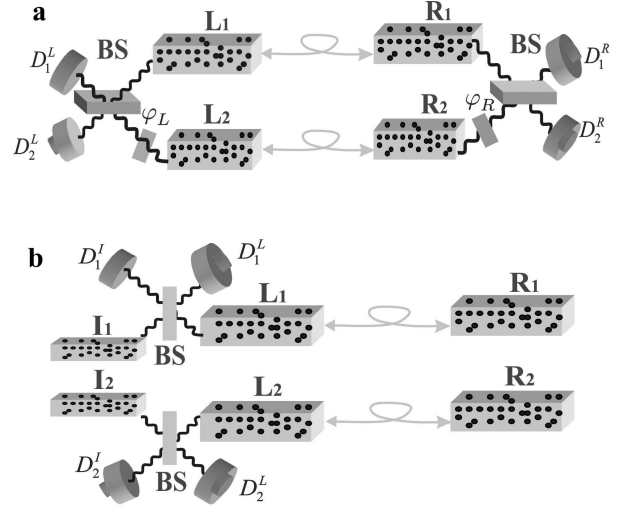


FIG. 20: (6a) Schematic setup for the realization of quantum cryptography and Bell inequality detection. Two pairs of ensembles L1, R1 and L2, R2 (or two pairs of metastable states as shown by Fig. (IV B 2b)) have been prepared in the EME states. The collective atomic excitations on each side are transferred to the optical excitations, which, respectively after a relative phase shift  $\varphi_L$  or  $\varphi_R$  and a 50%-50% beam splitter, are detected by the single-photon detectors  $D_1^L, D_2^L$  and  $D_1^R, D_2^R$ . We look at the four possible coincidences of  $D_1^R, D_2^R$  with  $D_1^L, D_2^L$ , which are functions of the phase difference  $\varphi_L - \varphi_R$ . Depending on the choice of  $\varphi_L$  and  $\varphi_R$ , this setup can realize both the quantum cryptography and the Bell inequality detection. (6b) Schematic setup for probabilistic quantum teleportation of the atomic “polarization” state. Similarly, two pairs of ensembles L1, R1 and L2, R2 are prepared in the EME states. We want to teleport an atomic “polarization” state  $(d_0 S_{I_1}^\dagger + d_1 S_{I_2}^\dagger) |0_a 0_a\rangle_{I_1 I_2}$  with unknown coefficients  $d_0, d_1$  from the left to the right side, where  $S_{I_1}^\dagger, S_{I_2}^\dagger$  denote the collective atomic operators for the two ensembles I1 and I2 (or two metastable states in the same ensemble). The collective atomic excitations in the ensembles I1, L1 and I2, L2 are transferred to the optical excitations, which, after a 50%-50% beam splitter, are detected by the single-photon detectors  $D_1^L, D_1^R$  and  $D_2^L, D_2^R$ . If there are a click in  $D_1^L$  or  $D_1^R$  and a click in  $D_2^L$  or  $D_2^R$ , the protocol is successful. A  $\pi$ -phase rotation is then performed on the collective mode of the ensemble R2 conditional on that the two clicks appear in the detectors  $D_1^L, D_2^L$  or  $D_2^L, D_1^L$ . The collective excitation in the ensembles R1 and R2, if appearing, would be found in the same “polarization” state  $(d_0 S_{R_1}^\dagger + d_1 S_{R_2}^\dagger) |0_a 0_a\rangle_{R_1 R_2}$ .

the ensemble state  $|0_a 0_a 0_a 0_a\rangle_{L_1 R_1 L_2 R_2}$ , have no contributions to the experimental results. So, for the measurement scheme shown by Fig. IV B 3, the ensemble state  $\rho_{L_1 R_1} \otimes \rho_{L_2 R_2}$  is effectively equivalent to the following “polarization” maximally entangled (PME) state (the terminology of “polarization” comes from an anal-



ogy to the optical case)

$$|\Psi\rangle_{\text{PME}} = \left( S_{L_1}^\dagger S_{R_2}^\dagger + S_{L_2}^\dagger S_{R_1}^\dagger \right) / \sqrt{2} |\text{vac}\rangle. \quad (74)$$

The success probability for the projection from  $\rho_{L_1 R_1} \otimes \rho_{L_2 R_2}$  to  $|\Psi\rangle_{\text{PME}}$  (i.e., the probability to get a click on each side) is given by  $p_a = 1/[2(c_n + 1)^2]$ . One can also check that in Fig. IV C 3, the phase shift  $\psi_\Lambda$  ( $\Lambda = L$  or  $R$ ) together with the corresponding beam splitter operation are equivalent to a single-bit rotation in the basis  $\{|0\rangle_\Lambda \equiv S_{\Lambda_1}^\dagger |0_a 0_a\rangle_{\Lambda_1 \Lambda_2}, |1\rangle_\Lambda \equiv S_{\Lambda_2}^\dagger |0_a 0_a\rangle_{\Lambda_1 \Lambda_2}\}$  with the rotation angle  $\theta = \psi_\Lambda/2$ . Now, it is clear how to do quantum cryptography and Bell inequality detection since we have the PME state and we can perform the desired single-bit rotations in the corresponding basis. For instance, to distribute a quantum key between the two remote sides, we simply choose  $\psi_\Lambda$  randomly from the set  $\{0, \pi/2\}$  with an equal probability, and keep the measurement results (to be 0 if  $D_1^\Lambda$  clicks, and 1 if  $D_2^\Lambda$  clicks) on both sides as the shared secret key if the two sides become aware that they have chosen the same phase shift after the public declare. This is exactly the Ekert scheme [111] and its absolute security follows directly from the proofs in [118, 119]. For the Bell inequality detection, we infer the correlations  $E(\psi_L, \psi_R) \equiv P_{D_1^L D_1^R} + P_{D_2^L D_2^R} - P_{D_1^L D_2^R} - P_{D_2^L D_1^R} = \cos(\psi_L - \psi_R)$  from the measurement of the coincidences  $P_{D_1^L D_1^R}$  etc. For the setup shown in Fig. IV C 3a, we would have  $|E(0, \pi/4) + E(\pi/2, \pi/4) + E(\pi/2, 3\pi/4) - E(0, 3\pi/4)| = 2\sqrt{2}$ , whereas for any local hidden variable theories, the CHSH inequality [120] implies that this value should be below 2.

We can also use the established long-distance EME states for faithful transfer of unknown quantum states through quantum teleportation, with the setup shown by Fig. IV C 3b. In this setup, if two detectors click on the left side, there is a significant probability that there is no collective excitation on the right side since the product of the EME states  $\rho_{L_1 R_1} \otimes \rho_{L_2 R_2}$  contains vacuum components. However, if there is a collective excitation appearing from the right side, its “polarization” state would be exactly the same as the one input from the left. So, as in the Innsbruck experiment [27], the teleportation here is probabilistic and needs posterior confirmation; but if it succeeds, the teleportation fidelity would be nearly perfect since in this case the entanglement is equivalently described by the PME state (74). The success probability for the teleportation is also given by  $p_a = 1/[2(c_n + 1)^2]$ , which determines the average number of repetitions for a successful teleportation.

#### 4. Noise and built-in entanglement purification

We next discuss noise and imperfections in the schemes for entanglement generation, connection, and applications. In particular we show that each step contains

built-in entanglement purification which makes the whole scheme resilient to the realistic noise and imperfections.

In the entanglement generation, the dominant noise is the photon loss, which includes the contributions from the channel attenuation, the spontaneous emissions in the atomic ensembles (which results in the population of the collective atomic mode  $s$  with the accompanying photon going to other directions), the coupling inefficiency of the Stokes signal into and out of the channel, and the inefficiency of the single-photon detectors. The loss probability is denoted by  $1 - \eta_p$  with the overall efficiency  $\eta_p = \eta'_p e^{-L_0/L_{\text{att}}}$ , where we have separated the channel attenuation  $e^{-L_0/L_{\text{att}}}$  ( $L_{\text{att}}$  is the channel attenuation length) from other noise contributions  $\eta'_p$  with  $\eta'_p$  independent of the communication distance  $L_0$ . The photon loss decreases the success probability for getting a detector click from  $p_c$  to  $\eta_p p_c$ , but it has no influence on the resulting EME state. Due to this noise, the entanglement preparation time should be replaced by  $T_0 \sim t_\Delta / (\eta_p p_c)$ . The second source of noise comes from the dark counts of the single-photon detectors. The dark count gives a detector click, but without population of the collective atomic mode, so it contributes to the vacuum coefficient in the EME state. If the dark count comes up with a probability  $p_{dc}$  for the time interval  $t_\Delta$ , the vacuum coefficient is given by  $c_0 = p_{dc} / (\eta_p p_c)$ , which is typically much smaller than 1 since the Raman transition rate is much larger than the dark count rate. The final source of noise, which influences the fidelity to get the EME state, is caused by the event that more than one atom are excited to the collective mode  $S$  whereas there is only one click in D1 or D2. The conditional probability for that event is given by  $p_c$ , so we can estimate the fidelity imperfection  $\Delta F_0 \equiv 1 - F_0$  for the entanglement generation by

$$\Delta F_0 \sim p_c. \quad (75)$$

Note that by decreasing the excitation probability  $p_c$ , one can make the fidelity imperfection closer and closer to zero with the price of a longer entanglement preparation time  $T_0$ . This is the basic idea of the entanglement purification. So, in this scheme, the confirmation of the click from the single-photon detector generates and purifies entanglement at the same time.

In the entanglement swapping, the dominant noise is still the losses, which include the contributions from the detector inefficiency, the inefficiency of the excitation transfer from the collective atomic mode to the optical mode [88, 90], and the small decay of the atomic excitation during the storage [88, 90]. Note that by introducing the detector inefficiency, we have automatically taken into account the imperfection that the detectors cannot distinguish the single and the two photons. With all these losses, the overall efficiency in the entanglement swapping is denoted by  $\eta_s$ . The loss in the entanglement swapping gives contributions to the vacuum coefficient in the connected EME state, since

in the presence of loss a single detector click might result from two collective excitations in the ensembles  $I_1$  and  $I_2$ , and in this case, the collective modes in the ensembles L and R have to be in a vacuum state. After taking into account the realistic noise, we can specify the success probability and the new vacuum coefficient for the  $i$ th entanglement connection by the recursion relations  $p_i \equiv f_1(c_{i-1}) = \eta_s \left(1 - \frac{\eta_s}{2(c_{i-1}+1)}\right) / (c_{i-1} + 1)$  and  $c_i \equiv f_2(c_{i-1}) = 2c_{i-1} + 1 - \eta_s$ . The coefficient  $c_0$  for the entanglement preparation is typically much smaller than  $1 - \eta_s$ , then we have  $c_i \approx (2^i - 1)(1 - \eta_s) = (L_i/L_0 - 1)(1 - \eta_s)$ , where  $L_i$  denotes the communication distance after  $i$  times entanglement connection. With the expression for the  $c_i$ , we can easily evaluate the probability  $p_i$  and the communication time  $T_n$  for establishing a EME state over the distance  $L_n = 2^n L_0$ . After the entanglement connection, the fidelity of the EME state also decreases, and after  $n$  times connection, the overall fidelity imperfection  $\Delta F_n \sim 2^n \Delta F_0 \sim (L_n/L_0) \Delta F_0$ . We need fix  $\Delta F_n$  to be small by decreasing the excitation probability  $p_c$  in Eq. (75).

It is important to point out that our entanglement connection scheme also has built-in entanglement purification function. This can be understood as follows: Each time we connect entanglement, the imperfections of the setup decrease the entanglement fraction  $1/(c_i + 1)$  in the EME state. However, the entanglement fraction decays only linearly with the distance (the number of segments), which is in contrast to the exponential decay of the entanglement for the connection schemes without entanglement purification. The reason for the slow decay is that in each time of the entanglement connection, we need repeat the protocol until there is a detector click, and the confirmation of a click removes part of the added vacuum noise since a larger vacuum components in the EME state results in more times of repetitions. The built-in entanglement purification in the connection scheme is essential for the polynomial scaling law of the communication efficiency.

As in the entanglement generation and connection schemes, our entanglement application schemes also have built-in entanglement purification which makes them resilient to the realistic noise. Firstly, we have seen that the vacuum components in the EME states are removed from the confirmation of the detector clicks and thus have no influence on the fidelity of all the application schemes. Secondly, if the single-photon detectors and the atom-to-light excitation transitions in the application schemes are imperfect with the overall efficiency denoted by  $\eta_a$ , one can easily check that these imperfections only influence the efficiency to get the detector clicks with the success probability replaced by  $p_a = \eta_a / [2(c_n + 1)^2]$ , and have no effects on the communication fidelity. Finally, we have seen that the phase shifts in the stationary channels and the small asymmetry of the stationary setup are removed automatically when we project the EME state to the PME state, and thus have no influence on the com-

munication fidelity.

The noise not correctable by our scheme includes the detector dark count in the entanglement connection and the non-stationary channel noise and set asymmetries. The resulting fidelity imperfection from the dark count increases linearly with the number of segments  $L_n/L_0$ , and from the non-stationary channel noise and set asymmetries increases by the random-walk law  $\sqrt{L_n/L_0}$ . For each time of entanglement connection, the dark count probability is about  $10^{-5}$  if we make a typical choice that the collective emission rate is about 10MHz and the dark count rate is  $10^2$ Hz. So this noise is negligible even if we have communicated over a long distance ( $10^3$  the channel attenuation length  $L_{att}$  for instance). The non-stationary channel noise and setup asymmetries can also be safely neglected for such a distance. For instance, it is relatively easy to control the non-stationary asymmetries in local laser operations to values below  $10^{-4}$  with the use of accurate polarization techniques [121] for Zeeman sublevels (as in Fig. IV C 2b).

### 5. Scaling of the communication efficiency

We have shown that each of our entanglement generation, connection, and application schemes has built-in entanglement purification, and as a result of this property, we can fix the communication fidelity to be nearly perfect, and at the same time keep the communication time to increase only polynomially with the distance. Assume that we want to communicate over a distance  $L = L_n = 2^n L_0$ . By fixing the overall fidelity imperfection to be a desired small value  $\Delta F_n$ , the entanglement preparation time becomes  $T_0 \sim t_\Delta / (\eta_p \Delta F_0) \sim (L_n/L_0) t_\Delta / (\eta_p \Delta F_n)$ . For an effective generation of the PME state (74), the total communication time  $T_{tot} \sim T_n/p_a$  with  $T_n \sim T_0 \prod_{i=1}^n (1/p_i)$ . So the total communication time scales with the distance by the law

$$T_{tot} \sim 2(L/L_0)^2 / (\eta_p p_a \Delta F_T \prod_{i=1}^n p_i), \quad (76)$$

where the success probabilities  $p_i, p_a$  for the  $i$ th entanglement connection and for the entanglement application have been specified before. The expression (76) has confirmed that the communication time  $T_{tot}$  increases with the distance  $L$  only polynomially. We show this explicitly by taking two limiting cases. In the first case, the inefficiency  $1 - \eta_s$  for the entanglement swapping is assumed to be negligibly small. One can deduce from Eq. (76) that in this case the communication time  $T_{tot} \sim T_{con} (L/L_0)^2 e^{L_0/L_{att}}$ , with the constant  $T_{con} \equiv 2t_\Delta / (\eta_p' \eta_a \Delta F_T)$  being independent of the segment and the total distances  $L_0$  and  $L$ . The communication time  $T_{tot}$  increases with  $L$  quadratically. In the second case, we assume that the inefficiency  $1 - \eta_s$  is considerably large. The communication time in this case is approximated by  $T_{tot} \sim T_{con} (L/L_0)^{[\log_2(L/L_0)+1]/2 + \log_2(1/\eta_s - 1) + 2} e^{L_0/L_{att}}$ , which increases with  $L$  still polynomially (or sub-exponentially

in a more accurate language, but this makes no difference in practice since the factor  $\log_2(L/L_0)$  is well bounded from above for any reasonably long distance). If  $T_{\text{tot}}$  increases with  $L/L_0$  by the  $m$ th power law  $(L/L_0)^m$ , there is an optimal choice of the segment length to be  $L_0 = mL_{\text{att}}$  to minimize the time  $T_{\text{tot}}$ . As a simple estimation of the improvement in the communication efficiency, we assume that the total distance  $L$  is about  $100L_{\text{att}}$ , for a choice of the parameter  $\eta_s \approx 2/3$ , the communication time  $T_{\text{tot}}/T_{\text{con}} \sim 10^6$  with the optimal segment length  $L_0 \sim 5.7L_{\text{att}}$ . This result is a dramatic improvement compared with the direct communication case, where the communication time  $T_{\text{tot}}$  for getting a PME state increases with the distance  $L$  by the exponential law  $T_{\text{tot}} \sim T_{\text{con}}e^{L/L_{\text{att}}}$ . For the same distance  $L \sim 100L_{\text{att}}$ , one needs  $T_{\text{tot}}/T_{\text{con}} \sim 10^{43}$  for direct communication, which means that for this example the present scheme is  $10^{37}$  times more efficient.

In summary, in this section we explained the recent atomic ensemble scheme for implementation of quantum repeaters and long-distance quantum communication. The proposed technique allows to generate and connect the entanglement and use it in quantum teleportation, cryptography, and tests of Bell inequalities. All of the elements of the scheme are within the reach of current experimental technology, and have the important property of built-in entanglement purification which makes them resilient to the realistic noise. As a result, the overhead required to implement the scheme, such as the communication time, scales polynomially with the channel length. This is in remarkable contrast to direct communication where the exponential overhead is required. Such an efficient scaling, combined with a relative simplicity of the proposed experimental setup, opens up realistic prospective for quantum communication over long distances.

#### D. Other Applications: quantum light memory and single-photon source

In this section, we investigate two other significant applications of atomic ensembles in quantum information processing: laser manipulation of atomic ensembles provides a simple experimentally feasible way to realize quantum light memory and single-photon source with controllable emission time, direction, and pulse shape. The realization of quantum light memory and controllable single-photon source constitutes two important steps towards implementation of a recently proposed quantum computation scheme [101]. In [101], a potentially scalable fault-tolerant quantum computation scheme is proposed based on the use of single-photon source, linear optics devices, and single-photon detectors. To realize that scheme, one is required (i) to have the ability of storing qubits (that is, quantum light memory is required to store optical qubits involved in that scheme), (ii) to have desired single-photon source with controllable

emission time and direction, (iii) and to maintain noise and imperfections in the involved physical setups below the percent level. Except the last requirement, which is still very challenging with the current experimental technology, atomic ensembles provide an ideal system for realization of the first two elements. Besides this potential application in quantum computation, quantum light memory and single-photon source are also important by themselves. For instance, single-photon source is important in the BB84 scheme for quantum key distribution to assure the absolute security and to increase the distribution efficiency [122]; and quantum light memory provides a powerful tool for eavesdropping in quantum cryptography.

##### 1. Quantum light memory

It is very hard to directly store photons for a reasonably long time. However, we know that coherence of atomic internal states can be maintained for a quite long time with the current technology. The basic idea of quantum light memory is to transfer the photonic excitation to the excitation in atomic internal states so that it can be saved, and afterwards, it should be possible to restore the excitation to photons without change of its quantum state. Quantum light memory has been investigated theoretically in Refs. [93, 94, 97, 100], and its experimental realization has been recently reported with either an ultracold Bose-Einstein condensate [88] or a hot atomic ensemble [90] as the storing medium. Ref. [100] described a method for irreversible mapping of the light state to the atomic state, and Refs. [93, 94] proposed the first quantum light memory schemes with reversible mapping between photonic and atomic states. Both schemes use the  $\Lambda$ -level configuration with a weak coupling cavity around the ensemble as described in Sec. II. The difference is that Ref. [93] is based on resonant coupling through adiabatic passages of dark states, and Ref. [94] is based on off-resonant coherent Raman absorption. Ref. [97] described the first scheme for storing light in a free-space atomic ensemble, which has been realized in the recent experiments [88, 90]. Here, to be consistent with other sections in this chapter, we will follow the off-resonant approach in Ref. [94] to review the principle for implementing quantum light memory. The readers interested in the schemes based on adiabatic passages are referred to Refs. [93, 97].

We consider an atomic ensemble with the  $\Lambda$ -level configuration as shown in Sec. 4.2 (see Fig. IV B 1). The input quantum optical signal is described by a continuous operator  $a_{\text{in}}(t)$ , with  $[a_{\text{in}}(t), a_{\text{in}}^\dagger(t')] = \delta(t - t')$ . We assume that input signal has a definite pulse shape  $f_{\text{in}}(t)$ . This is the case in most of the applications in quantum information processing. For instance, if we know that the signal comes from the output of a free cavity mode, the signal pulse has the shape  $f_{\text{in}}(t) =$

$\frac{\sqrt{\eta}}{\sqrt{1-e^{-\kappa T}}}e^{-\kappa t/2}$ , ( $0 \leq t \leq T$ ), where  $\kappa$  is the cavity decay rate and  $T$  denotes the pulse duration. For the input pulse with a definite shape, we can define an effective single-mode bosonic operator  $c_{in} = \int_0^T f_1(t) a_{in}(t) dt$  with  $[c_{in}, c_{in}^\dagger] = 1$  and a normalized shape function  $f_{in}(t)$ . Similarly for the output optical signal  $a_{out}(t)$  with a definite shape  $f_{out}(t)$ , we can also define a single-mode operator  $c_{out} = \int_0^T f_{out}(t) a_{out}(t) dt$ . The purpose of quantum light memory is to faithfully transfer the quantum state of the input optical mode  $c_{in}$  to the state of the collective atomic mode  $s \equiv (1/\sqrt{N_a}) \sum_{i=1}^{N_a} |1\rangle_i \langle 2|$ . The state can be stored in the atomic mode  $s$ , and afterwards we need to have ability to read out this state again to the output optical mode  $c_{out}$  with an arbitrary intentionally chosen pulse shape  $f_{out}(t)$ .

The light-atom interaction is described by the basic Langevin equation (56), with the effective coupling rate  $\kappa'(t) = 4N_a |\Omega_2(t) g_1|^2 / (\Delta^2 \kappa)$  adjustable by controlling the time dependence of the Rabi frequency  $\Omega_2(t)$  through change of the classical laser intensity. Equation (56) is linear and has the following simple solution

$$s(T) = s(0) e^{-\int_0^T \kappa'(t) dt/2} - \int_0^T e^{-\int_t^T \kappa'(\tau) d\tau/2} a_{in}(t) \sqrt{\kappa'(t)} dt. \quad (77)$$

To map the state of the input optical mode  $c_{in}$  to the atomic mode  $s$ , we choose the form of  $\Omega_2(t)$  so that the coupling rate  $\kappa'(t)$  satisfies the differential equation

$$\dot{\kappa}' = \frac{2\dot{f}_{in}}{f_{in}} \kappa' - \kappa'^2, \quad (78)$$

where  $f_{in}(t)$  is the shape of the input pulse. This differential equation is sometimes called the impedance matching condition [93, 103]. Under this condition, it can be seen from Eq. (77) that the collective atomic operator  $s_T$  at time  $T$  is given by

$$s_T = s(T) = \sqrt{M} s(0) - \sqrt{1-M} c_{in} \quad (79)$$

with the mapping inefficiency  $M = e^{-\int_0^T \kappa'(t) dt}$ . Since  $\kappa'(t)$  is positive, the mapping inefficiency  $M$  quickly tends to zero after a sufficiently long time  $T$ . With a zero  $M$ , the photonic state is faithfully mapped to the atomic state with  $s_T = -c_{in}$ . For a non-zero  $M$ , there will be a small inherent loss to the state mapping caused by the vacuum noise  $s(0)$ .

After mapping of the photonic state to the atomic state, the classical laser is turned off and the information can be stored in the atomic internal mode  $s_T$ . Then, after some time we want to read out this state to an output optical pulse with an intentionally chosen pulse shape  $f_{out}(t)$ , that is, we would like to map the state of the atomic mode  $s_T$  to the output optical mode  $c_{out} = \int_0^T f_{out}(t) a_{out}(t) dt$ . To attain this goal,

we turn on the classical laser to the transition  $|2\rangle \rightarrow |3\rangle$  (see Fig. IV B 1), and control its intensity so that the effective coupling rate  $\kappa'(t)$  satisfies the equation  $\dot{\kappa}' = \frac{2\dot{f}_{out}}{f_{out}} \kappa' + \kappa'^2$ , which is the time reverse of the impedance matching condition (78) for write-in of the photonic state. With this condition, one can deduce from Eq. (77) and the input-output relation  $a_{out}(t) = -a_{in}(t) - \sqrt{\kappa'} s$  that after time  $T$ , the outgoing optical mode is given by  $c_{out} = -\sqrt{M} c_T - \sqrt{1-M} s_T$ , where  $c_T$  is a single-mode vacuum noise operator. The matching inefficiency  $M$  has the same form as before, and tends to zero for a sufficiently long time  $T$ . In this case, the atomic state is faithfully read out with  $c_{out} = -s_T$ .

The physical setup of quantum light memory discussed above could have other applications. We note that the output pulse shape  $f_{out}(t)$  need not be the same as the input pulse shape  $f_{in}(t)$ . This means that the setup can work as a pulse shape modulator to change the shape of an optical pulse without alternation of its quantum state. The pulse shape modulator could be useful in quantum communication between two cavities [32]. For instance, if one wants to input a pulse from the free decay of a cavity to another cavity with the same decay rate, the pulse will be nearly completely reflected at the mirror of the second cavity [32]. However, if between the two cavities we insert a pulse shape modulator to change the pulse shape to be its time reversal, the pulse will be nearly completely absorbed by the second cavity since the input process is exactly the time reversal of the output process. Besides the application as a pulse shape modulator, the quantum light memory setup can also be used as a pulse shape splitter illustrated by Fig. IVD 1. Consider that we have two independent pulse modes superposed in the same time window  $[0, T]$ , with the shapes denoted by  $f_{in}(t)$  and  $h_{in}(t)$  respectively. The pulse shape functions are orthogonal to each other with  $\int_0^T f_{in}^*(t) h_{in}(t) dt = 0$  for independent modes. Now we want to split these two modes by selectively transferring one of the optical modes  $c_{in} = \int_0^T f_{in}(t) a_{in}(t) dt$  to the atomic mode  $s$  with the impedance matching condition. In this case, one can show from Eq. (77) and the input-output relation that the other mode  $d_{in} = \int_0^T h_{in}(t) a_{in}(t) dt$  is completely reflected. In fact, one has  $d_{out} \equiv \int_0^T h_{out}(t) a_{out}(t) dt = d_{in}$ , where  $d_{out}$  is the reflected optical mode with its pulse shape changed to  $h_{out}(t) = h_{in}(t) - (e^{R(T)} - 1) e^{-R(t)} f_{in}(t) \int_0^t f_{in}^*(\tau) h_{in}(\tau) d\tau$ , where  $R(t) \equiv \int_0^t \kappa'(\tau) d\tau$ . In this way, we obtain a pulse shape splitter to separate different shapes, just like a polarization beam splitter to separate different polarizations.

In the above we have shown how to store an effectively one-mode optical field in an atomic ensemble. It is also possible to store many optical modes in the same atomic ensemble with a step-by-step method to increase its memory capacity. For this we consider a one-dimensional

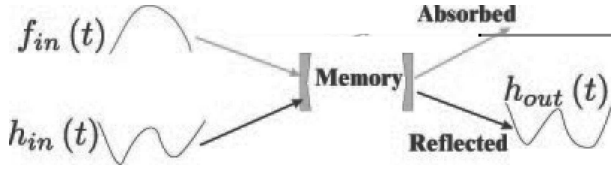


FIG. 21: Schematic setup to illustrate pulse shape splitter.

atomic ensemble with a length  $L_a$ . The coordinate of the  $j$  atom is denoted by  $x_j$ . We introduce a Fourier transformation to the individual atomic operator  $\sigma_{12}^j = |1\rangle_j \langle 2|$  with the form  $s_\mu \equiv \sum_j \sigma_{12}^j e^{i\mu x_j / L_a} / \sqrt{N_a}$  ( $\mu = 0, 1, \dots$ ). Under the weak excitation condition  $\langle |2\rangle_j \langle 2| \rangle \ll 1$ , the new modes  $s_\mu$  are independent and satisfy bosonic commutation relations  $[s_\mu, s_{\mu'}^\dagger] = \delta_{\mu\mu'}$ . We can induce a transition  $s_\mu \rightarrow s_{\mu+1}$  ( $\mu = 0, 1, \dots$ ) between the new modes by applying an electric field with spatial gradient for a suitable time to give a coordinate-dependent phase kick  $\sigma_{12}^j \rightarrow \sigma_{12}^j e^{i x_j / L_a}$ . To store in one atomic ensemble many optical pulse modes which come one after another, we transfer the first optical mode to the collective atomic mode  $s = s_0$  with the method described above, and then induce a transition  $s_\mu \rightarrow s_{\mu+1}$  by applying a phase kick. After the phase kick, the mode  $s$  is free to be used for storing the second optical mode. This process can be continued until many optical modes are stored in the atomic modes  $s, s_1, s_2, \dots$ . For releasing these atomic modes, we can simply reverse the above process.

In the real experiments, one cannot realize ideal quantum light memory with perfect state mapping between photons and atoms. As has been shown above, there is some inherent loss if the interaction time  $T$  is not much longer than the average effective coupling rate  $\bar{\kappa}$ . Additional to this, atomic spontaneous emissions will also contribute to loss with a signal-to-noise ratio given by  $R_{sn} \sim 4N_a |g_1|^2 / (\kappa \gamma_s)$  as described in Sec. 4.2. Assume that the overall inefficiency for all the loss effects in quantum light memory is denoted by  $\eta$ . In this case, if one inputs an optical mode in a coherent state  $|\alpha\rangle$  (which is commonly taken in experimental demonstrations), the read-out state from the memory is given by  $|\sqrt{1-\eta}\alpha\rangle$  with a state fidelity  $F = (\langle \alpha | \sqrt{1-\eta}\alpha \rangle)^2 = e^{-x_\eta |\alpha|^2}$ , where  $x_\eta = (1 - \sqrt{1-\eta})^2$ . With this imperfection, one would like to ask how to experimentally verify that one indeed realizes a quantum light memory, which should be better than any classical memory protocol. For instance, in a classical protocol, one can measure the input optical state to get some classical information, and then according to this information prepare a similar state after some time. The problem here is very similar to that in continuous variable quantum teleportation [29, 124], and we can use the result there to provide an experimentally testable criterion for quantum light memory. This criterion is given by measuring the input-output state fi-

delity  $F$ . Assume that the input state to the memory is randomly chosen from the set of coherent states  $\{|\alpha\rangle\}$  with a probability distribution  $p(\alpha) = (\lambda/\pi) e^{-\lambda|\alpha|^2}$ , where  $\lambda$  is a positive parameter, quantum light memory is verified with the confirmation to be better than any classical memory protocol if the measured average state fidelity  $F > F_{\text{cri}} = (1 + \lambda) / (2 + \lambda)$  [125]. With an overall loss inefficiency  $\eta$  for quantum light memory, the calculated average state fidelity in this case is given by  $F_{\text{cal}} = \lambda / (\lambda + x_\eta)$ . One can see that it is always possible to make  $F_{\text{cal}} > F_{\text{cri}}$  by choosing a large parameter  $\lambda$ , that is, by choosing the input coherent states close enough to the vacuum state. In a real experiment, there might be some technique noise which induces an additional fidelity decrease  $F_{\text{tec}}$  to the calculated value  $F_{\text{cal}}$ . In this case, one can verify that to meet the criterion  $F = F_{\text{cal}} - F_{\text{tec}} > F_{\text{cri}}$ , one has an optimal choice of the parameter  $\lambda$  to be  $\lambda = (1 - x_\eta) / (2F_{\text{tec}}) - 1 - x_\eta/2$ , and the technique fidelity decrease  $F_{\text{tec}}$  needs to be approximately below  $F_{\text{tec}} < (1 - x_\eta)^2 / 4$  for a successful demonstration of quantum light memory. In the experimental demonstrations [88, 90], the above criterion has not been checked, but it seems possible to meet this criterion with the current experimental technology.

## 2. Single-photon source

As has been mentioned before, single-photon source has many applications in quantum information processing. It is desirable to have a single-photon source with controllable emission time, direction, and pulse shape. This is required in some quantum information processing schemes since one needs to interfere two single-photon pulses, and this is generally available only when we can control the emission time, direction, and shape of the pulses. It is possible to produce single-photons with the setup of optical spontaneous parametric down conversion, which has been commonly used now in quantum communication experiments [123]. In this setup, photons are always generated in pairs due to the nonlinearity in the optical crystal. If we measure one output beam with a single-photon detector, conditional on a detector click the other output beam will be projected to a single-photon state. However, in this setup single photons will be produced at random times which are not controllable due to the randomness of spontaneous emissions. There are also proposals and experiments of using blockade mechanism in semiconductors or other solid-state materials to produce a source of single-photons [126–128], with the emission time fully controllable. To require the emitted single-photon pulses to be also directional, it seems that one needs to build a good cavity around the material. A fully controllable single-photon source is achievable if one could trap single-atoms in high-Q cavities for a sufficiently long time [129]. However, as we have mentioned before, this is possible but a experimentally challenging work. We show here that atomic ensembles can provide

another way to achieve a fully controllable single-photon source, which seems to be much easier for experimental demonstrations.

The principle of using an atomic ensemble to produce a single-photon source can be easily understood with the ideas explained in this chapter. The atomic ensemble working in the  $\Lambda$ -level configuration generates a correlated state in the form of Eq. (71) in the perturbative limit, which is an exact analogy of the optical spontaneous parametric down conversion process. We can measure the forward scattered signal with a single-photon detector, and conditional on a detector click, the collective atomic mode is projected to a single-excitation state. Since excitations can be stored for a reasonably long time in the ground-state manifold of the atoms, we can transfer the single-atomic excitation to the single-photon excitation at any desired time with the method described in the previous subsection. The emission time is controllable by when the repumping pulse is applied, and the emitted single-photon pulse is directed to the forward direction. The pulse shape is controllable by changing the time dependence of the Rabi frequency of the repumping pulse as in quantum light memory. This shows that the relatively simple system of an atomic ensemble can be used to produce single-photon pulses with fully controllable properties.

### E. Applications in continuous variable quantum information processing

In quantum information protocols, quantum information is normally carried by qubits, that is, by two-dimensional quantum systems. Similar to the classical case, quantum information can also be carried by some observables with continuous values, the canonical observables  $X$  and  $P$  for instance. The bosonic field (such as the optical field) provides a natural physical system to carry the continuous variable quantum information. Because of this, continuous variable quantum information processing has recently aroused a lot of interests. There have been proposals for continuous variable quantum teleportation [29, 124], cryptography [131], computation [130], error correction [134], entanglement purification [132], cloning [133], and etc., and continuous variable teleportation has been experimentally demonstrated by using single-mode optical fields [29]. We have seen from Sec. 4.2 that one can define a pair of canonical continuous-valued observables for atomic ensembles with suitable level schemes (the four-level scheme for instance). This property, combined with the ability of storing (qubit or continuous variable) quantum information in the ground-state manifold of atomic ensembles and the collectively enhanced coupling of the atomic mode in the ensemble to the optical mode, provides many possibilities for using atomic ensembles in continuous variable quantum information processing.

A good existing example to show these possibilities is

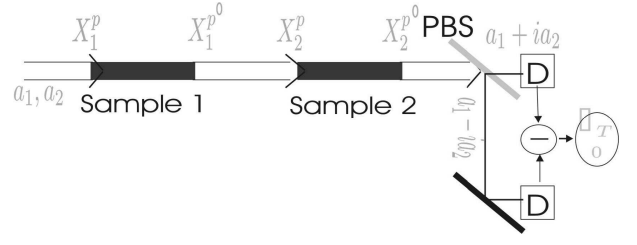


FIG. 22: Schematic setup for Bell measurements. A linearly polarized strong laser pulse (decomposed into two circular polarization modes  $a_1, a_2$ ) propagates successively through the two atomic samples. The two polarization modes  $(a_1 + ia_2)/\sqrt{2}$  and  $(a_1 - ia_2)/\sqrt{2}$  are then split by a polarizing beam splitter (PBS), and finally the difference of the two photon currents (integrated over the pulse duration  $T$ ) is measured.

given by the recent scheme for realizing continuous variable atomic quantum teleportation with laser manipulation of atomic ensembles [98]. Quantum teleportation of atomic states has not been realized yet due to the difficulty of achieving strong light-atom coupling. As we have seen, collective enhancement of the signal-to-noise ratio in atomic ensembles provides a possible way to go around this problem. There are two proposals to realize continuous variable teleportation with free-space atomic ensembles. Ref. [110] is based on the use of an external source of entanglement (non-classical light). Ref. [98] eliminates this requirement, and proposes a quantum teleportation scheme with the use of only coherent light. Based on the method in Ref. [98], a recent experiment has successfully generated entanglement between two distant macroscopic atomic ensembles [91], which is an important first step towards the final realization of atomic quantum teleportation. The following of this section is mainly devoted to a review of the scheme proposed in Ref. [98], and we will also briefly remark at the end of this section the possibilities of using atomic ensembles for realization of other continuous variable quantum information protocols.

The scheme in Ref. [98] is based on the four-level scheme described and analyzed in details in Sec. 4.2. The transformations (70) of the canonical atomic and optical observables induced by the light-atom interaction serve as the basic equations for understanding this scheme. To teleport continuous variable states from one atomic ensemble to the other, first we need to generate entanglement between the continuous observables  $X_1^a, P_1^a$  and  $X_2^a, P_2^a$  of two distant ensembles 1 and 2. This is done through a nonlocal Bell measurement of the EPR operators  $X_1^a - X_2^a$  and  $P_1^a + P_2^a$  with the setup depicted by Fig. IV E. This setup measures the Stokes operator  $X_2^{p'}$  of the output light. Using Eq. (70) and neglecting the small loss terms, we have  $X_2^{p'} = X_1^p + \kappa_c (P_1^a + P_2^a)$ , so we get a collective measurement of  $P_1^a + P_2^a$  with some inherent vacuum noise  $X_1^p$ . The efficiency  $1 - \eta$  of this measurement is determined by the parameter  $\kappa_c$  with  $\eta = 1/(1 + 2\kappa_c^2)$ . After this round of measurements,

we rotate the collective atomic spins around the  $x$  axis to get the transformations  $X_1^a \rightarrow -P_1^a$ ,  $P_1^a \rightarrow X_1^a$  and  $X_2^a \rightarrow P_2^a$ ,  $P_2^a \rightarrow -X_2^a$ . The rotation of the atomic spin can be easily obtained with negligible noise by applying classical laser pulses with detuning  $\Delta \gg \gamma$ . After the rotation, the measured observable of the first round of measurement is changed to  $X_1^a - X_2^a$  in the new variables. We then make another round of collective measurement of the new variable  $P_1^a + P_2^a$ . In this way, both the EPR operators  $X_1^a - X_2^a$  and  $P_1^a + P_2^a$  are measured, and the final state of the two atomic ensembles is collapsed into a two-mode squeezed state with variance  $\delta(X_1^a - X_2^a)^2 = \delta(P_1^a + P_2^a)^2 = e^{-2r}$ , where the squeezing parameter  $r$  is given by

$$r = \frac{1}{2} \ln(1 + 2\kappa_c^2). \quad (80)$$

Thus, using only coherent light, we generate continuous variable entanglement [135] between two nonlocal atomic ensembles. With the interaction parameter  $\kappa_c \approx 5$ , a high squeezing (and thus a large entanglement)  $r \approx 2.0$  is obtainable. Note that entanglement generation is the key step for many quantum information protocols, and as an example we show in the following how to use it to achieve quantum teleportation.

To achieve quantum teleportation, first the ensembles 1 and 2 are prepared in a continuous variable entangled state using the nonlocal Bell measurement described above. Then, a Bell measurement with the same setup as shown by Fig. IV E on the two local ensembles 1 and 3, together with a straightforward displacement of  $X_3^a$ ,  $P_3^a$  on the sample 3, will teleport an unknown collective spin state from the atomic ensemble 3 to 2. The teleported state on the ensemble 2 has the same form as that in the original proposal of continuous variable teleportation using squeezing light [124], with the squeezing parameter  $r$  replaced by Eq. (80) and with an inherent Bell detection inefficiency  $\eta = 1/(1 + 2\kappa_c^2)$ . The teleportation quality is best described by the fidelity, which, for a pure input state, is defined as the overlap of the teleported state and the input state. For any coherent input state of the sample 3, the teleportation fidelity is given by

$$F = 1 / \left( 1 + \frac{1}{1 + 2\kappa_c^2} + \frac{1}{2\kappa_c^2} \right). \quad (81)$$

Equation (81) shows, if there is no extra noise, a high fidelity  $F \approx 96\%$  would be possible for the teleportation of the collective atomic spin state with the interaction parameter  $\kappa_c \approx 5$ .

Finally, we need to incorporate several sources of noise in this scheme and analyze their influence on the teleportation fidelity. The noise includes the spontaneous emission noise described by Eq. (70), the detector inefficiency, and the transmission loss of the light from the first ensemble to the second one. The spontaneous emission noise can be included partly in the transmission loss and partly in the detector efficiency, so we do not analyze it

separately. The effect of the detector inefficiency  $\eta_d$  is to replace  $\kappa_c^2$  in Eqs. (80) and (81) with  $\kappa_c^2(1 - \eta_d)$ , and the teleportation fidelity is decreased by a term  $\eta_d/\kappa_c^2$ , which is very small and can be safely ignored. The most important noise comes from the transmission loss. The transmission loss is described by  $X_2^p = \sqrt{1 - \eta_t} X_1^p + \sqrt{\eta_t} X_s^t$  (see Fig. IV E), where  $\eta_t$  is the loss rate and  $X_s^t$  is the standard vacuum noise. The transmission loss changes the measured observables to be  $\sqrt{1 - \eta_t} X_1^a - X_2^a$  and  $\sqrt{1 - \eta_t} P_1^a + P_2^a$ . These two observables do not commute, and the two rounds of measurements influence each other. To minimize the influence on the teleportation fidelity, we choose the following configuration (for simplicity, we assume we have the same loss rate  $\eta_t$  from the sample 1 to 2 and from 1 to 3): In the nonlocal Bell measurements on the samples 1 and 2 (the entanglement generation process), we choose a suitable interaction coefficient  $\kappa_{c2}$  (where its optimal value will be determined below) for the second round measurement, whereas  $\kappa_{c1}$  for the first round of measurement is large with  $\kappa_{c1}^2 \gg \kappa_{c2}^2$  (the interaction coefficient can be easily adjusted, for instance, by changing the detuning). In the local Bell measurement, we choose the same  $\kappa_{c2}$  for the first round of measurement and the large  $\kappa_{c1}$  for the second round of measurement. For a coherent input state of the ensemble 3, the teleported state on the ensemble 2 is still a Gaussian state, and the teleportation fidelity  $F$  is found to be

$$F \approx 2 / \left( 2 + \frac{1}{\kappa_{c2}^2} + \kappa_{c2}^2 \eta_t \right) \leq 1 / (1 + \sqrt{\eta_t}), \quad (82)$$

which is independent of the coherent input state with suitable gain for the displacements [124]. The optimal value for  $\kappa_{c2}$  is thus given by  $\kappa_{c2} = 1/\sqrt{\eta_t}$ . Even with a significant transmission loss rate  $\eta_t \sim 0.2$ , quantum teleportation with a remarkable high fidelity  $F \sim 0.7$  is still achievable, which well exceeds the fidelity criterion  $1/2$  for continuous variable quantum teleportation with arbitrary coherent input states [125].

We have described the scheme in Ref. [98] for achieving continuous variable quantum teleportation of atomic spin state by laser manipulation of several atomic ensembles. The proposed scheme is within the reach of the current experimental technology, and has been partially demonstrated by the first-step experiment [91]. In general, one concerns about the possibilities of using laser manipulation of atomic ensembles to realize other continuous variable quantum information schemes. The four-level configuration used here and the  $\Lambda$ III-level configuration used in Sec. 4.3 have the ability to produce any squeezing operation. The  $\Lambda$ I-level configuration can be used to realize any beam-splitter like operation. One can also use the phase-kick technique discussed in quantum light memory subsection to manipulate many bosonic modes in one atomic ensemble, and the number of controllable modes can be further extended and is well scalable by connecting many atomic ensembles through optical pulses making use of the collective enhancement of the desired light-atom coupling in the ensembles. With these abilities, in

principle one can use laser manipulation of atomic ensembles to realize any scheme which is based on the following physical requirements, that is, a series of well controllable bosonic modes, and the ability of performing any desired squeezing or beam-splitter like operation on these modes. The schemes belong to this class include some continuous variable quantum cryptography scheme [131], the continuous variable quantum error correction scheme in Ref. [134], and the scheme in Ref. [133] for quantum cloning of Gaussian continuous variable states. To realize the continuous variable quantum computation scheme in Ref. [130] and the continuous variable entanglement purification scheme in Ref. [132], one needs another kind of operation, i.e., the Kerr operation, which is described by the single-mode Hamiltonian  $H_k = \chi_k (a^\dagger a)^2$ . There have been proposals of some level configurations to realize the Kerr operation in atomic ensembles using the phenomenon of electromagnetic field induced transparency (EIT) [136, 137]. Unfortunately, unlike the three configurations discussed in Sec. 4.2, the signal-to-noise ratio for the Kerr operation is not collectively enhanced [138], and as a result one basically still needs to build a high-Q cavity around the ensemble and has to enter the strong coupling regime for getting a good signal-to-noise ratio, which is experimentally very challenging. Therefore, it seems to be hard to realize continuous variable quantum computation and entanglement purification solely based on laser manipulation of atomic ensembles, but studies are going on in this direction, and possibly one can realize it with a combination of some other technique, using

direct interactions between atoms as in Refs. [102] for instance.

## F. Summary

This chapter has reviewed the recent advances of using atomic ensembles for quantum information processing. We put emphasis on the collective enhancement of the signal-to-noise ratio for the coupling between light and atomic ensembles with suitable level configurations. Due to the collectively enhanced coupling, we can do various kinds of interesting quantum information processing simply by laser manipulation of atomic ensembles in weak coupling cavities or even in free space, which greatly simplifies their experimental demonstration. All the theoretical schemes for quantum information processing reviewed in this chapter are within the scope of the near-future experiments. We hope that these example schemes have shown the promising future of using atomic ensembles for quantum information processing, with a combination of the advantages of a long coherence time and a collectively-enhanced coupling to light. The progress in this area is fast, and the important open questions include a full understanding of the interaction of light with hot and cold atomic ensembles in three-dimensional free space with various level configurations, and applications of these interaction configurations in physical realization of more quantum information protocols.

- 
- [1] A very good introduction to quantum information and its applications can be found in: PERES, A. *Quantum Theory: Concepts and Methods*, (Kluwer Academic) 1993; NIELSEN M. and CHUANG I., *Quantum computation and quantum information*, (Cambridge University Press), 2000; *The Physics of Quantum Information: Quantum Cryptography, Quantum Teleportation, Quantum Computation*, Edited by BOUWMEESTER D., EKERT A., and ZEILINGER A. (Springer-Verlag), 2000. On the other hand, most of the articles on the field can be found in <http://xxx.lanl.gov/archive/quant-ph>.
  - [2] SHOR P. W., *Proc. of the 3rd Annual Symposium on the Foundations of Computer Science* (IEEE Computer Society Press, Los Alamitos, Ca) 1994, pp. 124.
  - [3] EKERT A. and JOSZA R., *Rev. Mod. Phys.*, **68** (1995) 733.
  - [4] BRIEGEL H. J., DUR W., CIRAC J. I., ZOLLER P., *Phys. Rev. Lett.*, **81** (1998) 5932; DUR W., BRIEGEL H. J., CIRAC J. I., ZOLLER P., *Phys. Rev. A*, **59** (1999) 169.
  - [5] BELL J. S., *Physics* **1** (1964) 195.
  - [6] BENNETT C. H., BERNSTEIN H. J., POPESCU S., and SCHUMACHER B., *Phys. Rev. A*, **53** (1996) 2046.
  - [7] POPESCU S. and ROHRlich D., *Phys. Rev. A*, **56** (1997) 3319.
  - [8] LINDEN N. and POPESCU S., *Fortsch. Phys.*, **46** (1998) 567.
  - [9] GREENBERGER D. M., HORNE M., and ZEILINGER A., in *Bell's theorem, Quantum Theory and Conceptions of the Universe*, edited by M. Kafatos (Kluwer Academic, Dordrecht, The Netherlands) 1989, pp 69.
  - [10] DUR W., VIDAL G., and CIRAC J. I., *Phys. Rev. A*, **62** (2000) 62314.
  - [11] WERNER R. F., *Phys. Rev. A*, **40** (1989) 4277.
  - [12] PERES A., *Phys. Rev. Lett.*, **77** (1996) 1413.
  - [13] HORODECKI P., *Phys. Lett. A*, **232** (1997) 333.
  - [14] HORODECKI R., HORODECKI P., HORODECKI M., *Phys. Lett. A*, **210** (1996) 377.
  - [15] LEWENSTEIN W. *et al.*, *J. Mod. Opt.*, **77** (2000) 2481; TERHAL B. M., [quant-ph/0101032](http://arxiv.org/abs/quant-ph/0101032).
  - [16] BENNETT C. H., BRASSARD G., POPESCU S., SCHUMACHER B., SMOLIN J. A., and WOOTTERS W. K. *Phys. Rev. Lett.*, **76** (1996) 722; BENNETT C. H., DIVINCENZO D. P., SMOLIN J. A., and WOOTTERS W. K., *Phys. Rev. A*, **54** (1996) 3824.
  - [17] GISIN N., *Phys. Lett. A*, **210** (1996) 151.
  - [18] GIEDKE G., BRIEGEL H. J., CIRAC J. I., and ZOLLER P., *Phys. Rev. A*, **59** (1999) 2641.
  - [19] See, for example, DIVINCENZO D. P., *Fortschr. Phys.*, **48** (2000) 771.



- [20] Special issue of *Fortschr. Phys.* (edited by BRAUNSTEIN S. and LO H.-K.), **48** (2000) 769.
- [21] SHOR P. W., *Phys. Rev. A*, **52** (1995) 2493.
- [22] STEANE A. M., *Phys. Rev. Lett.*, **77** (1996) 793.
- [23] LAFLAMME R. *et al.*, *Phys. Rev. Lett.*, **77** (1996) 198.
- [24] GOTTESMAN D., *Phys. Rev. A*, **54** (1996) 1862.
- [25] SHOR P. W., in *37th Symposium on Foundations of Computing*, (IEEE Computer Society Press) 1996, pp. 56-65.
- [26] BENNETT C. H., BRASSARD G., CREPEAU C., JOZSA R., PERES A., and WOOTTERS W. K. *Phys. Rev. Lett.*, **70** (1993) 1895.
- [27] BOUWMEESTER D., PAN J.-W., MATTLE K., EIBL M., WEINFURTER H., ZEILINGER A., *Nature*, **390** (1997) 575.
- [28] BOSCHI D., BRANCA S., DE MARTINI F., HARDY L., and POPESCU S., *Phys. Rev. Lett.*, **80** (1998) 1121.
- [29] FURUSAWA A., SORENSEN J. L., BRAUNSTEIN S. L., FUCHS C. A., KIMBLE H. J., and POLZIK E. S., *Science*, **282** (1998) 706.
- [30] CIRAC J. I. and ZOLLER P., *Phys. Rev. Lett.*, **74** (1995) 4091.
- [31] PELLIZZARI T., GARDINER S.A., CIRAC J.I., and ZOLLER P., *Phys. Rev. Lett.*, **75** (1995) 3788.
- [32] CIRAC J. I., ZOLLER P., KIMBLE H. J., MABUCHI H., *Phys. Rev. Lett.* **78** (1997) 3221.
- [33] SORENSEN A. and MOLMER K., *Phys. Rev. Lett.*, **82** (1999) 1971.
- [34] POYATOS J.F., CIRAC J.I., and ZOLLER P. *Phys. Rev. Lett.*, **81** (1998) 1322.
- [35] JAKSCH D., BRIEGEL H.J., CIRAC J.I., GARDINER C.W., and ZOLLER P., *Phys. Rev. Lett.*, **82** (1999) 1975.
- [36] BRENNEN G., CAVES C., JESSEN P., and DEUTSCH I., *Phys. Rev. Lett.*, **82** (1999) 1060.
- [37] JAKSCH D., CIRAC J. I., and ZOLLER P., ROLSTON S.L., COTE R. and LUKIN M. D., *Phys. Rev. Lett.*, **85** (2000) 2208.
- [38] DUAN L.-M., CIRAC J. I., and ZOLLER P., *Science*, **292** (2001) 1695.
- [39] PACHOS J., ZANARDI P., RASETTI M., *Phys. Rev. A*, **61** (2000) 10305(R).
- [40] CIRAC J.I., PARKINS A. S., BLATT R., and ZOLLER P., *Adv. Atom. Mol. Opt. Phys.*, **37** (1996) 237.
- [41] STEANE A., *Appl. Phys. B*, **64** (1997) 623.
- [42] WINELAND D. J., MONROE C., ITANO W. M., LEIBFRIED D., KING B. E., and MEEKHOF D. M., *RES J. NIST*, **103** (1998) 259.
- [43] CIRAC J. I., ZOLLER P., *Nature*, **404** (2000) 579.
- [44] CALARCO T., CIRAC J. I., and ZOLLER P., *Phys. Rev. A*, **63** (2001) 62304.
- [45] LAW C.K. and EBERLY J.H., *Phys. Rev. Lett.*, **76** (1996) 1055.
- [46] GARDINER S. A., CIRAC J. I., and ZOLLER P., *Phys. Rev. A*, **55** (1997) 1683.
- [47] GARDINER C. W., ZOLLER P., *Quantum Noise* (Springer) 1999.
- [48] STENHOLM S., *Rev. Mod. Phys.*, **58** (1986) 699.
- [49] CIRAC J. I., BLATT R., ZOLLER P., and PHILLIPS W. D., *Phys. Rev. A*, **46** (1992) 2668.
- [50] MARZOLI I., CIRAC J. I., BLATT R., and ZOLLER P., *Phys. Rev. A*, **49** (1994) 2771.
- [51] MONROE C., MEEKHOF D. M., KING B. E., ITANO W. M., and WINELAND D. J., *Phys. Rev. Lett.*, **75** (1995) 4714.
- [52] KING B. E., WOOD C. S., MYATT C. J., TURCHETTE Q.A., LEIBFRIED D., ITANO W. M., MONROE C., and WINELAND D. J., *Phys. Rev. Lett.*, **7** (1998) 1525.
- [53] ROOS C.F., LEIBFRIED D., MUNDT A., SCHMIDT-KALER F., ESCHNER J., BLATT R., *Phys. Rev. Lett.*, **85** (2000) 5547.
- [54] NAGERL H. C., LEIBFRIED D., ROHDE H., THALHAMMER G., ESCHNER J., SCHMIDT-KALER F., BLATT R., *Phys. Rev. A*, **60** (1999) 145.
- [55] TURCHETTE Q. A., WOOD C. S., KING B. E., MYATT C. J., LEIBFRIED D., ITANO W. M., MONROE C., and WINELAND D. J., *Phys. Rev. Lett.*, **81** (1998) 3631.
- [56] SACKETT C.A. KIELPINSKI D., KING B.E., LANGER C., MEYER V., MYATT C.J., ROWE M., TURCHETTE Q.A., ITANO W.M., WINELAND D.J., *Nature*, **404** (2000) 256.
- [57] KIELPINSKI D., MEYER V., ROWE M. A., SACKETT C. A., ITANO W. M., MONROE C., and WINELAND D. J., *Science*, **291** (2001) 1013.
- [58] ROWE M. A., KIELPINSKI D., MEYER V., SACKETT C. A. ITANO W. M., MONROE C., WINELAND D. J., *Nature*, **409** (2001) 791.
- [59] JONATHAN D., PLENIO M. B., and KNIGHT P. L., *Phys. Rev. A*, **62** (2000) 42307.
- [60] ZANARDI P. and RASETTI M., *Phys. Lett. A*, **264** (1999) 94.
- [61] PACHOS J., ZANARDI P., LANL preprint available at <http://xxx.lanl.gov/abs/quant-ph/0007110>.
- [62] CIRAC J.I., PELLIZZARI T., ZOLLER P., *Science*, **273** (1996) 1207.
- [63] PELLIZZARI T., *Phys. Rev. Lett.*, **79** (1997) 5242.
- [64] TURCHETTE Q.A., HOOD C.J., LANGE W., MABUCHI H., and KIMBLE H. J., *Phys. Rev. Lett.*, **75** (1995) 4710.
- [65] MAITRE X., HAGLEY E., NOGUES G., WUNDERLICH C., GOY P., BRUNE M., RAIMOND J. M., and HAROCHE S., *Phys. Rev. Lett.* **79** (1997) 769.
- [66] RAUSCHENBEUTEL A., NOGUES G., OSNAGHI S., BERTET P., BRUNE M., RAIMOND J. M., and HAROCHE S., *Phys. Rev. Lett.*, **83** (1999) 5166.
- [67] RAUSCHENBEUTEL A., NOGUES G., OSNAGHI S., BERTET P., BRUNE M., RAIMOND J. M., and HAROCHE S., *Science*, **288** (2000) 2024.
- [68] OSNAGHI S., BERTET P., AUFEVES A., MAIOLI P., BRUNE M., RAIMOND J.M., and HAROCHE S., *Phys. Rev. Lett.*, **87** (2001) 37902.
- [69] BRATTKE S., VARCOE B.T.H., and WALTHER H., *Phys. Rev. Lett.*, **86** (2001) 3534.
- [70] S.-B. ZHENG, and G.-C. GUO, *Phys. Rev. Lett.*, **85** (2000) 2392.
- [71] GARDINER C.W., *Phys. Rev. Lett.*, **70** (1993) 2269.
- [72] CARMICHAEL H.J., *Phys. Rev. Lett.*, **70** (1993) 2273.
- [73] BOSE S., KNIGHT P.L., PLENIO M.B., and VEDRAL V., *Phys. Rev. Lett.*, **83** (1999) 5158.
- [74] VAN ENK S.J., CIRAC J.I., and ZOLLER P., *Phys. Rev. Lett.*, **78** (1997) 4293.
- [75] VAN ENK S.J., CIRAC J.I., and ZOLLER P., *Science*, **279** (1998) 205.
- [76] CALARCO T., HINDS E.A., JAKSCH D., SCHMIED-MAYER J., CIRAC J.I., and ZOLLER P., *Phys. Rev. A*, **61** (2000) 22304.

- [77] BRENNEN G.K., DEUTSCH I.H., JESSEN P.S., *Phys. Rev. A*, **61** (2000) 62309.
- [78] BRENNEN G.K., DEUTSCH I.H., WILLIAMS C.J., quant-ph/0107136 (*Phys. Rev. A*, in press)
- [79] WEINER J., BAGNATO V.S. and ZILIO S., JULIENNE P.S., *Rev. Mod. Phys.*, **71** (1999) 1.
- [80] JAKSCH D., BRUDER C., CIRAC J.I., GARDINER C.W., and ZOLLER P., *Phys. Rev. Lett.*, **81** (1998) 3108.
- [81] SCHLOSSER N., REYMOND G., PROTSSENKO I., GRANGIER P., *Nature*, **411** (2001) 1024.
- [82] BUCHKREMER F.B.J., DUMKE R., VOLK M., MUETHER T., BIRKL G., and ERTMER W., quant-ph/0110119
- [83] TIESINGA E., WILLIAMS C.J., MIES F.H., and JULIENNE P.S., *Phys. Rev. A*, **61** (2000) 63416.
- [84] GALLAGHER T.F., Rydberg Atoms (Cambridge University Press, New York, 1994).
- [85] Hald J., SORENSEN J. L., SCHORI C., and POLZIK E.S., *Phys. Rev. Lett.*, **83** (1999) 1319.
- [86] ROCH J.-F., VIGNERON K., GRELU Ph., SINATRA A., POIZAT J. -Ph., and GRANGIER Ph. *Phys. Rev. Lett.*, **78** (1997) 634.
- [87] HAU L. V., HARRIS S. E., DUTTON Z., and BEHROOZI C. H., *Nature*, **397** (1999) 594.
- [88] LIU C., DUTTON Z., BEHROOZI C. H., and HAU L. V., *Nature*, **409** (2001) 490.
- [89] KASH M. M., SAUTENKOV V. A., ZIBROV A. S., HOLLBERG L., WELCH G. R., LUKIN M. D., ROSTOVTSEV Y., FRY E. S., and SCULLY M. O., *Phys. Rev. Lett.*, **82** (1999) 5229.
- [90] PHILLIPS D. F., FLEISCHHAUER A., MAIR A., and WALSWORTH R. L., and LUKIN M. D., *Phys. Rev. Lett.*, **86** (2001) 783.
- [91] JULSGAARD B., KOZHEKIN A., POLZIK E. S., quant-ph/0106057, to appear in *Nature*.
- [92] KUZMICH A., BIGELOW N. P., and MANDEL L., *Europhys. Lett. A*, **42** (1998) 481.
- [93] LUKIN M. D., YELIN S. F., and FLEISCHHAUER M., *Phys. Rev. Lett.*, **84** (2000) 4232.
- [94] DUAN L.-M., CIRAC J. I., and ZOLLER P., talk at the IQEC-CLEO/Europe, (Nice, France) 2000.
- [95] DUAN L.-M., LUKIN M. D., CIRAC J. I., and ZOLLER P., quant-ph/0105105, to appear in *Nature*.
- [96] RAYMER M. A. and MOSTOWSKI J., *Phys. Rev. A*, **24** (1981) 1980.
- [97] FLEISCHHAUER M. and LUKIN M. D., *Phys. Rev. Lett.*, **84** (2000) 5094.
- [98] DUAN L.-M., CIRAC J. I., ZOLLER P., and POLZIK E. S., *Phys. Rev. Lett.*, **85** (2000) 5643.
- [99] RAYMER M. G., WALMSLEY I. A., MOSTOWSKI J., and SOBOLEWSKA B., *Phys. Rev. A*, **32** (1985) 332.
- [100] KOZHEKIN A. E., MOLMER K., POLZIK E. S., quant-ph/9912014.
- [101] KNILL E., LAFLAMME R., and MILBURN G. J., *Nature*, **409** (2001) 46.
- [102] LUKIN M. D., FLEISCHHAUER M., COTE R., DUAN L.-M., JAKSCH D., CIRAC J. I., and ZOLLER P., *Phys. Rev. Lett.*, **87** (2001) 037901.
- [103] FLEISCHHAUER M. and LUKIN M. D., quant-ph/0106066.
- [104] YE J., VERNOOY D. W., and KIMBLE H. J., *Phys. Rev. Lett.*, **83** (1999) 4987.
- [105] HAPPER W., *Rev. Mod. Phys.*, **44** (1972) 169.
- [106] HAPPER W. and ATHUR B. S., *Phys. Rev. Lett.*, **18** (1967) 577.
- [107] KUZMICH A., MANDEL L., and BIGELOW N. P., *Phys. Rev. Lett.*, **85** (2000) 1594.
- [108] TAKAHASHI Y., HONDA K., TANAKA N., TOYODA K., ISHIKAWA K., and YABUZAKI T., *Phys. Rev. A*, **60** (1999) 4974.
- [109] MOLMER K., *Eur. Phys. J. D*, **5** (1999) 301.
- [110] KUZMICH A. and POLZIK E. S., *Phys. Rev. Lett.*, **85** (2000) 5639.
- [111] EKERT A., *Phys. Rev. Lett.*, **67** (1991) 661.
- [112] KNILL E., R. LAFLAMME R., and ZUREK W. H., *Science*, **279** (1998) 342.
- [113] PRESKILL J., *Proc. R. Soc. Lond. A*, **454** (1998) 385.
- [114] ZUKOWSKI M., ZEILINGER A., HORNE M. A., and EKERT A., *Phys. Rev. Lett.*, **71** (1993) 4287.
- [115] HOOD C. J., LYNN T. W., DOHERTY A. C., PARKINS A. S., and KIMBLE H. J., *Science* **287** (2000) 1447.
- [116] PINKSE P. W. H., FISCHER T., MAUNZ T. P., and REMPE G., *Nature*, **404** (2000) 365.
- [117] CABRILLO C., CIRAC J. I., G-FERNANDEZ P., and ZOLLER P., *Phys. Rev. A*, **59** (1999) 1025.
- [118] LO H. K. and CHAU H. F., *Science*, **283** (1999) 2050.
- [119] SHOR P. W. and PRESKILL J., *Phys. Rev. Lett.*, **85** (2000) 441.
- [120] CLAUSER J. F., HORNE M. A., SHIMONY A., and HOLT R. A., *Phys. Rev. Lett.*, **23** (1969) 880.
- [121] BUDKER D., YASHUK V., and ZOLOTOREV M., *Phys. Rev. Lett.*, **81** (1998) 5788.
- [122] BRASSARD G., LÜTKENHAUS N., MOR T., and SANDERS B. C., *Phys. Rev. Lett.*, **85** (2000) 1330.
- [123] ZEILINGER A., *Rev. Mod. Phys.*, **71** (1999) S288.
- [124] BRAUNSTEIN S. L. and KIMBLE H. J., *Phys. Rev. Lett.* **80** (1998) 869.
- [125] BRAUNSTEIN S. L., FUCHS C. A., and KIMBLE H. J., quant-ph/9910030.
- [126] KIM J., BENSON O., KAN H., and YAMAMOTO Y., *Nature*, **397** (1999) 500.
- [127] MICHLER P., KIRAZ A., BECHER C., SCHOENFELD W. V., PETROFF P. M., ZHANG L., HU E., and IMAMOGLU A., *Science*, **290** (2000) 2282.
- [128] BEVERATOS A., BROURI R., GACON T., POIZAT J.-P., and GRANGIER P., quant-ph/0104028.
- [129] GHERI K. M., SAAVEDRA C., TORMA P., CIRAC J. I., and ZOLLER P., *Phys. Rev. A*, **58** (1998) R2627.
- [130] BRAUNSTEIN S. L. and LLOYD S., *Phys. Rev. Lett.* **82** (1999) 1789.
- [131] GOTTESMAN D. and PRESKILL J., *Phys. Rev. A*, **63** (2001) 022309 and refs. therein.
- [132] DUAN L.-M., GIEDKE G., CIRAC J. I., and ZOLLER P., *Phys. Rev. Lett.*, **84** (2000) 4002; *Phys. Rev. A* **62** (2000) 032304.
- [133] CERF N. J. and ROTTENBERG A. X., *Phys. Rev. Lett.*, **85** (2000) 1754.
- [134] BRAUNSTEIN S. L., *Nature*, **394** (1998) 47.
- [135] DUAN L.-M., GIEDKE G., CIRAC J. I., and ZOLLER P., *Phys. Rev. Lett.* **84** (2000) 2722.
- [136] IMAMOGLU A., SCHMIDT H., WOODS G., and DEUTSCH M., *Phys. Rev. Lett.* **79** (1997) 1467.
- [137] LUKIN M. D., IMAMOGLU A., *Phys. Rev. Lett.*, **84** (2000) 1419.
- [138] GHERI K. M., ALGE W., and GRANGIER P., *Phys.*

*Rev. A*, **60** (1999) R2673.